



**IUTAM**

International Union of Theoretical  
and Applied Mechanics

# **2011 IUTAM SYMPOSIUM ON IMPACT BIOMECHANICS IN SPORT**

**SYMPOSIUM PROCEEDINGS**

**UNIVERSITY COLLEGE DUBLIN, DUBLIN, IRELAND**

**JULY 7-9 2011**

## EVENT SPONSORS



- University College Dublin
- UCD School of Electrical, Electronic and Mechanical Engineering
- Bertram Broberg Memorial Fund
- International Union of Theoretical and Applied Mechanics
- Royal Irish Academy



## SCIENTIFIC COMMITTEE

Prof. Mike Caine	Sports Technology, Mechanical & Manufacturing Engineering, Loughborough University, England	M.P.Caine@lboro.ac.uk
Prof. Dick van Campen (IUTAM representative)	Mechanical Engineering, Eindhoven University Technology, Eindhoven, Netherlands	d.h.v.Campen@tue.nl
Prof. Michael Gilchrist (Chairman)	School of Electrical, Electronic & Mechanical Engineering, University College Dublin, Ireland	Michael.Gilchrist@ucd.ie
Prof. Richard Greenwald	Thayer School of Engineering at Dartmouth, Hanover NH, USA	richard.greenwald@dartmouth.edu
Prof. Mont Hubbard	Mechanical & Aeronautical Engineering, University of California, Davis, Davis CA, USA	mhubbard@ucdavis.edu
Prof. Andrew McIntosh	School of Safety Science, University of New South Wales, Sydney, Australia	a.mcintosh@unsw.edu.au
Prof. Gerald Nurick	Dept. of Mechanical Engineering, University of Cape Town, South Africa	Gerald.Nurick@uct.ac.za
Prof. Stephen Reid	School of Engineering, University of Aberdeen, Scotland	steve.reid@abdn.ac.uk
Prof. Renato Rodano	Politecnico di Milano, Italy	renato.rodano@biomed.polimi.it
Prof. Josef Vander Sloten	Division of Biomechanics and Engineering Design, Katholieke Universiteit Leuven, Belgium	jos.vandersloten@mech.kuleuven.be

## LOCAL ORGANIZING COMMITTEE

Dr. Brian Caulfield	School of Physiotherapy & Performance Science, Health Sciences Centre, University College Dublin	b.caulfield@ucd.ie
Prof. David FitzPatrick	School of Electrical, Electronic and Mechanical Engineering, University College Dublin	david.fitzpatrick@ucd.ie
Dr. Manuel A. Forero Rueda (Secretary)	School of Electrical, Electronic and Mechanical Engineering, University College Dublin	manuel@ucd.ie
Prof. Michael Gilchrist (Chairman)	School of Electrical, Electronic and Mechanical Engineering, University College Dublin	michael.gilchrist@ucd.ie
Dr. Ciaran Simms	Department of Mechanical & Manufacturing Engineering, Trinity College Dublin	csimms@tcd.ie

## PROGRAMME

DAY 1: JULY 7, 2011		
8:00 – 9:00	<b>Registration and Welcome</b>	
9:00 – 9:45	<b>Keynote lecture</b> - Adding insult to injury: The dynamics of human tissues	K. T. Ramesh
9:45 – 10:15	Modelling the anisotropic behaviour of skin	A. Ní Annaidh
10:15 – 10:45	Experimental characterization of the mechanical properties of the superior sagittal sinus – bridging vein complex	K. Baeck
10:45 – 11:15	<b>Coffee Break</b>	
11:15 – 11:45	Modelling the impact response of cranial bone	J. Motherway
11:45 – 12:15	A new method to determine the young's modulus from fresh bone flaps	E. Forausbergher
12:15 – 12:45	Mechanical properties of brain tissue in tension at high strain rates	B. Rashid
12:45 – 14:15	<b>Lunch</b>	
14:15 – 15:00	<b>Keynote lecture</b> - Biomechanics of traumatic brain injuries and head injury criteria	S. Kleiven
15:00 – 15:30	The egg Injury criterion. Can we learn more about head injury with an egg surrogate?	A. Short
15:30 – 16:00	Injury data from unhelmeted football head impacts evaluated against critical strain tolerance curves	D. A. Patton
16:00 – 16:30	<b>Coffee Break</b>	
16:30 – 17:00	Traumatic brain injuries investigation using finite element modeling of rat brain	M. Gilchrist
17:00 – 17:30	Impact performance of ice hockey helmets: head acceleration versus focal force dispersion	R. Ouckama
18:00 -	<b>Irish Pub Night – Pickup at 18:00</b>	
DAY 2: JULY 8, 2011		
9:00 – 9:45	<b>Keynote lecture</b> - Biomechanical considerations in the design of equipment to prevent sports injury	A. McIntosh
9:45 – 10:15	Analysis of loading curve characteristics on the production of brain deformation metrics	A. Post
10:15 – 10:45	Computational protective helmet component analysis	M. A. Forero
10:45 – 11:15	<b>Coffee Break</b>	
11:15 – 11:45	Dynamic impact response characteristics of ice hockey helmets using a centric and non-centric impact protocol	E. Walsh
11:45 – 12:15	The application of brain tissue deformation values in assessing the safety performance of ice hockey helmets	B. Hoshizaki
12:15 – 12:45	Impact assessment of jockey helmet liner materials	D. A. Patton
12:45 – 14:15	<b>Lunch</b>	
14:15 – 15:00	<b>Keynote lecture</b> - Passive and active muscle effects on impacts	M. T. G. Pain
15:00 – 15:30	Validated 3d finite element model of wrist joint	V. Balden
15:30 – 16:00	Trampoline frame impact attenuation: padded metal-frame vs soft-edge system	D. Eager
16:00 – 16:30	<b>Coffee break</b>	
16:30 – 17:00	Falls into via ferrata climbing sets can cause severe injuries for lightweight climbers	S. Litzenberger
17:00 – 17:30	Upload your head injury! A novel method for biomechanical prediction. Is it feasible?	A. Glenn
17:30 – 18:00	A comparison of peak linear and angular response between the Hybrid III and the Hodgson-WSU headforms	M. Kendall
18:00 -	<b>Symposium Banquet – Departure at 18:00, Radisson pick up at 18:15</b>	
DAY 3: JULY 9, 2011		
9:00 – 9:45	<b>Keynote lecture</b> - Collision injuries in Rugby Union	J. Ryan
9:45 – 10:15	Classification of Collisions in Elite Level Rugby Union using a Wearable Sensing Device	G. Coughlan
10:15 – 10:45	An integrated measurement system for analysing impact biomechanics in the rugby scrum	G. Treawartha
10:45 – 11:15	<b>Coffee break</b>	
11:15 – 11:45	Impact reconstruction from damage to pedal- and motor-cycle helmets	A. McIntosh
11:45 – 12:15	Head impact conditions in case of bicyclist falling	P. Carreira
12:15 – 12:45	Human brain tolerance thresholds for traumatic brain injury from reconstructions	A. Post

## TABLE OF CONTENTS

<b>Day 1: July 7, 2011</b>			
Title	Presenting Author	Institution	Page
<b>Keynote lecture</b> - Adding insult to injury: The dynamics of human tissues	K. T. Ramesh	JHU	1
Modelling the anisotropic behaviour of skin	A. Ní Annaidh	UCD	3
Experimental characterization of the mechanical properties of the superior sagittal sinus – bridging vein complex	K. Baeck	KULeuven	5
Modelling the impact response of cranial bone	J. Motherway	UCD	7
A new method to determine the young's modulus from fresh bone flaps	E. Forausbergher	KULeuven	9
Mechanical properties of brain tissue in tension at high strain rates	B. Rashid	UCD	11
<b>Keynote lecture</b> - Biomechanics of traumatic brain injuries and head injury criteria	S. Kleiven	KTH	13
The egg Injury criterion. Can we learn more about head injury with an egg surrogate?	A. Short	U. of Melbourne	14
Injury data from unhelmeted football head impacts evaluated against critical strain tolerance curves	D. A. Patton	UNSW	16
Traumatic brain injuries investigation using finite element modeling of rat brain	M. Gilchrist	UCD / Strasbourg University	18
Impact performance of ice hockey helmets: head acceleration versus focal force dispersion	R. Ouckama	McGill University	20
<b>Day 2: July 8, 2011</b>			
Title	Presenting Author	Institution	Page
<b>Keynote lecture</b> - Biomechanical considerations in the design of equipment to prevent sports injury	A. McIntosh	UNSW	22
Analysis of loading curve characteristics on the production of brain deformation metrics	A. Post	U. of Ottawa	24
Computational protective helmet component analysis	M. A. Forero	UCD	26
Dynamic impact response characteristics of ice hockey helmets using a centric and non-centric impact protocol	E. Walsh	U. of Ottawa	28
The application of brain tissue deformation values in assessing the safety performance of ice hockey helmets	B. Hoshizaki	U. of Ottawa	30
Impact assessment of jockey helmet liner materials	D. A. Patton	UNSW	32
<b>Keynote lecture</b> - Passive and active muscle effects on impacts	M. T. G. Pain	Loughborough U.	34
Validated 3d finite element model of wrist joint	V. Balden	U. of Cape Town	36
Trampoline frame impact attenuation: padded metal-frame vs soft-edge system	D. Eager	U. of Tech. Sydney	38
Falls into via ferrata climbing sets can cause severe injuries for lightweight climbers	S. Litzenberger	UAS Technikum Wien	40
Upload your head injury! A novel method for biomechanical prediction. Is it feasible?	A. Glenn	U. of Melbourne	42
A comparison of peak linear and angular response between the Hybrid III and the Hodgson-WSU headforms	M. Kendall	U. of Ottawa	44
<b>Day 3: July 9, 2011</b>			
Title	Presenting Author	Institution	Page
<b>Keynote lecture</b> - Collision injuries in Rugby Union	J. Ryan	Leinster Rugby	46
Classification of Collisions in Elite Level Rugby Union using a Wearable Sensing Device	G. Coughlan	UCD	48
An integrated measurement system for analysing impact biomechanics in the rugby scrum	G. Treawartha	U. of Bath	50
Impact reconstruction from damage to pedal- and motor-cycle helmets	A. McIntosh	UNSW	52
Head impact conditions in case of bicyclist falling	P. Carreira	Oxylane Research	54
Human brain tolerance thresholds for traumatic brain injury from reconstructions	A. Post	U. of Ottawa	56

## ADDING INSULT TO INJURY: THE DYNAMICS OF HUMAN TISSUES

K.T. Ramesh

Department of Mechanical Engineering, The Johns Hopkins University  
Baltimore, MD 21218, ramesh@jhu.edu

### INTRODUCTION

Computational models are often used as a tool to study impact biomechanics. They are also utilized to develop protective restraints in automobiles, to design protective gear in sports and military applications, and to develop a better understanding of the mechanisms that lead to traumatic brain injury (TBI). The fidelity of such models relies heavily on the accurate representation of the internal structure, an accurate description of the behavior of the materials involved, and the use of an appropriate measure of injury. Impact problems in general have several unique features: high stresses as a result of inertial confinement, shock propagation and shock damage, the triggering of vibrational modes, and accelerations that may be injurious in themselves. We attempt here to delineate some of the key issues in the dynamics of human soft tissues, and consider a specific injury mechanism in some detail.

We begin by discussing experimental techniques needed to measure the dynamic properties of soft tissues, and then discuss the specific problem of diffuse axonal injury.

### EXPERIMENTAL METHODS

The major difficulty associated with the study of soft tissues under mechanical loading arises from the dramatic difference between the response of such tissues to hydrostatic pressure and shear stress. Soft tissues are generally nearly incompressible, but have relatively low shear moduli. As a consequence, a number of traditional experimental methods are not very sensitive to the material properties of the tissue itself, particularly in shear. We have, therefore, focused on the development of experimental techniques that are able to separate out the responses in hydrostatic compression and shear.

The primary experimental technique for the measurement of the high-strain-rate behaviour of materials is the Kolsky bar (sometimes called the split-Hopkinson pressure bar). This technique has been widely used for metals and ceramics, but cannot be

used in conventional form for studying soft tissues. We have developed two specialized experimental techniques based on the Kolsky bar for measuring the dynamic properties of human tissues: a confined experiment for measuring the bulk modulus at 100 microsecond time scales, and a double-lap shear configuration for measuring the shear behaviour at high strain rates. These techniques are described in detail by Saraf et al. [1]. In the case of the bulk technique, the specimens are flat discs, while the shear specimens are thin strips. These techniques have been used to study human liver, lung, heart, stomach, and brain tissues. We discuss some of the latter results here.

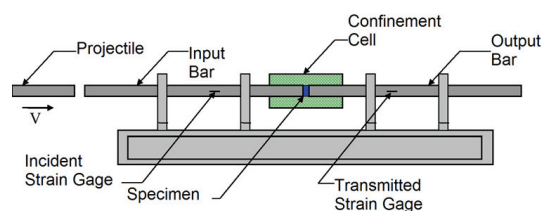


Figure 1. Schematic of the Dynamic Bulk Compressibility Experiment described by Saraf et al., 2007 [1].

The dynamic response of human brain tissues to hydrostatic compression is of interest to simulations of the mechanical loadings and deformations associated with traumatic brain injury. We have compared the behaviours of samples obtained from the cerebrum and cerebellum regions, and find slightly different bulk moduli for the two regions.

### DIFFUSE AXONAL INJURY

Diffuse axonal injury (DAI) accounts for a large percentage of deaths due to brain trauma and is characterized by damage to neural axons. This neural damage occurs primarily in the deep white matter regions of the brain. Understanding this injury therefore requires the understanding of both the constitutive behaviour of white matter and the injury thresholds associated with functional damage of the tissue.

The constitutive description of white matter must take into account the fibrous nature of the tissue. We have chosen to model the tissue as transversely isotropic, using a nonlinear elastic description with a reinforcing strain energy function based on previous work in the literature [4]. The model is fundamentally anisotropic, accounting for the orientation of the fibres. The parameters of the strain energy function are determined by comparing the constitutive description to the available experimental data [2]. We use diffusion tensor imaging data to incorporate the structural orientation of the neural axons into the computational model.

Once the constitutive description of the white matter has been developed, an injury criterion must be specified in order to define an injury model. There are several existing injury models in the literature, primarily based on macroscopic measures such as the acceleration of the head, or based on computed measures such as the von Mises stress or the pressure at a point in the brain as a result of the dynamic loading.

We choose instead to use a cellular injury criterion, based on the fundamental experiments of Bain & Meaney [3] on the tensile strain needed to functionally damage an axon. We relate this cellular injury criterion to the deformation of the tissue by identifying the tensile strain along the fibre direction in the model as the effective axonal strain, and defining that region of the tissue as being damaged when the effective axonal strain reaches a threshold value defined by the experiments of Bain & Meaney.

Using this approach, we are able to identify both the locations of injury and the likelihood of injury through simulations of the brain that incorporate the local fibrous structure through the diffusion tensor imaging data. We show that the degree of injury that is predicted in a computational model of DAI is highly dependent on the incorporation of the axonal orientation information and the inclusion of anisotropy into the constitutive model for white matter.

## DISCUSSION

Both our experiments and our simulations suggest that the dynamic behaviours of tissues and the onset of injury under dynamic loading are the result of the couplings between inertia, wave propagation, constitutive response and cellular organization (and perhaps also subscale phenomena). The importance of inertia in the design and analysis of dynamic experiments on soft tissues should not be underestimated. Further, the order-of-magnitude differences in the compressive and shear responses of soft tissues can lead to the separation of the timescales for injury as a result of pressure and shear loadings,

and can lead to a variety of phenomena that would not appear in static or slow loading problems.

The particular case of brain injury as a result of dynamic loading of the head presents examples of all of the couplings discussed previously. Our analysis suggests that the explicit incorporation of fibre orientation information using diffusion tensor imaging may have promise for the development of improved injury thresholds for automotive, sports and defence applications.

## REFERENCES

1. Saraf H, Ramesh KT, Lennon AM, Merkle AC and Roberts JC. Measurement of the dynamic bulk and shear response of soft human tissues. *Experimental Mechanics* 2007; 47:439-449.
2. Velardi F, Fraternali F and Angelillo M. Anisotropic constitutive equations and experimental tensile behavior of brain tissue. *Biomechanics and Modeling in Mechanobiology* 2006; 5 (1):53-61.
3. Bain AC and Meaney DF. Tissue-level thresholds for axonal damage in an experimental model of central nervous system white matter injury. *Journal of Biomechanical Engineering-Transactions of the ASME* 2000; 122:615-622.
4. Wright R and Ramesh KT, An Axonal Strain Injury Criterion for Traumatic Brain Injury. *Biomechanics and Modeling in Mechanobiology* 2011; in press.

## MODELLING THE ANISOTROPIC BEHAVIOUR OF SKIN

A. Ní Annaidh<sup>1,2</sup>, K. Bruyère<sup>3</sup>, M. Destrade<sup>4</sup>, M. Gilchrist<sup>1,5</sup>, C. Maurini<sup>2</sup>, M. Otténio<sup>3</sup>, G. Saccomandi<sup>6</sup>

1. School of M&ME, University College Dublin; aisling.niannaigh@ucd.ie
2. Institut Jean Le Rond D'Alembert, UMR 7190, CNRS-UPMC, 4 place Jussieu, Paris
3. Université de Lyon, Iftstar, LBMC, Bron, Université Lyon 1, Villeurbanne
4. School of Mathematics, Statistics and Applied Mathematics, NUIG, Galway, Ireland
5. School of Human Kinetics, University of Ottawa, Ontario K1N 6N5, Canada
6. Dipartimento di Ingegneria Industriale, Università degli Studi di Perugia, Perugia, Italy

### INTRODUCTION

The mechanical properties of skin are important for a number of applications including surgery, dermatology, impact biomechanics and forensic science. Skin is a complex multi-layered material which can broadly be divided into two main layers, the epidermis and the dermis. The epidermis consists of cells and cellular debris, and the dermis consists of mostly networks of the fibrous proteins collagen<sup>1</sup>. Collagen fibres govern many of the mechanical properties of soft tissues, in particular their anisotropic behaviour. In order to capture the anisotropic behaviour of soft tissues, modelling now often incorporates a collagen fibre distribution. Here we have developed an automated process for detecting the orientation and distribution of collagen fibres in the dermis using a combination of histological and image processing techniques. Data obtained using this method, together with uniaxial extension tests of excised human skin allow us to evaluate the parameters of the popular Gasser-Ogden-Holzapfel (GOH) anisotropic model<sup>2</sup>.

### MATERIALS AND METHODS

The GOH model applies to incompressible solids with two preferred directions of collagen fibres. The strain energy function can be manipulated to give the following expression for the Cauchy stress,  $\sigma$ .

$$\sigma_{11} = \mu(\lambda_1^2 - \lambda_1^{-2}\lambda_2^{-2}) + 4\mu k_1 \alpha e^{k_2 \alpha^2} [\kappa(\lambda_1^2 - \lambda_1^{-2}\lambda_2^{-2}) + (1-3\kappa)\lambda_1^2 \cos^2 \gamma] \quad \text{Eq.1}$$

$$\sigma_{22} = \lambda_2^2 - \lambda_1^{-2}\lambda_2^{-2} + 4\mu k_1 \alpha e^{k_2 \alpha^2} [\kappa(\lambda_2^2 - \lambda_1^{-2}\lambda_2^{-2}) + (1-3\kappa)\lambda_2^2 \sin^2 \gamma] \quad \text{Eq.2}$$

$$\alpha = \kappa(\lambda_1^2 + \lambda_2^2 + \lambda_1^{-2}\lambda_2^{-2}) + (1-3\kappa)(\lambda_1^2 \cos^2 \gamma + \lambda_2^2 \sin^2 \gamma) - 1$$

When Eq.1 is linearised in the neighbourhood of small strains,  $\lambda_i \approx 1 + \varepsilon_i$ , we find the following expression

for the infinitesimal Young's Modulus in the 1-direction

$$E_1 = \frac{3 + 8k_1(1-3\kappa)^2(1-3\cos^2 \gamma \sin^2 \gamma)}{1 + 2k_1(1-3\kappa)^2 \sin^4 \gamma} \mu \quad \text{Eq.3}$$

Combining Eq.1, Eq.2 and Eq.3;  $\mu$ ,  $k_1$ ,  $k_2$  and  $\lambda_2$  can be obtained through non-linear curve-fitting. The parameter  $\gamma$  refers to the angle between the axis of principle stress and the preferred orientation of collagen fibres and  $\kappa$  the collagen dispersion factor respectively. Both parameters are obtained directly through image analysis of histology slides.

Skin biopsies were procured from samples prior to mechanical testing. Histology slides were stained using Van Gieson which makes collagen appear red/pink. Images were taken of each slide using a Nikon E80i Transmission microscope. The orientation of collagen fibres were then calculated in a fully-automated customised MATLAB routine using the Image Processing Toolbox. A brief algorithm is given below and the main steps of the algorithm are illustrated in Fig.1.

- The RGB image was converted to a binary image where white pixels indicate collagen and black pixels for all other areas.
- After thinning operations, individual fibres bundles are identified using *bwlabel*.
- An ellipse was approximated about each fibre bundle and the orientation of the major axis of each ellipse was calculated.
- The dispersion factor<sup>2</sup>,  $\kappa$ , was then calculated assuming a Von Mises distribution,  $\rho(\theta)$ , where  $\theta$  is the orientation of individual collagen bundles.

$$\kappa = \frac{1}{4} \int_0^\pi \rho(\theta) \sin^3 \theta d\theta \quad \text{Eq.4}$$

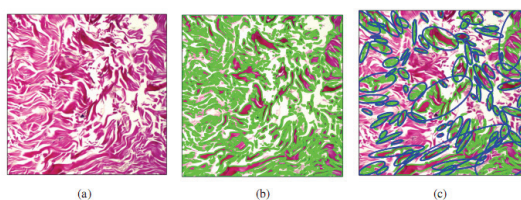


Fig.1 (a) Original histology slide. (b) All identified collagen bundles outlined in green (c) Best fit ellipse about each fibre bundle.

## RESULTS

The mean collagen dispersion,  $\kappa$ , was calculated to be  $0.2553 \pm 0.0232$ , where a value of 0.3333 indicates complete isotropy and a value of 0 indicates transverse isotropy. Fig.2 illustrates the fit between the experimental data obtained through uniaxial extension tests, and the model prediction. Table 1 displays the evaluated model parameters.

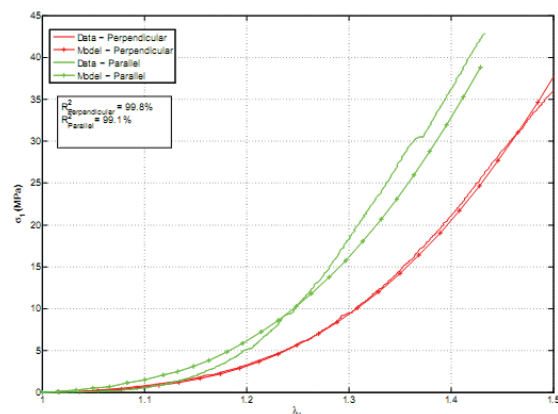


Fig.2: Comparison of a skin sample parallel to the Langer lines and perpendicular to the Langer lines (i.e. with two different mean orientations,  $\theta$ ), and their fit to the GOH model.

Table 1: Values obtained through curve-fitting for the parameters  $\mu$ ,  $k_1$ ,  $k_2$ . Also displayed is the  $R^2$  a measure of goodness of fit, and  $\gamma$  and  $\kappa$  which were calculated directly from the automated image analysis technique.

Orientation of Langer lines	$\mu$ MPa	$k_1$	$k_2$	$\kappa$	$\gamma$ °	$R^2$ %
Perpendicular	0.7861	97.51	0.1	0.2752	50	99.8
Parallel	0.7861	97.51	0.1	0.2414	43	99.1

## DISCUSSION

In this study we have developed a simple automated process which can detect the orientation of collagen fibres. This technique can be easily implemented in MATLAB and can be adapted to detect other biological features, such as certain cells, leading to applications in diagnostics. We have applied this technique to skin biopsies and provided new quantitative data on the orientation of collagen fibres in the human dermis. So far, the availability of

accurate structural data has lagged behind the progress of anisotropic constitutive modelling. Here we have provided the structural data required to accurately make use of advances in constitutive modelling, and help fill the void of experimental data. The model parameters of the GOH model have been evaluated for skin using experimental data. These sets of parameters will provide invaluable data for those wishing to model the anisotropic behaviour of skin.

## REFERENCES

1. G. L. Wilkes, I. A. Brown and R. H. Wildnauer. *The biomechanical properties of skin*. CRC Critical Reviews in Bioengineering 1973, vol:1(4).
2. Gasser, T., R. Ogden, Holzapfel, G. Hyperelastic modelling of arterial layers with distributed collagen fibre orientations. *Journal of the Royal Society Interface* 2006; vol: 3:15-35

## EXPERIMENTAL CHARACTERIZATION OF THE MECHANICAL PROPERTIES OF THE SUPERIOR SAGITTAL SINUS – BRIDGING VEIN COMPLEX

K. Baeck<sup>1</sup>, A. Asiminei<sup>2</sup>, E. Verbeken<sup>3</sup>, J. Goffin<sup>2</sup>, J. Vander Sloten<sup>1</sup>

1. Division of Biomechanics and Engineering Design, K.U.Leuven, Belgium, Katrien.Baeck@mech.kuleuven.be
2. Division of Experimental Neurosurgery and Neuroanatomy, K.U.Leuven, Belgium
3. Morphology and Molecular Pathology Section, K.U.Leuven, Belgium

### INTRODUCTION

Next to skull fracture and brain contusion, one of the most frequent head injuries in bicycle related accidents is acute subdural hematoma (ASDH) <sup>[1]</sup>. An ASDH can develop through three different mechanisms where rupture of a bridging vein (BV), connecting the cortex to one of the draining venous sinuses, is one. Finite element head models <sup>[2]</sup> are nowadays widely used to study the mechanisms of ASDH but an accurate description of the BV material behaviour is currently missing. Therefore, to understand the biomechanical etiology of ASDH and BV rupture and to support the design of FE head models, an accurate characterization of the BV material failure properties is essential.

The objective of this study is to determine the BV material properties under axial loading conditions at high strain rates and to investigate a possible gender variation and strain rate dependency in their failure mechanism.

### MATERIALS AND METHODS

A total of 63 BV-units were dissected from the cerebral hemispheres of 6 fresh cadavers of both sexes (4 male, 2 female), with ages ranging from 72y.o. to 92y.o. and without medical history of vascular pathology. The dissections were performed under permanent perfusion of physiological saline solution and at maximum 5 days post mortem to ensure the preservation of the biological tissue quality. Each dissected BV-unit included a small strip from the superior sagittal sinus (SSS) attached to the vein. Prior to experiments, the geometrical parameters of the SSS-BV junction (wall thickness and width of the BV and SSS) were measured on stereomicroscopy images obtained for each specimen. Subsequently, 46 BVs were clamped at both ends using laparoscopy surgical clamps and stretched until failure at high strain rates ( $14.28 \pm 5.26\text{s}^{-1}$ ) using a BOSE test bench as shown in figure 1. To verify a uniform deformation and no

slippage of the specimens, all tests were recorded using a high-speed video camera (MotionXtra<sup>®</sup> HG-100K).

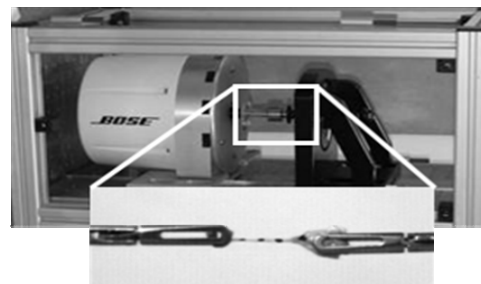


Figure 1: Bose test bench with close up of a BV-SSS unit between surgical clamps

For every BV test, the time, load and displacement data were recorded at 4 kHz sampling frequency and further processed using Matlab software to calculate the biomechanical parameters: ultimate stress and strain, yield stress and strain and Young's modulus. The ultimate stress  $\sigma_u$  and strain  $\epsilon_u$  were calculated at the point of maximum axial load whereas the yield stress  $\sigma_Y$  and strain  $\epsilon_Y$  were calculated for the point of maximum Young's modulus as shown in figure 2.

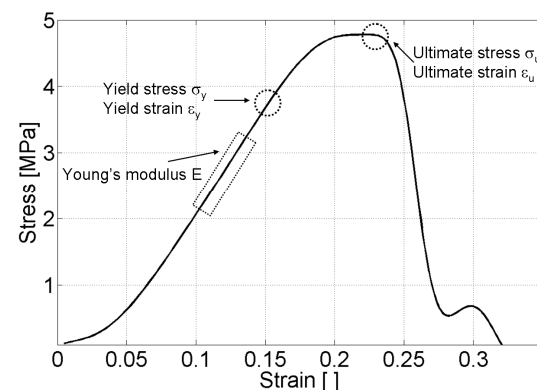


Figure 2: Typical stress-strain curve used for further calculation of the mechanical parameters

## RESULTS

Due to technical problems during the microscopy stage, no microscopic images were available for 5 dissected veins. For the remaining 58 dissected bridging veins (20 female and 37 male), the geometrical description in terms of BV width and wall thickness was obtained and listed in table 1 for both male and female specimens. The biomechanical parameters: ultimate stress and strain, yield stress and strain and Young's modulus were determined for 40 successful BV tests based on the obtained stress strain curves and they are also listed per gender in table 1. BV tests where slippage or failure due to the surgical clamps occurred were rejected from the dataset.

Table 1: Experimental test results

<b>BV geometry</b>	<b>Female</b>	<b>Male</b>
BV width [mm]	2.43±1.16	3.56±1.32
BV wall thickness [mm]	0.049±0.023	0.039±0.011
<b>BV material</b>	<b>Female</b>	<b>Male</b>
Young modulus [MPa]	28.35±19.64	26.65±15.18
Yield stress [MPa]	1.36±1.13	1.17±0.74
Yield strain [%]	8.99±5.75	6.85±5.63
Ultimate stress [MPa]	4.48±2.09	2.99±1.38
Ultimate strain [%]	28.9±12.53	23.81±10.29

## DISCUSSION

A gender influence is seen in both the BV's geometry and the calculated mechanical parameters. The average cross sectional area of male BVs is larger than female BVs which lead to higher mechanical failure parameters for female than male BVs.

For all the tested veins at high strain rates ( $14.28 \pm 5.26s^{-1}$ ) presented in table 1, the results in terms of Young's modulus, ultimate stress and strain are in the same range as the reported values in literature<sup>[3,4]</sup> on low strain rate ( $1.32 \pm 1.12s^{-1}$ ) BV tests. A substantial difference was however observed for the yield stress and strain between high and low strain rate BV tests. The high inter- and intra-individual variability of the BV specimens (size, origin, etc.) can be the first cause for the observed differences. A second cause could be the definition of the yield point (point of maximum Young's modulus) which might not be the most appropriate one to describe soft tissue material behavior. Based on the presented results, the differences between the biomechanical parameters of low<sup>[3,4]</sup> and high strain rates are not large enough to conclude a strain rate dependency of the BV material properties.

A failure of the SSS-BV complex occurred in 80% off the BV tests along the vein lumen and for only 8 cases, the failure was localised close to the SSS, which supports previously published histological

observations<sup>[5]</sup> describing a unique and stronger architecture for this SSS region.

## CONCLUSION

The paper presents the biomechanical behaviour of the SSS-BV complex at high strain rates. The microscopy method, applied to visualize the BV specimens, is a new approach to describe the SSS and BV geometry and allows for further estimation of the regional mechanical parameters and gender differences.

A gender influence was seen in both the BV's geometry and the calculated mechanical parameters. The comparison of the presented data at high strain rates with low strain rate data was made, but a strain rate dependency could not yet be concluded. Therefore, more BV tests at even higher strain rates are required to give a final conclusion.

## REFERENCES

1. Depreitere B, Van Lierde C, Maene S, et al. Bicycle-related head injury: a study of 86 cases. *Accid Anal Prev* 2004; 36:561-567.
2. Horgan TJ and Gilchrist MD, The creation of three-dimensional finite element models for simulating head impact biomechanics. *Int J of Crashworthiness* 2003; 8:353-366.
3. Delye H, Goffin J, Verschueren P, Vander Sloten J, Van der Perre G, et al., Biomechanical properties of the superior sagittal sinus-bridging vein complex. *Stapp Car Crash J* 2006; 50:625-636.
4. Monson KL, Goldsmith W, Barbaro NM, Manley GT, Significance of source and size in the mechanical response of human cerebral blood vessels. *J Biomech* 2005; 38:737-744.
5. Pang Q, Lu X, Gregersen H, von Oettingen G and Astrup J, Biomechanical properties of porcine cerebral bridging veins with reference to the zero-stress state. *J Vasc Res* 2001; 38:83-90.

## MODELLING THE IMPACT RESPONSE OF CRANIAL BONE

Julie Motherway, M.D. Gilchrist

University College Dublin; Julie.Motherway@ucd.ie, Michael.Gilchrist@ucd.ie

### INTRODUCTION

Linear and depressed skull fractures are frequently mechanisms of head injury and are often associated with traumatic brain injury. Accurate knowledge of the fracture of cranial bone can provide insight into occurrences of lesions of soft neural tissue and can help in designing energy absorbing head protection systems and safety helmets. Cranial bone is a complex material comprising of a three-layered structure: external layers consisting of compact, high-density cortical bone and a central layer consisting of a low-density, irregularly porous structure.

Human cranial bone has previously been tested in compression, tension and bending. The majority of these studies concentrate on fetal cranial bone at quasi-static testing speeds. However, fetal and adult cranial bones are vastly different materials. Fetal cranial bone is a thin, non-homogeneous cortical bone layer with a highly directional fibre orientation [1]. Mature adult cranial bone has stiff outer cortical strata and an inner energy absorbing porous lightweight core, the diploë. Thus the elastic modulus of adult cranial bone is higher [2] and the diploë acts to increase its thickness thereby increasing its bending strength. Furthermore, the diploë is an efficient energy absorbing layer and stiffens the whole sandwich structure. The aim of this study is to characterize the response of adult cranial bone in bending under dynamic impacts and to use that information to validate high resolution finite element simulations of the tests.

### MATERIALS AND METHODS

Adult cranial bone specimens were extracted from the parietal and frontal cranial bones of 8 cadaver subjects (F=4, M=4; 81±11 years old). 63 specimens (6 cm×1 cm) were obtained from the parietal and frontal bones. Prior to testing, specimens were scanned using a  $\mu$ CT scanner.

The specimens were tested in three-point bend set-up at dynamic speeds (0.5, 1 and 2.5 m/s), Figure 1. Each test was captured using high-speed video and the

corresponding force-deflection curves recorded. The mechanical properties that were calculated for each specimen included: the sectional elastic modulus, the maximum force at failure, the energy absorbed until failure, the average strain rate and the maximum bending stress.

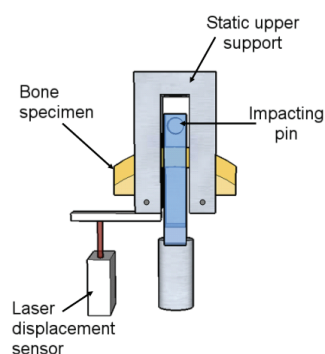


Figure 1: The experimental 3-point bend test set-up.

Structurally detailed, specimen-specific 3D finite element (FE) models of the dynamic tests were developed from the  $\mu$ CT data using Simpleware software. The models were run using Abaqus 6.9-1 on a high performance computer cluster (ICHEC). The models were fully verified and validated against the experimental results according to best practises outlined in the literature [3-5]. A full convergence study of the meshes produced was completed and the sensitivity of the models to the boundary conditions, material type and element type were also explored.

### RESULTS

The force-displacement curve of each test was recorded, Figure 2. The calculated mechanical properties were consistent with those previously reported in the literature. The cranial bone was significantly stiffer at the higher strain rates. The cranial sampling site was also a significant factor in the resulting mechanical properties. More details can be found in a paper by Motherway et al. [6].

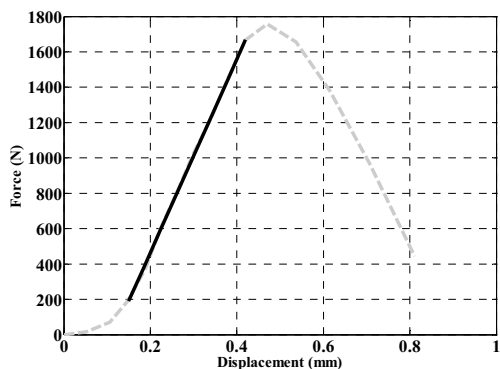


Figure 2. Measured force-displacement graph for a cranial specimen tested at 2.5m/s

It was possible to produce high quality FE meshes of the specimens from  $\mu$ CT data, Figure 3. Full convergence studies were carried out and a number of material models were examined. The failure of the bone specimens were compared to the FE models.

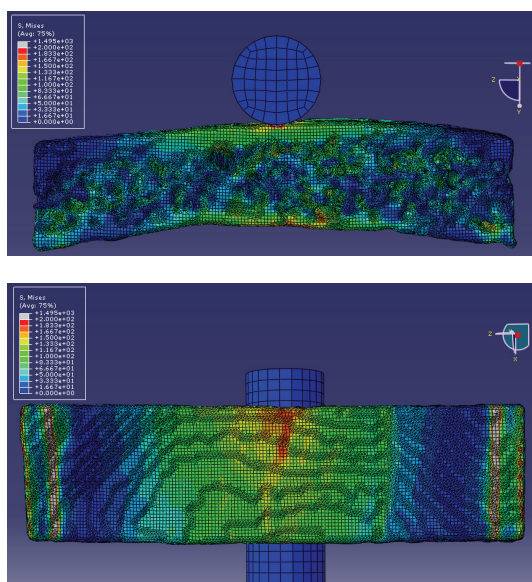


Figure 3. A deformed finite element model of a specimen tested at 2.5m/s.

Of the material models tested, a model by Carter and Hayes [7] shows the most promising results. The Carter and Hayes model allows for the calculation of a linear elastic modulus taking into account strain rate and the ash density:

$$E = 3790 \dot{\epsilon}^{0.06} \rho^3$$

The density was calculated from the  $\mu$ CT scan sets and related to density using a calibration phantom. The Poisson's ratio was set at 0.3.

## DISCUSSION

High resolution finite element models were fully verified and validated against an experimental study. It was found that these models could provide useful insight into the failure of cranial bone specimens under bending. The results from this work can be used to improve the skull material and failure definitions in the UCD 3D-FE model of the skull-brain complex, currently used to aid helmet design.

## ACKNOWLEDGEMENTS

The authors wish to acknowledge the SFI/HEA Irish Centre for High-End Computing (ICHEC) for the provision of computational facilities and support.

The authors also wish to acknowledge the help of Dr. P. Verschueren, Prof. G. Van der Perre and Prof J. Vander Sloten from the Division of Biomechanics and Engineering Design, K.U. Leuven, Belgium with the experimental aspects of this work.

## REFERENCES

1. McPherson, G. K., Kriewall, T. J., The elastic modulus of fetal cranial bone: A first step towards an understanding of the biomechanics of fetal head molding. *Journal of Biomechanics* 1980; 13: 9-16.
2. Margulies, S. S., Thibault, K. L., Infant skull and suture properties: Measurements and implications for mechanisms of pediatric brain injury. *Journal of Biomechanical Engineering* 2000; 122: 364-371.
3. Anderson, A.E. et al., Verification, Validation and sensitivity studies in computational biomechanics. *Computer Methods in Biomechanics and Biomedical Engineering* 2007; 10: 171-184.
4. Oberkampf, W.L. et al., Verification, validation, and predictive capability in computational engineering and physics. Presented at: *Foundations for Verification and Validation in the 21<sup>st</sup> Century Workshop* 2002, Johns Hopkins University, Laurel, Maryland.
5. ASME Committee (PT60) on Verification and Validation in Computational Solid Mechanics, Guide for verification and validation in computational solid mechanics. *American Society of Mechanical Engineers*, 2006.
6. Motherway, J.A., Verschueren, P., Van der Perre, G., Vander Sloten, J., Gilchrist, M.D., The mechanical properties of cranial bone: The effect of loading rate and cranial sampling position. *Journal of Biomechanics* 2009; 42: 2129-2135.
7. Carter, D.R. and Hayes, W.C., The compressive behavior of bone as a two-phase porous structure. *The Journal of Bone and Joint Surgery* 1977; 59:954-962.

## A NEW METHOD TO DETERMINE THE YOUNG'S MODULUS FROM FRESH BONE FLAPS

Esmeralda Forausbergher<sup>1</sup>, Hans Delye<sup>2</sup>, Jos Vander Sloten<sup>1</sup>, Jan Goffin<sup>2</sup>, Georges Van der Perre<sup>1</sup>

1. Division of Biomechanics and Engineering Design, K.U.Leuven, Belgium – [esmeralda.forausbergher@mech.kuleuven.be](mailto:esmeralda.forausbergher@mech.kuleuven.be)
2. Division of Experimental Neurosurgery and Neuroanatomy, K.U.Leuven, Belgium

### INTRODUCTION

A prediction tool such as a finite element model should have all the input elements defined as well as possible for the result to be reliable. Beside geometry, boundary conditions and loading, the material definition plays a major role for the reliability of the finite element model outcome. For a finite element model of the head, there are a number of materials that have to be characterized i.e. brain tissue, bridging veins, skull bone etc. The focus of this particular work is on the skull bone.

The properties of an adult human skull are well documented, however *in vivo* data are seldom and mostly they concern the auditory response of the skull or stresses related to mastication [1,2].

The most established methods to extract the elastic modulus of the bone are destructive such as the three point bending test. None the less, the results from such tests are reliable for the given specimens. However, these specimens are embalmed or fresh frozen but never fresh.

In case of child skull bone, the data is very scarce in literature [3-9]. Given the limited number of child cadavers, some of the research has been focused on failure test of animal skull bone. Using such an animal model makes the examination of time-bound changes in skull bone properties possible. However, the extrapolation to human situation is not straight forward [8].

This research presents a vibration based non destructive method to assess the elasticity modulus  $E$  of skull bone flaps.

### MATERIALS AND METHODS

This method is a combination of experimental and computational tools. The test equipment, presented in figure 1, consists of a fixing device which

is attached to a small shaker, small (2g) PCB accelerometers, amplifier and the Pimento testing system (LMS<sup>®</sup>). All the equipment that comes in touch or close to the bone flap is sterilized prior to testing.

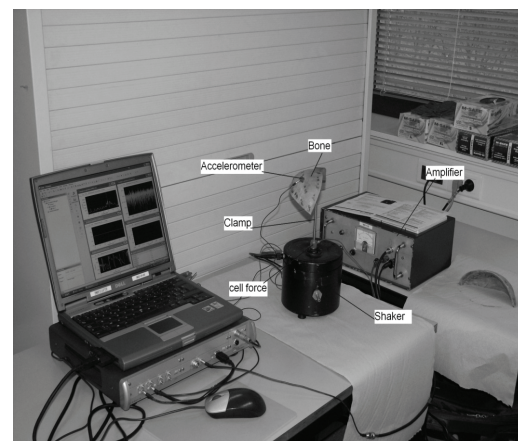


Figure 1: Test set-up

The accelerometers are attached to the bone flap which is then fixed to the shaker and excited. The input and response vibrations are recorded, frequency response function is computed and an experimental modal analysis (EMA) is performed.

A finite element model (FEM) of the bone flaps is extracted from the patient's CT after the operation. To this bone mesh, a mesh of the fixing clamp is attached and then boundary conditions are applied.

A finite element modal analysis (FEMA) is performed and the results are compared with results from the EMA. The Young's modulus of each specimen is then estimated by numerically optimizing the Young's modulus of each model so that simulation results matched with corresponding experimental data.

## RESULTS

A summary of the results from the tested bone flaps during surgery are presented in table 1. The number of patients is not enough for a valid statistical analysis. As it can be seen, infant bone density is lower than adult density and the same also holds for the Young's modulus.

Table 1: Results from tested bone flaps during surgery

	Sex	Age	Density (g/cm <sup>3</sup> )	E (Mpa)
P1	M	53 y.o.	1.512	3750
P2 – in1-1	F	5 m.o.	0.6028	30
P2-inf1 – 2	F	5 m.o.	0.6975	40
P3	F	69 y.o.	1.958	11000
P4	F	72 y.o.	1.141	2000
P5-inf2	M	4.4 m.o.	0.1888	30

## DISCUSSION

As expected, Young's modulus of infant skull bone is around three orders of magnitude lower than that of an adult. The skull bone density of a child is around one third of the density of an adult bone. The limited number of tests to date does not allow for a significant statistical analysis with respect to the evolution in time of the E modulus. However, we are confident that by using this technique we will be able to gather further information about age dependency of bone properties. Therefore, we proposed in this work a new non-destructive technique for the evaluation of fresh bone E modulus.



Figure 2. MD using the test set-up

As the equipment can be entirely sterilized, the duration of the measurement itself is very short and the manipulation of the bone flaps and accelerometer can be easily performed by a medical doctor (MD) (figure 2). Therefore, this technique was successfully used during head surgeries.

## REFERENCES

1. Endo B. Experimental studies on the mechanical significance of the form of the human facial skeleton. *J Faculty Sci Univ Tokyo* 1966; 3:1–101.
2. Endo B. Analysis of stresses around the orbit due to masseter and temporalis muscles respectively. *Am J Anthropol Soc Nippon* 1970; 78:251–266.
3. Kriewall TJ. Structural, Mechanical, and Material Properties of Fetal Cranial Bone. *Am. J. Obstet. Gynecol.* 1982; 143:707–714.
4. Kriewall TK et al. Bending Properties and Ash Content of Fetal Cranial Bone. *J. Biomech.* 1981; 14:73–79.
5. McPherson GK and Kriewall TJ. The Elastic Modulus of Fetal Cranial Bone: A First Step Towards an Understanding of the Biomechanics of Fetal Head Molding. *J. Biomech.* 1980; 13:9–16.
6. Gefen A, Gefen N, Zhu Q, Raghupathi R and Margulies SS. Age-dependent changes in material properties of the brain and braincase of the rat. *J Neurotrauma* 2003; 20(11):1163-77.
7. Margulies SS and Thibault KL. Infant skull and suture properties: measurements and implications for mechanisms of pediatric brain injury. *J Biomech Eng.* 2000; 122(4):364-71.
8. Coats B and Margulies SS. Material properties of human infant skull and suture at high rates. *J Neurotrauma.* 2006; 23(8):1222-32.
9. Prange MT, Luck JF, Dibb A, Van Ee CA, Nightingale RW and Myers BS. Mechanical Properties and Anthropometry of the Human Infant Head. *Stapp Car Crash Journal*, 2004; 48:279-299.

## MECHANICAL PROPERTIES OF BRAIN TISSUE IN TENSION AT HIGH STRAIN RATES

Badar Rashid<sup>1</sup>, Michel Destrade<sup>2,1</sup>, Michael Gilchrist<sup>1,3</sup>

<sup>1</sup>School of Electrical, Electronic, and Mechanical Engineering, University College Dublin, Belfield, Dublin 4, Ireland

<sup>2</sup>School of Mathematics, Statistics and Applied Mathematics, National University of Ireland Galway, Galway, Ireland

<sup>3</sup>School of Human Kinetics, University of Ottawa, Ontario K1N 6N5 Canada

### INTRODUCTION

During the last decade, 3D FE models have been developed by various researchers which contain detailed geometric descriptions of anatomical features of the human head, in order to investigate internal dynamic responses to multiple loading conditions. Fidelity of these models, however, is highly dependent on the accuracy of the material properties used to model biological tissues.

In this study extensive tensile experiments were performed on porcine brain tissue at high strain rates of 30 - 90 s<sup>-1</sup>. The precise determination of material parameters at high strain rates would be more suitable during finite element analysis to predict brain injuries due to TBI.

### MATERIALS AND METHODS

Eight fresh porcine brains were collected from a local slaughter house and preserved in physiological saline solution at 4 to 6°C prior to being within six hours of post-mortem. All brain samples (mixed white and gray matter) were extracted perpendicular to the sagittal plane randomly from the cerebral cortex and corpus callosum regions in order to determine average properties of brain tissue (Fig. 1). All samples were prepared and tested at 22°C. Ten tensile tests were performed at each loading velocity of 120, 240, 360 and 480 mm/s corresponding to strain rates of 30, 60, 90 and 120 s<sup>-1</sup> respectively, in order to analyze the strain rate dependency of brain tissue in extension.

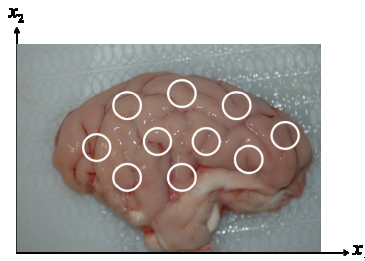


Fig. 1 Locations of sample extractions.

### CONSTITUTIVE MODELS

During the tension tests, the principal stretch ratio  $\lambda$  was calculated from the measure of the elongation  $e$

using equation:  $\lambda = 1 + e$  and for compression tests,  $\lambda = 1 - e$ . The nominal /Lagrange stress  $S_{11}$  was evaluated as  $S_{11} = F / A$ , where  $F$  is the tensile or compressive force, as measured in Newtons by the load cell, and  $A$  is the area of a cross section of the sample in its undeformed state. The experimentally measured nominal stress was then compared to the predictions of the hyperelastic models from the relation  $S_{11} = -S_{11} = -\frac{d\tilde{W}}{d\lambda}$ ,

#### Fung Strain Energy Function

The Fung strain energy is often used for the modelling of soft biological tissues. It depends on the first strain invariant only, as

$$W(I_1) = \frac{\mu}{2b} \left[ e^{b(I_1-3)} - 1 \right] \quad (1)$$

$$S_{11} = \mu e^{b(\lambda^2+2\lambda^{-1}-3)} (\lambda - \lambda^{-2}) \quad (2)$$

#### Gent Strain Energy Function

The Gent strain energy describes rapidly strain-stiffening materials in a very satisfying way. It also depends on the first strain invariant only, as

$$W(I_1) = -\frac{\mu}{2} J_m \ln \left( 1 - \frac{I_1 - 3}{J_m} \right) \quad (3)$$

$$S_{11} = \frac{\mu J_m}{J_m - \lambda^2 - 2\lambda^{-1} + 3} (\lambda - \lambda^{-2}) \quad (4)$$

#### Ogden Strain Energy Function

Soft biological tissue is proven to be represented well by the Ogden formulation and most of the mechanical test data available for brain tissue in the literature are fitted with an Ogden hyperelastic function (Ogden 1972). The one-term Ogden hyperelastic function is given by

$$W = \frac{2\mu}{\alpha^2} (\lambda_1^\alpha + \lambda_2^\alpha + \lambda_3^\alpha - 3) \quad (5)$$

$$S_{11} = \frac{2\mu}{\alpha} \left\{ \lambda^{\alpha-1} - \lambda^{-\left(\frac{\alpha}{2}+1\right)} \right\} \quad (6)$$

Here in each case  $\mu > 0$  (infinitesimal shear modulus) and  $b, J_m, \alpha$  are stiffening parameters.

## RESULTS

Ten uniaxial tensile tests were conducted on cylindrical porcine brain samples at each strain rate. The tissue specimens with an initial thickness of  $4.0 \pm 0.1$  mm were fully stretched approximately up to 2.4 mm, thus producing 60% strain. The average of ten tensile experiments at each strain rate was taken and stress behaviour was analyzed (Fig. 2). The deformation encountered in very soft tissue biomechanics never exceeds strain levels of about 30%. Beyond this limit tissues suffer permanent damage Miller (2001). Moreover, we have also observed that the maximum stress is approximately at 32% strain, which shows that the brain tissue is damaged permanently at this strain.

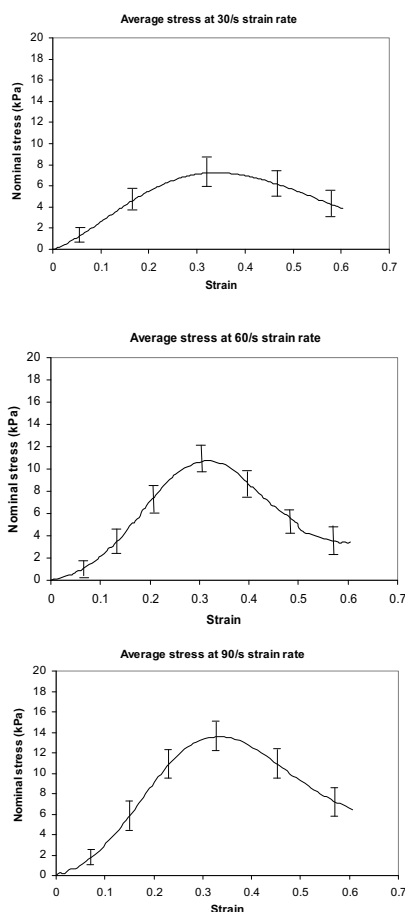


Fig. 2 Average of ten uniaxial tensile tests at each strain rate.

To investigate the combined behaviour of brain tissue in compression and tension, the compression data up to 30% (tests performed earlier) and the tensile data up to 30% strain only was used for the curve fitting of strain energy functions. Excellent agreement of experimental data to two terms Ogden model is

achieved ( $R^2 \approx 0.9992$ ) at all strain rates (Fig. 3). Other models have not been mentioned to achieve brevity.

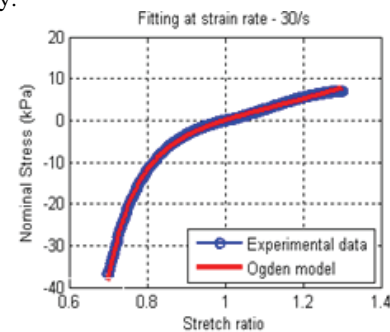


Fig. 3 Fitting of Ogden at 30/s strain rate to compression and tension data.

After curve fitting process, the material parameters ( $\mu_1 = 6.0623$  kPa,  $\mu_2 = 3.8794$  kPa,  $\alpha_1 = 4.604$ ,  $\alpha_2 = -9.021$ ) were derived, which can be used for the finite element analysis. Similarly, procedure was also adopted for 60 and 90/s train rate.

## DISCUSSION

In this research we have accurately determined the mechanical properties of porcine brain tissue simultaneously from the combined experimental data (tension + compression) up to 30% strain at strain rates of 30, 60 and 90  $s^{-1}$  (known thresholds of axonal injury). The results obtained from *in vitro* experiments showed that the deformation of porcine brain tissue is quite different under compression and tension.

Moreover, it was observed that the maximum average stress in compression was approximately five times higher than in tension at the same strain (30%) and strain rates (30, 60 and 90/s). The maximum nominal stress up to 30% strain at strain rates of 30, 60 and 90  $s^{-1}$  in compression was  $35.54 \pm 6.33$ ,  $51.34 \pm 7.53$  and  $66.0 \pm 8.25$  kPa (mean  $\pm$  SD) and in tension was  $7.25 \pm 0.60$ ,  $10.8 \pm 1.45$ ,  $13.58 \pm 1.44$  kPa (mean  $\pm$  SD) respectively. The material parameters determined after fitting of various strain energy functions to experimental data would be very useful for the biofidelic finite element human head models to predict brain injuries under impact conditions.

## REFERENCES

1. Miller K. How to test very soft biological tissues in extension? J Biomech; 2001, 34: 651– 657.
2. Ogden R. W. Large deformation isotropic elasticity - on the correlation of theory and experiment for incompressible rubber like solids, Proceedings RSL Series A, Vol. 326, No. 1567 (Feb. 1, 1972), pp. 565-584.

## BIOMECHANICS OF TRAUMATIC BRAIN INJURIES AND HEAD INJURY CRITERIA

Svein Kleiven

Royal Institute of Technology, Stockholm, Sweden; sveink@kth.se

### INTRODUCTION

If no new actions are initiated, the incidence of traffic related accidents worldwide is expected to be ranked the third most common disease in all categories within two decades. Consequences of head injuries are not limited to the victim alone but have impact on the society as a whole through the large costs involved, not to mention the tragedies and the suffering. It should be noted that very little is understood about the true mechanisms associated with head injury, but many theories exist. The biomechanics of the human head can be seen as a motion of the brain inside an externally loaded skull. At present, mainly a one-dimensional criterion, named the Head Injury Criterion (HIC), is used in the development of safety devices, where a rigid dummy head is launched towards specific locations in the car. However, the human head behaves in a more complex way. One of the advantages with the finite element (FE) method is the possibility to model the anatomy with great detail, thus it is possible to study the kinematics of the head as well as the stresses and strains in the Central Nervous System (CNS) tissues.

### MATERIALS AND METHODS

When evaluating the consequences of an impact to the head, different injury criteria are used. However, present injury criteria do not account for rotational or directional dependency. This paper primarily focuses on summarizing current efforts, and to outline future strategies in human head injury prediction. The influence of inertial forces to all the degrees of freedom of the human head was evaluated with a detailed FE model. Also, evaluation of existing and proposed head injury criteria was performed. The models were used to investigate the differences in terms of strains in the brain, due to variation in impact direction and duration.

### RESULTS AND DISCUSSION

Various local tissue predictors for traumatic brain injuries (TBI) have been evaluated based upon FE modelling of sports accidents, experiments on brain tissue cultures, and FE modelling of animal experiments. However, several different local injury metrics are promoted, and the combined results are inconclusive. The maximal principal strain has usually been chosen as a predictor of diffuse axonal injuries, as well as for mechanical injury to the blood-brain barrier. Other local brain tissue injury measures have also been proposed and evaluated, such as von Mises stresses, product of strain and strain rate, strain energy, and the accumulative volume of brain tissue enduring a specific level of strain, the Cumulative Strain Damage Measure (CSDM). Since so many local brain injury measures are proposed, a thorough evaluation of the correlation between brain injury and some specified local threshold was performed. Detailed FE models of the adult human head were imposed the kinematics of 58 sports accidents. A reconstruction of a motocross accident was also performed. This accident was well documented by motion pictures, which simplified the reconstruction. Also, CT images of the injured driver were available. It was possible, through this reconstruction, to recreate the injury pattern in the brain of the injured rider. Further on, this study underlines earlier findings that the local brain injury measures are very sensitive to the choice of stiffness for the brain tissue. With a proper understanding of the mechanisms following trauma to the human brain, better protective systems such as helmets can be developed.

## THE EGG INJURY CRITERION

CAN WE LEARN MORE ABOUT HEAD INJURY WITH AN EGG SURROGATE?

Wen Yang<sup>1</sup>, Tania Adithama<sup>1</sup>, Shrey Makkar<sup>1</sup>, Wenting Wang<sup>1</sup>, Andrew Short<sup>1,2</sup>

1. University of Melbourne, Biomedical Engineering Department, ashort@dvexperts.net
2. BioForensic Consulting, Melbourne

### INTRODUCTION

Head Injury Criteria (HIC) has been developed to predict the probability of life threatening head injury from a particular impact<sup>1,2,3 & 4</sup>. However, HIC mainly predicts fracture and sports injuries such as concussion are becoming more prominent which may require another predictor. In a two stage process this abstract considers impact speed as an injury predictor. Then on-line video could be used to consider impact speed as a predictor for concussion.

Although it is an important and widely utilized benchmark, there are some limitations to the HIC as human concussion is not well predicted and calculations as they are complex and require human tissues and expensive equipment. From the study performed by Prasad and Mertz in 1985<sup>1</sup>, an S-shaped HIC curve was selected to be the best fit because it can be used for both skull fracture and brain damage. However in terms of an R<sup>2</sup> parameter, it does not fit the raw data well. Additionally, the cumulative curve is just an empirical output which has no clear underlying analytical understanding of system.

In order to consider an alternative method that is simple statistical and based on drop height (or impact speed) egg surrogates were used. Eggs were chosen due to the similarity of shape and physical properties between eggs and human heads. In addition, many tests can be rapidly performed without an ethical barrier. Injury type from different drop heights was recorded. The cumulative curve for egg data exhibits a similar trend as Prasad's results. This supports the egg as a suitable alternative experimental candidate to study HIC. A graph of percentage of linear and non-linear injury against dropping height was drawn and it was noticed that the shape of two curves seemed to match a normal distribution within error bounds. This offers a mathematical method to model a large variety of random variables with one statistical analysis. With further study and if more data can be obtained, a probability model of head injury can be developed.

### MATERIALS AND METHODS

Egg samples used in the experiment were purchased from local market of two different brands; caged and free range. The size and weight of each sample was measured prior to the experiment. No protective layer was used to minimize the test surface. Multiple eggs were dropped from each of a number of different heights. The fracture type were recorded for each drop height.

### RESULTS

An egg injury scale (EIS) was created for the purposes of the experiments performed, and is summarized in the Table 1. In the case where more than one fracture type is observed, only the more severe one was taken into account.

Table 1. EIS categorization

EIS	Description
1	Linear Fracture
2	Ringed Fracture
3	Depressed Fracture
4	Yolk broken

Given that different parameters are presented, it is assumed that impact speed in collision is acceleration. It can be seen in Figure 1(b) that the profile of the cumulative probability of a more severe injury occurring at increasing drop height is very similar to the one obtained for the skull (Figure 1a). This shows that the egg is indeed a good surrogate of the head and can be used to obtain general trends. Additionally, the similarity between the two graphs also shows that differences in the physical properties of the egg do not affect the shape of the graph. There has been extensive research done on formulating general expressions for various features of the head such as skull thickness, brain size and head diameter [3, 4], but the injury profile of the eggs have shown physical properties does not affect the trend of the curve and that they

may be a worthwhile surrogate. This is a significant finding as it will shift the focus of research in many automotive industries.

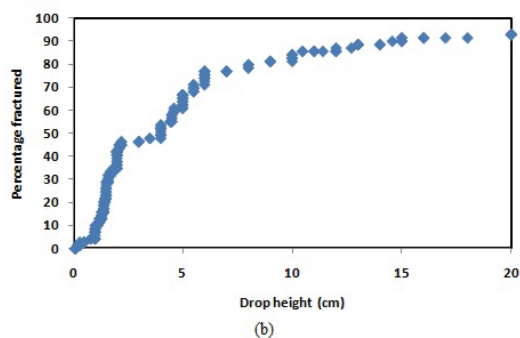
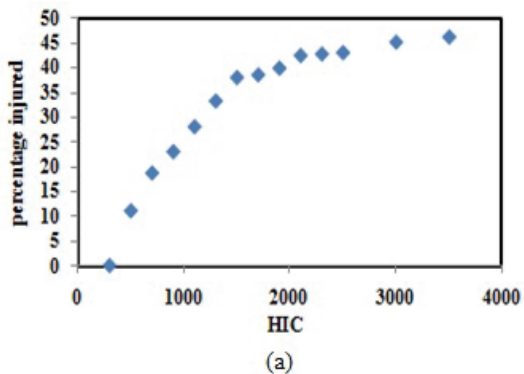


Figure 1. The cumulative curve of a) the percentage of injury against HIC (Prasad); b) the percentage of fracture against egg drop height in our experiments.

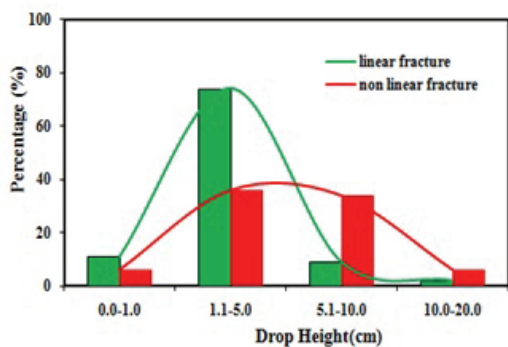


Figure 1. The graph of percentage linear and non-linear (EIS 2+) fracture against drop height

While there is limited data available Figure 2 shows that a normal distribution could model this data. For instance, the system can be described in terms of its normal distribution function

$$f(x) = \frac{1}{\sqrt{2\pi\sigma^2}} e^{-\frac{(x-\mu)^2}{2\sigma^2}}$$

where  $\sigma^2$  is the variance  $\mu$  is the mean of the system

For the linear case, this was found to be:

$$f(x_L) = 0.19e^{-\frac{(x-2.81)^2}{8.90}}$$

And for the non-linear case the expression was

$$f(x_{NL}) = 0.12e^{-\frac{(x-4.07)^2}{23.52}}$$

## DISCUSSION

Parallels can be drawn between the normal distribution function and the Weibull probability density function

$$f(T) = \frac{\beta}{\eta} \left(\frac{T-\gamma}{\eta}\right)^{\beta-1} e^{-\left(\frac{T-\gamma}{\eta}\right)^\beta}$$

where  $\eta$  is the scale parameter,  $\beta$  is the shape or slope parameter and  $\gamma$  is the location parameter as they have similar form and both include exponents.

We consider whether enough cadaver data is available to determine which is the best fit and if an egg surrogate dropped in the region of 2000 times can help understanding.

This abstract indicates that the egg may well be a good surrogate and that impact speed may be as strong a head injury predictor as HIC, albeit in a statistical sense.

## REFERENCES

1. P. Prasad and H. J. Mertz, "The position of the United States delegation to the ISO working group on the use of HIC in the automotive environment," *SAE transactions*, vol. 94, pp. 106-116, 1985.
2. C. Alvarez-Caldas, *et al.*, "Head injury criterion: the best way to evaluate head damage?," *International Journal of Vehicle Design*, vol. 45, pp. 411-425, 2007.
3. D. Gao and C. W. Wampler, "Head injury criterion," *Robotics & Automation Magazine, IEEE*, vol. 16, pp. 71-74, 2009.
4. J. Hutchinson, *et al.*, "The head injury criterion (HIC) functional," *Applied mathematics and computation*, vol. 96, pp. 1-16, 1998.

## INJURY DATA FROM UNHELMETED FOOTBALL HEAD IMPACTS EVALUATED AGAINST CRITICAL STRAIN TOLERANCE CURVES

D.A. Patton<sup>1</sup>, A.S. McIntosh<sup>1</sup>, S. Kleiven<sup>2</sup>, B. Fréchéde<sup>1</sup>

1. Risk and Safety Sciences, UNSW, Australia; declan@student.unsw.edu.au
2. Department of Neuronic Engineering, School of Technology and Health, KTH, Sweden

### INTRODUCTION

Concussion has been identified in recent research as being the most commonly occurring head injury in sports [1]. Many studies have reconstructed and analysed impact cases from American-football [2, 3]; however, very few studies have focused on impacts occurring in unhelmeted football codes [4, 5].

The concept of angular kinematics being the mechanism of brain injury was first published nearly 70 years ago [6]. It was stated that angular kinematics was the main cause of brain injury because it resulted in shear strains in the tissue. The magnitude of these shear strains in a particular region of the brain were thought to be an indication of the probability of injury in that region.

A threshold for diffuse axonal injury (DAI), which accounts for rotational loads in the coronal plane, was developed from animal impact tests, physical model experiments and analytical model simulations [7]. The critical strain tolerance curves presented are in agreement with the hypothesis of Holbourn (1943). It was stated that DAI exists as part of continuum of axonal injury severity, ranging from mild concussion to severe DAI; however, this theory has not been assessed for sports concussions.

In a later study, using a simple head-vehicle impact reconstruction model for actual pedestrian accidents, the relationship between the critical strain tolerance curves proposed by Margulies & Thibault (1992) and the parameters of impact was examined [8]. It was found that the 10% critical strain tolerance curve largely separated the cases with injury to the corpus callosum from the no-injury cases.

Finite element (FE) human head models are powerful tools for investigating intracranial stresses and brain tissue deformations during impact. The KTH FE Human Head Model is a detailed and parameterised finite element model, which was developed as a research tool to investigate various head impact injuries [9]. The model has been extensively validated

against cadaveric experimental data for intracranial pressure, intracerebral acceleration, relative brain-skull motion and skull fracture. The model was used to reconstruct concussion and no-injury impact cases occurring in American-football and various global- and local-level injury predictors were evaluated [2]. It was identified that strain in the corpus callosum was a good predictor of injury and a value of 0.21 related to a 50% probability of concussion.

### MATERIALS AND METHODS

In a previous study, 27 cases of unhelmeted concussive head impacts involving football players were reconstructed as rigid body simulations [4]. All cases had been chosen from a larger database of 100 videos of concussive head impacts that had been analysed quantitatively to obtain estimates of the players closing speeds [5]. Medical reports were used to grade each case using the revised Cantu Concussion Scale, with nine cases falling into each of the three grades. A further study reconstructed 13 head impact cases where no injury was sustained. Unlike the pedestrian study, the cases were not selected to replicate the experimental conditions upon which the critical strain tolerance curves were based.

From the rigid body reconstructions, the component curves of linear and angular head acceleration were obtained at the centre of gravity. The skull of the KTH FE Head Model was approximated to be rigid and the component acceleration output pulses were prescribed to the model's centre of gravity; driving the inertial loading. The maximum strain level in the corpus callosum was calculated for each case using FE simulations.

The aim of this study was to investigate the relationship between the kinematic results from the unhelmeted football head impact cases, the critical strain tolerance curves proposed by Margulies & Thibault (1992) and the strain levels in the corpus callosum calculated from FE simulations.

## RESULTS

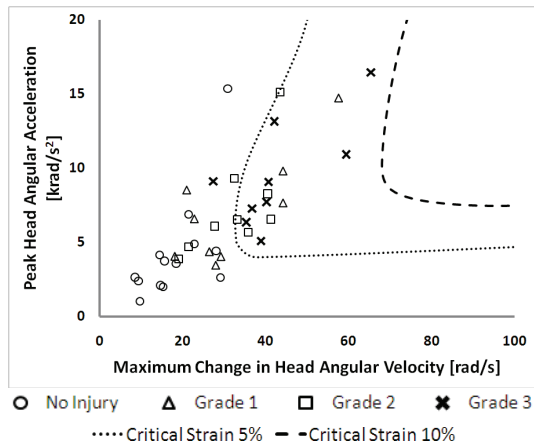


Figure 1: Distribution of unhelmeted football impact cases, classified by concussion grade (Revised Cantu Scale), against critical strain tolerance curves proposed by Margulies & Thibault (1992).

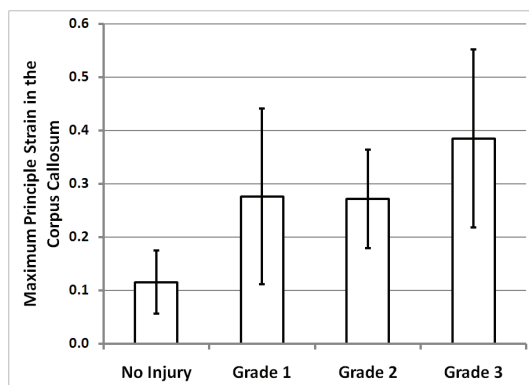


Figure 2: Average levels of strain in the corpus callosum for unhelmeted football impact cases, classified by concussion grade (Revised Cantu Scale).

	Grade 1	Grade 2	Grade 3
No Injury	0.002	0.0001	< 0.0001
Grade 1		0.754	0.225
Grade 2			0.069

Table 1: Significance levels relating to results in Figure 2 (P-values from two-tailed t-test for unequal variance).

## DISCUSSION

The relationship between the kinematic results from the rigid body reconstructions of unhelmeted football impact cases and the critical strain tolerance curves proposed by Margulies & Thibault (1992) was investigated. It was found that there was no clear separation between the grade 1 and grade 2 cases; however, the no-injury and grade 3 cases were largely separated by the 5% critical strain tolerance curve (see Figure 1). The absolute value of the critical shear strains require conversion to principle strains before representing actual strains in the brain tissue [7].

The reconstructed pedestrian cases presented by Ryan & Vilenius (1995) were all fatally injured and no-injury cases were defined by the absence of visible injury to the corpus callosum. Therefore, concussion may have occurred in these cases, which were mainly distributed between the 5% and 10% critical strain tolerance curves. This explains why the pedestrian no-injury cases were distributed in the same region as the unhelmeted football concussion cases.

The strain levels in the corpus callosum for the grade 3 cases were significantly higher than for the no-injury cases (see Figure 2 and Table 1). It is suggested that the 5% critical strain tolerance curve equates to a principle strain level of approximately 0.20. Strain based injury predictors are highly sensitive to the choice of brain tissue stiffness [2]; therefore, this tentative injury tolerance level is specific to the KTH FE Human Head Model.

This study demonstrates that the 5% critical strain tolerance curve is associated with impacts involving loss of consciousness longer than one minute. It is suggested that there is a high probability of a grade 3 concussion injury occurring during an impact with rotational kinematics above 4000 rad/s<sup>2</sup> and 30 rad/s for peak angular acceleration and maximum change in angular velocity, respectively.

## REFERENCES

1. McCrory, P.R., *The Nature of Concussion: A Speculative Hypothesis*. British Journal of Sports Medicine, 2001. 35(3): p. 146-147.
2. Kleiven, S., *Predictors for Traumatic Brain Injuries Evaluated Through Accident Reconstructions*, in 51<sup>st</sup> Stapp Car Crash Conference. 2007, SAE: San Diego, CA, USA. p. 81-114.
3. Pellman, E.J., et al., *Concussion in Professional Football: Part 1 - Reconstruction of Game Impacts and Injuries*. Neurosurgery Online, 2003. 53(4): p. 799-814.
4. Fréchède, B. and A.S. McIntosh, *Numerical Reconstruction of Real-Life Concussive Football Impacts*. Medicine & Science in Sports & Exercise, 2009. 41(2): p. 390-398.
5. McIntosh, A.S., P.R. McCrory, and J. Comerford, *The Dynamics of Concussive Head Impacts in Rugby and Australian Rules Football*. Medicine & Science in Sports & Exercise, 2000. 32(12): p. 1980-1984.
6. Holbourn, A.H.S., *Mechanics of Head Injuries*. The Lancet, 1943. 2: p. 438-441.
7. Margulies, S.S. and L.E. Thibault, *A Proposed Tolerance Criterion for Diffuse Axonal Injury in Man*. Journal of Biomechanics, 1992. 25(8): p. 917-923.
8. Ryan, G.A. and A.T.S. Vilenius, *Field and Analytic Observations of Impact Brain Injury in Fatally Injured Pedestrians*. Journal of Neurotrauma, 1995. 12(4): p. 627-634.
9. Kleiven, S., *Finite Element Modeling of the Human Head*. Doctoral Thesis. 2002, KTH - Royal Institute of Technology: Stockholm, Sweden.

## TRAUMATIC BRAIN INJURIES INVESTIGATION USING FINITE ELEMENT MODELING OF RAT BRAIN

Daniel Baumgartner<sup>1</sup>, Michael Gilchrist<sup>2</sup>, Michael Lamy<sup>1</sup>, Rémy Willinger<sup>1</sup>, Johan Davidsson<sup>3</sup>

1. University of Strasbourg, Strasbourg, France; daniel.baumgartner@unistra.fr

2. University College Dublin, Dublin, Ireland

3. Chalmers University of Technology, Göteborg, Sweden; johan.davidsson@chalmers.se

### INTRODUCTION

Traumatic Brain Injuries (TBI) constitute a significant portion of all injuries occurring as a result of automotive, sports and domestic accidents. Especially in sports, such kind of injuries can range from mild to severe when going from soft sports with poor head trauma possibility, to motor sports at the other extreme even if a protection device is worn. To determine the physiological and mechanical factors inducing TBI, experiments on animals have been used over the past few years. It has been inferred that angular accelerations are a main cause for such injuries as diffuse axonal injuries. However, studies concerning the accurate biomechanics of the mild TBI are still scarce.

In order to improve knowledge on TBI, a finite element model (FEM) of the rat's brain was developed in this study.

The short term aim of this model is to numerically reconstruct mechanical impacts which were generated by real experiments on rat's heads. As a consequence, the influence of the material parameters of the FEM is a crucial point; thus, parametric studies were led on them.

The long term goal of the FEM of the rat's head is to determine TBI mechanisms and tissue tolerance limits. This will be achieved by comparing injuries observed in experimental cases on one hand, and mechanical results extracted from the FEM on the other hand.

### MATERIALS AND METHODS

The FE model's geometry was obtained thanks to medical imaging techniques: micro Computed Tomography was performed for the bones while Magnetic Resonance Imaging was used for soft tissue geometry. Thresholding techniques allowed extracting an "outer surface" of the rat brain.

This surface delimited a volume which was then meshed, with the HYPERMESH© software. The final mesh of the brain consists of the following main

features: a cerebrum, a cerebellum, a brainstem, olfactory bulbs, a rigid skull on the outside, and a layer of elements for the interface between the brain and the skull. The FE mesh is continuous, all its components (except the skull) being made of a total of 17,972 hexahedral elements, with an average edge size of 0.45mm. The skull is made of 3,220 shell elements.

Material properties were selected from the data available in the literature and included in the FEM thanks to the HYPERCRASH© software. All the elements were alleged to be homogenous and isotropic. Skull properties were taken from Baumgartner [1], while the brain/skull interface behavior was based upon studies from Mao [4]. Both of these components were assumed to be linear elastic. All the other components were defined with a viscous elastic behaviour, adopting a Boltzman model (table1, from Gefen [3] and Mao [4]).

Table 1 reports the reference values of our model. However it should be noted that studies in literature stress that available material data remains limited. Moreover, reported mechanical behavior values can greatly vary from one experiment to another depending on the protocol. Therefore, parametric studies are needed to assess the influence of material properties in FEM in general and in the present model in particular.

A reference input was defined for the parametric study, adapted from Davidsson [2] experimental impacts on rats. It consists in a case of pure rearward rotational acceleration loading in the sagittal plane. The duration of its main pulse is 0.5ms, while its maximum amplitude is 1.6Mrad/s<sup>2</sup>.

The reference analysis consisted to submit the FEM of the rat's head to the input from figure 1 with the reference material characteristics from table 1. The following simulations, achieved thanks to the RADIOSS CRASH© software, were identical to the reference analysis case, except for one sole parameter of the brain being modified. The parameters that were subjected to such variations are the short and long term shear moduli, the bulk modulus and the decay constant for brain.

For every simulation, two mechanical outputs were considered: brain pressure and Von Mises stress (which is indeed considered as an injury criterion by a great amount of authors).

Short term shear modulus	Long term shear modulus	Bulk modulus	Decay constant	Density
1,721 Pa	508 Pa	2.19 GPa	0.125 s <sup>-1</sup>	1,040 kg.m <sup>-3</sup>

Table 1 Parameters of the viscous elastic brain

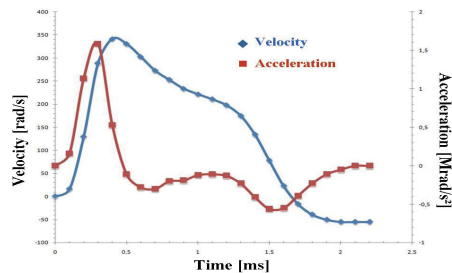


Figure 1 Reference input of the parametric study

## RESULTS AND DISCUSSION

The pattern of Von Mises stresses is depicted in figure 2. The main stresses are situated in cingulate cortex. The second region with high stresses is the vicinity of the corpus callosum, closer to the central part of the brain. Value of the maximal stress is about 0.6kPa, and is reached after 1.4ms. When it comes to pressures, maximal values of around 120kPa are observed in the lower olfactory bulb, after 0.3ms.

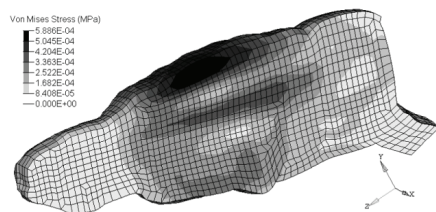


Figure 2 Brain Von Mises stresses distribution.

During the parametric studies, pressures did not appear to be influenced, as any change in one of the aforementioned mechanical parameters never resulted in a significant variation in values or pattern. Besides, brain Von Mises stresses offered a greater insight on the importance of the values that were attributed to these parameters. Short term shear modulus variations (170Pa to 17kPa) did not modify the stress anatomical distribution, but the calculated values increased linearly with the shear modulus. Long term shear modulus (varying from 50Pa to 5kPa) affected neither the pattern of stresses nor their values. The same observation was made for the the brain decay constant. Eventually, when bulk modulus was modified from 219MPa to 21.9GPa, the Von Mises stresses decreased with it, following a power function, while distribution remained unchanged.

Thus, brain short term shear modulus and bulk modulus appear to be the most crucial of the parameters. Concerning the bulk modulus, though the parametric study explores a wider array, two values (1.125GPa and 2.19GPa) are generally assumed for brain matter. However, when it comes to the short term shear modulus, reported values can change a hundredfold, with no general consensus. In spite of this, the described model still appears reliable. First, the Von Mises stresses distribution is consistent, independently from the value of brain short term shear modulus. Then, this distribution seems to relate to the experimental model, as Davidsson [2] reported haemorrhages on the upper cortex surface, and diffuse axonal injuries in the corpus callosum; both regions have displayed important Von Mises stresses in the numerical model. Moreover, the stresses increase linearly with the short term shear modulus: the issue of the definition of its value can consequently be seen as mainly a linear scaling problem.

## CONCLUSION

A FEM of the rat's brain was developed to improve the knowledge on TBI. Such a digital tool is a powerful way to establish a correlation between observed injuries on the one hand and intracranial metrics on the other hand. Thus, having some more accurate knowledge on more or less severe brain injury mechanisms, it becomes possible to improve protection devices, against these mechanisms. Especially in a great deal of sport activities, in which situations can lead to head impact, new protection techniques may then be designed. That outcome can be used, for example, for ice hockey helmets improvement, as it has been underlined in past studies by Mihalik [5] and Rousseau [6].

## REFERENCES

- Baumgartner D. and Willinger R., Human head tolerance limits to specific injury mechanisms inferred from real world accident numerical reconstruction. *Revue Européenne des Eléments Finis*, 2004, vol. 14, pp. 421-444.
- Davidsson J., Risling M. and Angeria M., A new model and injury threshold for sagittal plane rotational induced diffuse axonal injuries in the brain. *Proceedings of the 2009 IRCOB Conference*, 2009.
- Gefen A., Gefen N., Zhu Q., Raghupathi R. and Margulies S., Age-dependent changes in material properties of the brain and braincase of the rat. *Journal of Neurotrauma*, 2003, vol. 20, pp. 1163-1172.
- Mao H., Zhang L., Yang K.H. and King A.I., Application of a finite element model of the brain to study traumatic brain injury mechanisms in the rat. *Stapp Car Crash Journal*, 2006, vol. 50, pp. 583-600.
- Mihalik J.P., Guskiewicz K.M., Jeffries J.A., Greenwald R.M. and Marshall S.W., Characteristics of head impacts sustained by youth ice hockey players, *Journal of Sports Engineering and Technology*, 2008, vol. 222(1), pp. 45-52.
- Rousseau P., Post A. And Hoshizaki T.B., The effect of impact management materials in ice hockey helmets on head injury criteria, *Journal of Sports Engineering and Technology*, 2009, vol. 223(4), pp. 159-165.

## IMPACT PERFORMANCE OF ICE HOCKEY HELMETS: HEAD ACCELERATION VERSUS FOCAL FORCE DISPERSION

Ryan Ouckama, David J. Pearsall

Department of Kinesiology and Physical Education, McGill University, Montréal, Québec,  
Canada. ryan.ouckama@mail.mcgill.ca; david.pearsall@mcgill.ca

### INTRODUCTION

International helmet impact standards primarily utilize linear acceleration measures as a criterion to assess a helmet's ability to reduce force transmission to the head. Modern sport helmets certified to these impact safety standards have practically eliminated the incidence of skull fracture and fatal brain injury in football and ice hockey.<sup>1</sup> However, the incidence of diffuse brain injuries, such as concussion or mTBI, remains high.

While linear acceleration has been linked to mTBI, other factors may be considered. For example, some researchers have speculated that mTBI risk may also be related to rotational acceleration<sup>2</sup> and impact contact mechanics (e.g. area, pressure, duration) between the colliding surface / helmet / head.<sup>3,4</sup> Each variable provides unique information about the impact phenomenon. For instance, recent findings have demonstrated that global linear head acceleration criterion do not necessarily correspond to local foam contact mechanics.<sup>5</sup>

The purpose of this was to demonstrate the feasibility of capturing localized load distribution data during standardized helmet drop impact testing, and to compare various models of ice hockey helmets according to these measures.

### MATERIALS AND METHODS

An EN960 575mm magnesium half-headform was instrumented with an accelerometer at the center of mass along with 25 flexible force sensors (Flexiforce® A201-100, Tekscan, Boston). The 5x5 sensor array, covering a 80x60 mm area was centered about the prescribed location for impacts to the front of the head as defined by ice hockey helmet test standards (CSA z262.1-09). Prior to attachment, the sensors were dynamically calibrated using a 5kg mass guided by a vertical drop rig. A high density vinyl cylinder (d=9.5mm mm, h=13 mm) was adhered to the impactor which served both to dampen the impact and ensure all force was transferred directly to the active sensor area. Ten calibration trials were recorded for each sensor. The Flexiforce® output was correlated to a piezoelectric force plate (Type 9215M113, Kistler, Switzerland) which served as the impact base. Data were collected using a 32 channel acquisition device

(NI-9205) at 9 kHz. Three non-helmeted impacts (collected pre and post-testing) served as reference conditions and were used to verify repeat performance of the net force calculated from the sensor array.

Five different models of commercially available ice hockey helmets, representing several material types, were obtained for testing. Test factors included temperature (21°C, -25°C) and location (front, side, rear) for the repeated measure of impact (3). Testing procedure followed that of the CSA Z262.1 standard. At the present time only front impacts will be considered.

### RESULTS

Average (n=250) peak calibration force of the Flexiforce® sensor was  $960 \pm 244$ N (mean  $\pm$  sd) with impact duration lasting an average time of  $13.8 \pm 0.9$  ms. These characteristics were selected to maximize the load measurement range of each sensor while matching the average load profile time ( $13.6 \pm 0.9$  ms) of all 4.5m/s helmet impacts. Average R<sup>2</sup> values for the correlation of Flexiforce® sensor voltage with the force plate were  $0.983 \pm 0.001$ . Average percent error (rms error/range) was  $3.3 \pm 0.01\%$ . Only the rising portion of force curves forces were used for calibration.

Obvious differences in load distribution were visible between helmets types. Average (n=5) load distribution patterns for the first impact of the bare headform and five helmet models are presented in Figure 1. Multivariate repeated-measures ANOVA revealed significant differences ( $p < 0.05$ ) for both peak acceleration and peak focal force for the between-subject effects of helmet model, temperature, and helmet\*temperature (Figure 2). Within subject effects of impact, impact\*helmet, impact\*temperature, and impact\*helmet\*temperature were all significant ( $p < 0.05$ ). Average drop velocity for helmet impacts was  $4.52 \pm 0.02$  m/s and all trials were within 2% of the 4.5 m/s standard requirement. Pre- and post-test results of the bare headform drop were compared using the maximum net force of all 25 sensors. This identified a 7.4% reduction in net force between conditions. A 0.4% increase in global force was calculated from the same trials using the load cell data. Slight rotation of the clamping mechanism over the testing period may have contributed to this result.

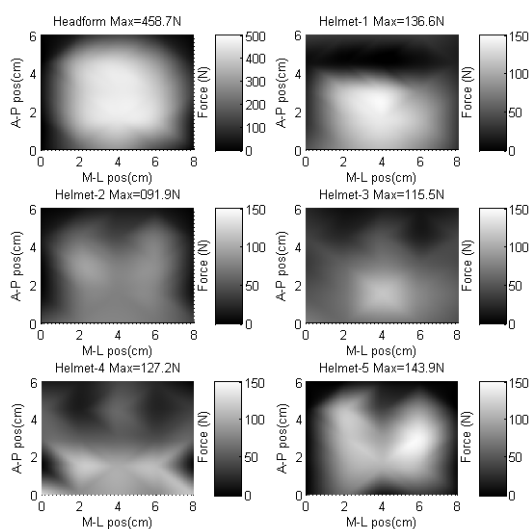


Figure 1: Plot of average ( $n=5$ ) load distribution between ambient conditions of a bare headform impact (top left) and five models of ice hockey helmets. Data were interpolated (quadratic) between the 25 sensor array.

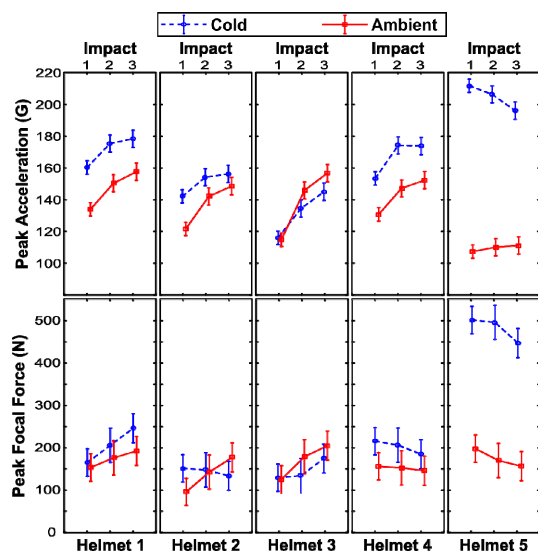


Figure 2: Repeated-measures results by helmet model for both acceleration (top) and peak focal force (bottom) values. Note: peak focal force does not exhibit the same trend as peak acceleration.

## DISCUSSION

The focal force pattern at the front impact site varied between helmet models. Indeed all 5 helmets displayed distinct regional load distributions. For example the bare headform condition (Figure 1) demonstrated a focal impact about the central sensor with radial dispersion. In the helmeted conditions we see inferiorly shifted focal dispersion (helmets 1 & 3), bilateral contact (helmets 2 & 4) and a rather variable load distribution (helmet 5). These patterns can be

attributed to the construction methods, choice of impact attenuating material and the juxtaposition of materials (layering, gaps between pads). Therefore, modelling load transmission response should not assume an even focal force distribution as may be the case in many simulations. The implications of these results are that FEM analyses should replicate specific helmet traits in order to further refine the prediction of cranial and deep neurovascular tissue responses. Further, the methods used can help identify high load concentration areas, conspicuously located with respect to specific helmet components. While bone failure at these high load concentrations is unlikely, the peak pressure calculated based on sensor area reached upwards of 8.4 MPa, which is substantial and approaching tissue failure magnitude.<sup>6</sup> This would be of particular concern at thinner more vulnerable areas of the skull, particularly the temporal squamous bone.

Our findings suggest that peak focal force was not proportional to peak global acceleration. Helmet 5 for example had the lowest acceleration values during ambient testing, yet focal forces were in the same range as all other models. Global acceleration alone cannot provide an assessment of the local/intercranial tissue response<sup>4</sup> meaning that the risk level attributed to acceleration may not represent the risk level associated at the impact site<sup>7</sup>. Further testing will examine high speed projectile impacts from the puck.

## ACKNOWLEDGEMENTS

Funding support for this work was provided by the NSERC/FQRNT Industrial Innovation Scholarship, in collaboration with the Bauer Hockey Corp.

## REFERENCES

- Mueller FO. Fatalities from head and cervical spine injuries occurring in tackle football: 50 years' experience. *Clin Sports Med.* 1998; 17: 169-82.
- Pellman EJ, Viano DC, Tucker AM *et al.* (2003) Concussion in professional football: reconstruction of game impacts and injuries. *Neurosurgery* 53:799-814
- Forero Rueda MA, Cui L and Gilchrist MD. Optimisation of energy absorbing liner for equestrian helmets. Part I: Layered foam liner. *Materials and Design.* 2009; 30: 9.
- Marjoux D, Baumgartner, D, *et al.* Head injury prediction capability of the HIC, HIP, SIMon and ULP criteria. *Accid Anal Prev.* 2008; 40: 1135-48.
- Ouckama R and Pearsall DJ. Evaluation of a flexible force sensor for measurement of helmet foam impact performance. *J Biomech.* 2011; 44: 904-9.
- Motherway *et al.* The mechanical properties of cranial bone: the effect of loading rate and cranial sampling position. *J Biomech.* 2009; 42: 2129-35.
- Bishop PJ and Arnold J. The effectiveness of hockey helmets in limiting localized loading on the head. In: Castaldi PJ, Bishop PJ and E.F. H, (eds.) *Safety in Ice Hockey.* Philadelphia: American Society for Testing Materials, 1993, p. 175-82.

## BIOMECHANICAL CONSIDERATIONS IN THE DESIGN OF EQUIPMENT TO PREVENT SPORTS INJURY

McIntosh AS<sup>1 2</sup>

1. Risk and Safety Sciences; UNSW, Australia, a.mcintosh@unsw.edu.au
2. The Australian Centre for Research into Sports Injury and its Prevention (ACRISP), Monash University, Australia

### INTRODUCTION

The international market for sports equipment is enormous. One component of that market is explicitly equipment to prevent injury and ideally all equipment should enable performance without causing injury. Although some athletes might be interested in the science behind the technology, biomechanical design inputs should be largely transparent to the user. In contrast, biomechanical principles, data, understanding of injury mechanisms and human tolerance should be central to the design process. This paper will describe a biomechanical approach to the design of equipment to prevent sports injury and provide some examples of successes, partial successes and failures.

### DESIGN APPROACH

The following elements need to be considered in equipment design:

1. Injury risk management objective
2. Injury mechanisms
3. Human tolerance
4. Range of sports loads: normal and abnormal
5. Objectives of sport and sports skills
6. Efficacy and effectiveness of current and past equipment
7. User expectations: usability, mass, aesthetics
8. Standards
9. Performance objectives
10. Materials and properties
11. Material and component testing
12. Prototype testing
13. Final product
14. Product evaluation and continuous control

The injury risk management objective is central to the design process. The objective should represent the reduction in severity or elimination of a known injury, and/or the reduction in its likelihood. American football helmets are an example of a device that addressed successfully the original objective of reducing severe and fatal head injuries. In the last decade a second objective has been added, to reduce

concussion. As will be discussed, a spread of objectives can be very challenging to satisfy.

The mechanism/s of the target injury/ies must be well understood. Great success has been achieved in reducing severe head injury through impact acceleration management and load distribution, but attention has only turned recently to other mechanisms of brain injury, such as angular acceleration. Impacts cause many injuries, but there are other loading mechanisms in non-contact knee ligament injuries and shoulder dislocation, for example.

Human tolerance to loads experienced in sport and the magnitude of typical loads has been studied in some areas, eg. the head, but not others, eg. the shoulder. Figure 1 presents likelihood curves for concussion, skull fracture and AIS 3/4 head injury vs. AIS < 3 against linear acceleration. All relationships plotted are significant at  $P < 0.05$ . Figure 1 identifies the difficulties of optimising design to manage linear acceleration in high energy and moderate energy impacts in the same helmet to reduce all severities of head injury.

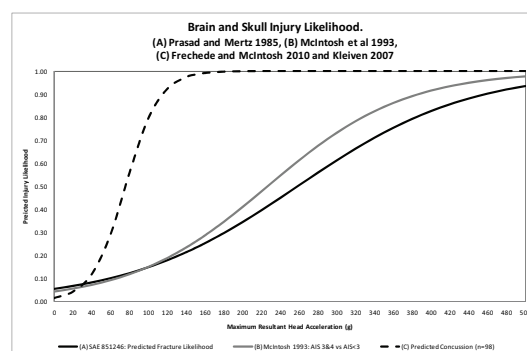


Figure 1: Brain and skull injury likelihood [1,2,3,4]

The load on the shoulder has recently been studied in the tackle in rugby union football and found to be around 2000 N [5]. This provides both normative data and a reference for the impact tolerance of the anterior/superior shoulder.

The objective of the sport skill during which the injury occurs is an important consideration. Ski bindings need to release before transmitted loads reach levels capable of causing tibial fractures or knee ligament injury. On the other hand, an expert skier does not expect the bindings to release during the execution of a high-speed turn despite the loads being substantial. In other situations the use of equipment could make the skill impractical, eg. heading the ball in football while wearing padded headgear.

Laboratory tests, case-control studies, cohort studies, ecologic studies, and randomised control trials of equipment provide an understanding of the efficacy and effectiveness of equipment. However, for the equipment designer, the information requires interpretation or may be unusable [6,7]. Controls may not be satisfactory from a biomechanical perspective and the range of loads experienced by the cohort may be large, meaning that equipment might have been 'effective' as designed, but not as used.

Satisfying usability, user expectations and aesthetics is a challenge for designers and biomechanists. In many sports weight, comfort, mobility and thermal comfort are critical. A biomechanical approach that might encase an athlete will be impractical and unsuccessful in many situations. Although it is feasible for an ice hockey goal-keeper to wear equipment from head to toe, the same is not true for the jockey. The outcome of meeting standards' requirements in terms of equipment weight and usability needs special consideration. However, it is also apparent that some equipment does not perform any safety function, despite the expectations of athletes, but is satisfactory aesthetically, light weight and usable.

Standards provide a very good benchmark for what should be the minimum level of performance. In recent years the need has been expressed for standards that address equipment for elite ('high risk') sport and general ('moderate risk') sport. However, this approach has not always been successful when put into practice. It is believed that no helmet was manufactured and sold commercially that met the very comprehensive high impact performance jockey helmet standard (EN 14572). One reason for this outcome, that is possibly relevant to other sports, is that the market for equipment for elite sport is miniscule compared to general sport. Therefore, without incentives and support, manufacturers may only reluctantly seek to meet standards for very limited applications.

Having considered points one to eight, it is possible to specify the equipment's performance objectives. These could be to meet a specific standard or more comprehensive and innovative. For example, the objectives for a hypothetical helmet for snow sports might be to: eliminate the risk of any head injury greater than AIS 2 in all foreseeable crashes and halve the risk of brain injuries less than AIS 1; meet SNELL

and EN standards; maintain adult helmet mass to less than 750 gm and provide child sized scaled versions; provide user options for electronic devices; include a mini accelerometer - GPS device that transmit a distress signal when a serious impact has occurred; and, maintain thermal comfort.

To meet the performance objectives above, it would be necessary to examine thoroughly materials and undertake an iterative design process comprising, most likely, impact testing and computer modelling, moving from components to the whole helmet. In this application the performance of materials in sub-zero temperatures must be considered. It would also be necessary to have reference data on the range of impacts that can occur, human tolerance and user information, as already described. In the author's experience, there is only limited publicly available information on materials used in devices that attenuate impact energy. Therefore, a careful review of the literature, discussions with colleagues and materials manufacturers comprises an essential first step.

Having determined materials and the performance of components, prototypes need to be made. The fabrication process is critical in maintaining the characteristics observed in component testing. Differences in performance due to the realisation of curved planes, eg. in a helmet, or the need for the device to drape comfortably around a body part, are to be expected. Having reached this point, there are many non-biomechanical factors that contribute to the final product.

To conclude, there is a need to focus on biomechanical inputs, as well as a human-centred ergonomics approach, in the design of equipment to prevent sports injury.

## REFERENCES

1. Prasad P and Mertz H, The Position of the U.S. Delegation to the ISO Working Group 6 on the use of HIC in the Automotive Environment. *SAE Technical Paper Series* 1985; 851246
2. McIntosh A Kallieris D Mattern R and Miltner E, Head and Neck Injury Resulting from Low Velocity Direct Impact. *Proceedings of the 37th. STAPP Car Crash Conference* 1993; SAE 933112
3. Fréchède B and McIntosh AS, Numerical Reconstruction of Real-Life Concussive Football Impacts. *MSSE* 2009; 41: 390-396
4. Kleiven S, Predictors for traumatic brain injuries evaluated through accident reconstructions. *Stapp Car Crash Journal* 2007; 51: 81-114
5. Usman J McIntosh AS and Fréchède B, An investigation of shoulder forces in active shoulder tackles in rugby union football, *JSAMS* 2011; in press
6. Finch CF Ullah S and McIntosh AS, Combining Epidemiology and Biomechanics in Sports Injury Prevention Research: A New Approach for Selecting Suitable controls, *Sports Medicine* 2011; 41: 59-72

## ANALYSIS OF LOADING CURVE CHARACTERISTICS ON THE PRODUCTION OF BRAIN DEFORMATION METRICS

Andrew Post<sup>1</sup>, Evan Walsh<sup>1</sup>, Blaine Hoshizaki<sup>1,2</sup>, Michael Gilchrist<sup>1,2</sup>

1. University of Ottawa Neurotrauma Impact Science Lab; apost@uottawa.ca
2. School of Mechanical and Materials Engineering; University College Dublin

### INTRODUCTION

Brain injury in everyday life and sport has high costs associated with it. In car crashes brain injury often results in severe neurological defects or in the worst cases, death. In sports, traumatic brain injuries have largely been eliminated due to helmet use, but concussions have remained prevalent, and may have unmeasured long term effects on neural tissue [1].

Diffuse injuries such as concussion are highly dependent on the amount of rotation an impact delivers to the brain along with the linear component [2]. Even more significant is how these linear and rotational acceleration time histories interact with brain tissue. As a result of this research it has been concluded that the best predictor of risk of injury would be to measure brain deformation using simulation [2]. This has led to the measurement of brain tissue deformation through the use of finite element models of the human head. This method is useful because it accounts for the influence of the linear and rotational acceleration loading curves on brain tissue and human brain geometry.

Many researchers to date have estimated the amount of deformation which may be associated with various risks of injury using a finite element model [3]. Some have used complete computer based simulations [4] while others have used physical models to generate the linear and angular acceleration loading curves which define the results of a potentially injurious impact [3]. As a result it has been suggested that maximum principal strain and Von Mises stress could potentially be important dependent variables used to measure brain deformation associated with concussive brain injury.

While these parameters have been identified by past research, it remains unclear how the linear and angular acceleration time histories contribute to brain deformation. Research by Post et al. [5] has examined some basic loading curve shapes. This research supported the notion that simply examining the peak linear and rotational acceleration values may not be descriptive enough to predict the severity of the resulting brain deformation.

The purpose of this research is to examine how the linear and rotational acceleration time history characteristics from a series of centric and non-centric impacts to hockey helmets influence peak maximum principal strain and Von Mises stress.

### MATERIALS AND METHODS

A pneumatic linear impactor was used to impact the hockey helmets. The linear impactor consists of a frame housing the impacting arm and a sliding table to which a Hybrid III head and neck form were attached. The mass of the impacting arm was  $16.6 \pm 0.1$  kg and was propelled into the helmeted Hybrid III head form at 5.0 m/s. The tip of the impacting arm is capped with a hemispherical nylon pad covering a MEP disc.

Twenty four individual helmets were impacted, of which 12 were vinyl nitrile and 12 were expanded polypropylene. The helmets were impacted at five sites designed to create different linear and rotational loading curve responses. These linear and rotational loading curves were then used as input for the model.

The finite element model of the human brain used in this research was developed in Dublin, Ireland and is known as the University College Dublin Brain Trauma Model (UCDBTM) [6]. The head was comprised of scalp, three part skull, pia, falx, tentorium, CSF, grey matter, white matter, cerebellum and brain stem. The validation of the model was carried out against intracranial pressure and brain motion from neutral density tracking responses from cadaveric impact research. Overall, the model was comprised of 10,192 hexahedral elements.

For curve analysis the linear and rotational acceleration loading curves were broken down into five measurable characteristics: 1) peak value, 2) total duration, 3) slope to peak, 4) time to peak, and 5) integral of the entire loading curve (figure 1). A principal component analysis was used to identify how much variance each characteristic in x, y and z components accounts for the resulting brain deformation metric. The maximum principal strain and Von Mises stress were broken down into increments of 5% and 1,000 Pa to establish comparable categories.

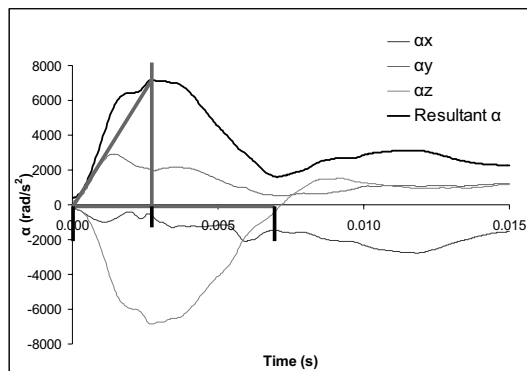


**Figure 1.** Example loading curve for a Hybrid III headform with curve characteristics identified: A) time to peak; B) duration of impact; C) slope to peak; and D) time to peak.

## RESULTS

The results are presented in tables 1 and 2. Table 1 depicts the variables accounting for the variance and chance of correctly predicting the maximum principal strain and table 2 shows the variables and chance of correctness for Von Mises stress.

**Table 1.** Analysis results showing the variables found to account for the variance in maximum principal strain and percent correct prediction

	Maximum principal Strain			
	Grey matter	White matter	Cerebrum	Brain stem
resultant angular integral	y angular time to peak	y linear integral	z linear integral	
z linear slope	z linear time to peak	x linear integral	z linear peak	
y angular integral	resultant angular integral	resultant linear integral	y angular time to peak	
		x angular slope	resultant angular peak	
		y angular time to peak	z angular time to peak	
		y angular integral	linear duration	
		angular duration		
% correct	43	59	87	86

**Table 2.** Analysis results showing the variables found to account for the variance in Von Mises stress and percent correct prediction

	Von Mises stress			
	Grey matter	White matter	Cerebrum	Brain stem
resultant angular integral	-no variables qualified-	x linear peak	x angular slope	
z linear integral		y angular integral	z linear integral	
		x linear integral		
		x angular slope		
		resultant angular time to peak		
% correct	27	n/a	62	48

The results indicate that for maximum principal strain and Von Mises stress there were no commonalities amongst the five curve characteristics chosen to predict the brain deformation metrics. There were also no commonalities in curve shape characteristic between the variables included in the analysis between maximum principal strain and Von Mises stress.

Overall, the ability of the variables chosen for the analysis to correctly predict the resulting maximum principal strain was low for the grey and white matter, at 43 and 59%. The values were higher for the cerebrum and the brain stem (87% and 86%), however the values for these two groups were

assigned to 3 or 4 groups and thus increases the predictive likelihood of success. The ability of the variables to predict the Von Mises stress were also low (table 2), and notably no variables accounted for the variance in the white matter.

## DISCUSSION

Of the five curve characteristics that were used in this analysis, none of them consistently appear to account for variance in maximum principal strain and Von Mises stress. Amongst the variables used in this analysis, peak resultant linear acceleration was not found to account for any variance in brain deformation metric. This supports previous research reporting low correlations between peak dynamic variables and brain deformation metrics [7]. In addition, as a result of the wide variety of curve characteristic combinations used to account for deformation variance, it could be suggested that using one variable as a predictor of brain deformation may be inadequate. Since finite element models use the entire dynamic response curve to calculate brain injury metrics it may be a better tool to predict risk of injury.

The limitations inherent to this research lie in the assumptions surrounding the model and the method used to break down the model. The model is a simulation of human response and while validated, is an approximation of true physical response. The variables chosen in this study to represent the characteristics of the dynamic response curve may not have been adequate in predicting brain deformation. The slope, for example is simplified into a straight line, when the shape of the curve to the peak is much more complex.

## REFERENCES

- Wennberg, R.A. and Tator, C.H. National Hockey League reported concussions, 1986-87 to 2001-02. *Can. J. Neurol. Sci.* 2003; 30: 206-209.
- King, A.I., Yang, K.H., Zhang, L. et al. Is head injury caused by linear or angular acceleration. *IRCOBI conference 2003*; Lisbon, Portugal.
- Kleiven, S. Predictors for traumatic brain injuries evaluated through accident reconstruction. *Stapp Car Crash J.* 2007; 51: 81-114.
- Doorly, M.C. and Gilchrist, M.D. The use of accident reconstruction for the analysis of traumatic brain injury due to head impacts arising from falls. *Comput Method Biomec* 2006; 9(6): 371-377.
- Post, A., Hoshizaki, T.B. and Gilchrist, M. Finite element analysis of the effect of loading curve shape on brain injury predictors. *8<sup>th</sup> Conference of the ISEA 2010*; Vienna, Austria.
- Horgan, T.J. and Gilchrist, M.D. The creation of three-dimensional finite element models for simulating head impact biomechanics. *IJCrash* 2003; 8(4): 353-366.
- Oeur, A., Post, A., Hoshizaki, T.B. et al. The correlation between brain deformation metrics and acceleration using a linear and non-linear impact protocol. *XXIII ISB 2011*; Brussels, Belgium.

## COMPUTATIONAL PROTECTIVE HELMET COMPONENT ANALYSIS

Manuel A. Forero Rueda, Michael D. Gilchrist

School of Electrical, Electronic and Mechanical Engineering, University College Dublin, Belfield, Dublin 4, Ireland; manuel@ucd.ie, michael.gilchrist@ucd.ie

### INTRODUCTION

The power and potential of applying computer modelling for helmet research is just beginning to be utilized. Equestrian helmets have improved considerably throughout the years, but empirical methods can only advance equestrian helmets to a certain point. From that point on, analytical research techniques can be employed to analyse helmet performance in detail and assist the design process. Computer methods can assist in understanding the behaviour of the helmet's individual components, beyond merely the headform output as it is usually done in a laboratory environment.

The helmet design process can be shortened by using computational modelling techniques. The initial concept testing phases could be substituted by computer modelling, therefore reducing the number of prototypes and tests to perform on the final few best options. Validation and testing on the actual manufactured product will still be needed; therefore computer modelling cannot be used to substitute the design/research process in its entirety.

This study uses a similar methodology as in previous research by the authors where the helmet liner material properties were studied, to analyse other aspects of helmet design. While the helmet liner is of vital importance for energy absorption, other modifications can also serve to improve its performance.

### MATERIALS AND METHODS

The equestrian helmet model (Fig. 1) previously developed and analysed by the authors [1-3] will be used in this study. The helmet shell and geometrical factors such as a gap between the liner and shell, ventilation holes and ridges on the helmet liner were studied to observe their influence on helmet performance. Standard flat anvil impact test simulations were done at 4.4, 5.4 and 7.7 m/s according to the equestrian helmet standards EN 1384:1997 and EN 14572:2005.

The helmet performance was analysed in light of changes to shell stiffness properties. Five helmet shell stiffnesses were used: 2, 7.25 (baseline), 20, 35 and 50 GPa. The headform peak linear acceleration, contact area of the shell with the helmet liner and the headform with the helmet liner, Von Mises stress distribution on the helmet liner and average Dissipated Plastic Energy Density (DPED) of the helmet liner are shown and discussed.

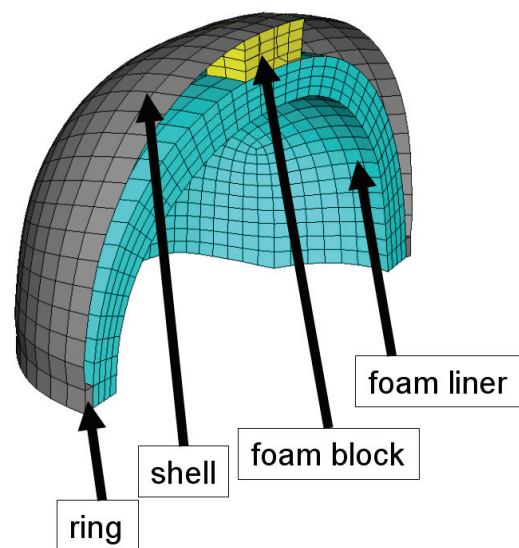


Figure 1: FE Equestrian helmet model.

Also, the fibre reinforced composite model was tested with the helmet model to evaluate its capability of modelling an equestrian helmet shell and to reach a response close to that of an actual equestrian helmet during impact.

The equestrian helmet model was modified by removing the foam block and generating a new helmet shell flush with the outer surface of the helmet liner. Impacts were done on a rigid flat anvil at three impact speeds, and the results were compared with those of the original helmet model. The variables analysed were headform peak linear acceleration and time

history, Von Mises stress distribution on the helmet liner, and contact area time history.

Two helmet liner types were generated based on the baseline helmet model. 20 mm diameter holes were created on the intended area of impact of the helmet liner for one case, and a rectangular ridge of 7 mm thickness, 15 mm wide and 61 mm in length was created for the second case. The features were added on the impact site. Linear acceleration, contact area, Von Mises stress volume proportion and average DPED were calculated for both cases and compared to the baseline helmet.

Finally, combinations of helmet modifications were done to determine whether it was possible to achieve a helmet configuration that reaches closer to the minimum EN 14572:2005 standard requirements. Two helmet types were generated and implemented in impact simulations to determine the best performing configuration for each helmet type.

## RESULTS

Stiff and compliant shells perform favourably for respectively high and low impact energies. If compliant and stiff shells were to be used for high and low energies respectively, a stiff shell at low impact energy would spread the load too much on the helmet liner and would not allow the liner to absorb energy. This in turn leads to high acceleration values (Fig 2). A compliant shell at a high impact energy concentrates the load on a small area which would yield excessively if the impact energy is sufficiently high. This would also lead to undesirable high levels of acceleration.

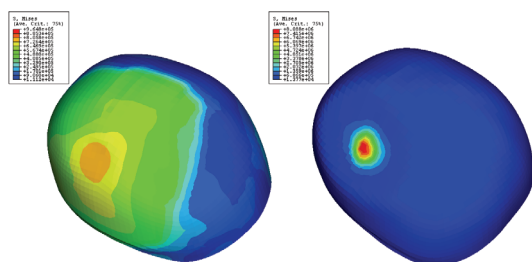


Figure 2: Von Mises Stress contour plots at peak headform acceleration for stiff shell (left) and compliant shell (right).

The presence of the air gap in the baseline helmet seems to contribute significantly to the linear acceleration reduction. The accelerations are lower than those without the air gap by 13, 15 and 21% for the low, medium and high speed impact cases respectively. The time that the acceleration exceeded 150 g for the medium and high impact speeds was also less.

The linear acceleration is slightly reduced when the ventilation holes or the ridge were included on the

helmet liner for the low and medium impact speed cases. Adding ventilation holes increases the impact dissipation capacity for lower impact energies, while for the high impact case it actually slightly decreases it. The ridge was seen to be effective at low impact energies as well, but it did not change performance for the high energy impact.

## DISCUSSION

Changing the helmet shell stiffness can radically affect the helmet's impact attenuation performance. Use of a low stiffness shell allows for the foam liner to deform more as it reduces the contact area on the helmet liner. This is useful when low impact energies are involved. Higher stiffness shells spread the impact energy to more of the helmet liner which allows the liner to withstand higher impact energies without deforming excessively.

The air gap present in the majority of current equestrian helmet designs can play an important role in impact attenuation. Without adding significant additional material (and consequently cost), the air gap improves the helmet performance by a significant margin. The air gap delays the impact duration and in this manner it spreads the impact energy, and consequently reduces the peak linear accelerations.

Adding geometric features on the helmet liner such as ventilation holes or ridges can help alter the energy absorbing performance of the helmet liner. Geometric structures can help concentrate and direct impact loads to improve energy absorption on the liner impact region.

By studying helmet design variations in terms of other variables different from headform linear acceleration, it is possible to not only determine which helmet configurations perform better, but also why they perform the way they do and how efficiently they are performing. This can assist the design and optimization process to suggest models which optimise cost, weight and helmet size.

## REFERENCES

1. Forero Rueda, M.; Cui, L. and Gilchrist, M. Optimisation of energy absorbing liner for equestrian helmets. Part I: Layered foam liner. *Materials and Design*, 2009, 30, 3405-3413.
2. Cui, L.; Forero Rueda, M. & Gilchrist, M. Optimisation of energy absorbing liner for equestrian helmets. Part II: Functionally graded foam liner. *Materials and Design*, 2009, 30, 3414-3419.
3. Cui, L.; Kiernan, S. & Gilchrist, M. Designing the energy absorption capacity of functionally graded foam materials. *Materials Science and Engineering A*, 2009, 507, 215-225.

## DYNAMIC IMPACT RESPONSE CHARACTERISTICS OF ICE HOCKEY HELMETS USING A CENTRIC AND NON-CENTRIC IMPACT PROTOCOL

Evan Stuart Walsh, Andrew Post, Phil Rousseau, Marshall Kendall, Clara Karton, Anna Oeur, Scott Foreman Thomas Blaine Hoshizaki

University of Ottawa Neurotrauma Impact Science Laboratory; ewals056@uottawa.ca

### INTRODUCTION

Protective headgear serves as a means of reducing the incidence and severity of head injuries in many impact and collision sports. In ice hockey, helmets meeting the Canadian Standards Association's Z262.1-09 or equivalent certification standards have resulted in near elimination of traumatic head injuries in the sport. The centric nature of the standards elicits a primarily linear head response that has been associated with a risk of skull fracture and traumatic brain injury. In contrast, the rate of concussive injuries in impact and collision sports, including ice hockey, has remained unchanged despite the advancement of centric test standards and associated protective equipment. This disparity may be primarily attributed to the lack of non-centric impact conditions within the standards. Non-centric impacts have been shown to cause higher angular accelerations, which in turn have been linked to concussive injuries. Suggestions that linear and angular accelerations are highly correlated are not supported and primarily occur under centric impact conditions. Unfortunately, practically all helmet standards employ centric or linear dominant impacts and as a result report high correlations between linear and angular accelerations. To properly assess sports helmet performance, it is important to select realistic impact conditions that represent the highest risk of brain injury. In developing centric and non-centric helmet assessment protocols, the influence of impact vector rotation on the complete dynamic impact response, or the orthogonal components of linear and angular accelerations, of the head must be considered. The efficacy of ice hockey helmets in preventing brain injuries can then be evaluated based on proposed linear and angular acceleration thresholds for both traumatic and mild traumatic brain injuries.

### MATERIALS AND METHODS

A linear impactor system consisting of a weighted, pneumatically driven impactor arm; a Hybrid III head- and neckform on an adjustable sliding table; and a computerized collection system was used to produce measurable three-dimensional helmeted headform impacts for six commercially available ice hockey helmets.

The linear impactor consisted of a stationary steel frame secured to a cement floor supported a cylindrical, free-moving impactor arm (length  $1.28 \pm 0.01$  m; mass  $16.6 \pm 0.1$  kg). Consistent system

compliance was attained through a hemispherical nylon striker (diameter  $0.132 \pm 0.001$  m; mass  $0.677 \pm 0.001$  kg) containing a vinyl nitrile 602 foam layer (thickness  $0.0357 \pm 0.0001$  m) that capped the impactor arm. The compliance afforded by the foam layer of the striker protected the linear impactor and headform from mechanical deterioration. The impactor arm and striker were accelerated pneumatically to a velocity of  $7.5\text{m}\cdot\text{s}^{-1}$  following an electronic trigger. Impactor parameters of mass, velocity, and compliance were unchanged throughout the testing procedure.

A helmeted 50th percentile adult male Hybrid III headform (mass  $4.54 \pm 0.01$  kg) instrumented according to Padgaonkar's orthogonal 3-2-2-2 linear accelerometer array protocol was fixed to a 50th percentile Hybrid III neckform (mass  $1.54 \pm 0.01$  kg) with a resulting forward headform pitch of  $2.5^\circ$ . Headform angular acceleration components were calculated based on the first principles of rigid body dynamics and linear accelerations from the orthogonally arranged sensor array. The complete Hybrid III structure was connected to a sliding table (mass  $12.78 \pm 0.01$  kg) and linear rail system and was adjustable linearly in all three axes and rotationally in the y- and z-axes using a locking device. The linear rails were aligned longitudinally with the impactor arm and allowed for the sliding table to displace linearly (length  $0.54 \pm 0.01$  m).

Inbound impactor velocity was measured using an electronic time gate (width  $0.2525 \pm 0.0001$  m) and recorded by computer. The nine mounted single-axis Endevco 7264C-2KTZ-2-300 accelerometers were sampled at 20 kHz and filtered using the SAE J211 class 1000 protocol. The accelerometer signals were passed through a TDAS Pro Lab system before being processed by TDAS software. Data collection was triggered when any of the accelerometers reached a 3g threshold and terminated after 15 ms.

A condensed version of the University of Ottawa Test Protocol (uOTP<sup>5</sup>), employing five centric and non-centric impact conditions, was used to assess the dynamic impact response of six commercially available ice hockey helmets. Each of the helmets was certified to both the Canadian Standards Association's Z262.1-09 and Hockey Equipment Certification Council ASTM F1045-07 centric safety standards.

Table 1. uOTP<sup>5</sup> Conditions

Site	Location	Impact Angle
1	Anterior intersection of the mid-sagittal and absolute transverse planes	15° elevation in the mid-sagittal plane towards the impactor
2	Right intersection of the coronal and absolute transverse planes	No vertical or horizontal rotation was applied to the vector
3	Midpoint between the anterior mid-sagittal and right coronal planes in the transverse plane	45° rotation in the transverse plane
4	Midpoint between the posterior mid-sagittal and right coronal planes in the transverse plane	-45° rotation in the transverse plane
5	Posterior intersection of the mid-sagittal and absolute transverse planes	-45° rotation in the transverse plane

Three identical helmets of each model were impacted three times at the five conditions for a total of forty-five impacts per helmet. The dynamic impact responses were ranked and also compared statistically between helmets using analyses of variance. Additionally, the results were rated against proposed brain injury thresholds to evaluate the severity of the impacts across helmet and condition and determine the appropriateness of the dependent variables.

## RESULTS

When the mean peak linear and angular acceleration values were ranked for the five impact conditions across the six helmets, the average rank difference between the two forms of acceleration was eleven out of thirty. This was particularly evident in the non-centric impact conditions, such as Site 4, where linear acceleration values were all in the top ten and angular accelerations were in the bottom ten.

Table 2. Mean Peak Dynamic Impact Response by Helmet

Helmet	Peak a (g)		Peak $\alpha$ (rad/s <sup>2</sup> )	
	Mean	St Dev	Mean	St Dev
A	78.2	13.4	6962	1787
B	80.8	11.2	7151	1241
C	72.0	10.5	5870	1114
D	76.4	8.1	6966	1219
E	80.2	10.2	6353	1220
F	80.7	9.4	7393	1723

None of the certified ice hockey helmets tested had linear acceleration values deemed to be of high risk of brain injury; however, all but one of the helmets had at least one impact condition above an 80% risk of mild traumatic brain injury when angular acceleration was considered. Three-quarters of the angular accelerations elicited that represented a high risk of mild traumatic brain injury were the result of non-centric impact vectors.

## DISCUSSION

Angular acceleration was found to add important information regarding the assessment of helmet efficacy with respect to risk of mild traumatic injury. Although no helmet approached the linear accelerations associated with traumatic brain injury, five of the six models had angular accelerations that would be associated with mild traumatic brain injury. It may therefore be concluded that angular acceleration should be included as a dependent variable in helmet assessment protocols. High risk of mild traumatic brain injury was also primarily associated with the non-centric impact conditions, reinforcing the need for such impact vector rotations in helmet certification standards.

## REFERENCES

- King, A.I., Yang, K.H., Zhang, L. et al. Is head injury caused by linear or angular acceleration? *IRCOBI conference 2003*; Lisbon Portugal.
- Padagaonkar, A.J., Krieger, K.W. and King, A.I. Measurement of angular acceleration of a rigid body using linear accelerometers. *J. Appl. Mech.* 1975; 42: 552–556.
- Walsh, E.S. and Hoshizaki, T.B. Sensitivity analysis of a hybrid III head- and neckform to impact angle variations. *ISEA conference 2010*; Vienna Austria.
- Walsh, E.S., Rousseau, P., Foreman, S. and Hoshizaki, T.B. The determination of novel impact conditions for the assessment of linear and angular headform accelerations. *ISBS conference 2009*; Limerick, Ireland.
- Walsh, E.S., Rousseau, P. and Hoshizaki, T.B. The influence of impact location and angle on the dynamic impact response of a hybrid III headform. *Sp. Eng.* 2011; 13: 135-143.
- Wenneberg, R.A. and Tator, C.H. National Hockey League reported concussions, 1986-87 to 2001-02. *Can. J. Neurol. Sci.* 2003; 30: 206-209.
- Zhang, L., Yang, K.H. and King, A.I. A proposed injury threshold for mild traumatic brain injury. *J. Biomech. Eng.* 2004; 126: 226-236.

## THE APPLICATION OF BRAIN TISSUE DEFORMATION VALUES IN ASSESSING THE SAFETY PERFORMANCE OF ICE HOCKEY HELMETS

Blaine Hoshizaki<sup>1</sup>, Evan Walsh<sup>1</sup>, Andrew Post<sup>1</sup>, Philippe Rousseau<sup>1</sup>, Marshall Kendall<sup>1</sup>, Clara Karton<sup>1</sup>, Anna Oeur<sup>1</sup>, Scott Foreman<sup>1</sup> and Michael Gilchrist<sup>1,2</sup>

1. University of Ottawa Neurotrauma Impact Science Laboratory; thoshiza@uottawa.ca
2. University College Dublin College of Engineering, Mathematical and Physical Sciences

### INTRODUCTION

Head injuries and concussion in particular have become a major concern in contact sports especially ice hockey. The inclusion of helmets in sports has successfully reduced the incidence of traumatic brain injury, however the incidence of concussion injuries seems to be unaffected [1].

A possible reason for this continuing incidence of concussion is the method in which helmets are designed and tested. Currently, helmets are required to adhere to certification standards which use peak resultant linear acceleration as the dependent variable measuring protective performance [2]. This dependent variable is associated with traumatic brain injury, but is not correlated with concussion. Concussion has been described as a rotationally dominant injury, and such rotations are not measured using linear acceleration [3]. Currently no certification standard uses both linear and rotational accelerations to evaluate sport helmet performance [2].

Previous research measuring the ability of ice hockey helmets to manage linear and rotational acceleration have reported that while they may be similar for linear impacts, they show differences in the rotational response [4]. These differences are also present in centric and non-centric testing protocols of American football helmets [5]. Attempts to predict brain injuries using peak linear and angular accelerations have not been particularly successful. The development of finite elements models for the head and brain provide an opportunity to use brain deformation values to access the ability of helmets to manage the risk of brain injuries.

Finite element modelling of the brain during an impact provides an opportunity to study the influence of the brain tissue on complex loading curves. This allows for the characteristics of the loading curve to be used to predict brain deformations, which have a higher significance in predicting nervous system tissue injury [6]. This approach is expected to provide more

information describing the impact management characteristics of helmets and identify how divergences between linear and rotational acceleration affect brain tissue with respect to injury.

The purpose of this research was to evaluate ice hockey helmets using brain tissue deformation values under centric and non-centric impact conditions.

### MATERIALS AND METHODS

A pneumatic linear impactor was used to impact certified ice hockey helmets at 7.5 m/s in centric and non-centric conditions. The linear impactor is formed of a table housing a helmeted hybrid III headform and the main frame which holds the impacting arm. The mass of the impacting arm was  $16.6 \pm 0.1$  kg and had a VN600 foam pad with a nylon cap affixed to the end. The hybrid III headform was equipped with accelerometers in a 3-2-2 arrangement for measurement of three-dimensional kinematics.

Six different models were tested under the impact conditions, three impacts per helmet per condition. The liners of the helmets were vinyl nitrile, expanded polypropylene or engineered structure. The resulting three dimensional loading curve responses were applied to the centre of gravity of the finite element model to produce measurements of the brain deformations. The deformation metrics chosen for this study include Von Mises stress (VMS) and maximum principal strain (MPS).

The University College Dublin Brain Trauma Model (UCDBTM) was used to complete the finite element model the impact deformations of the human brain [7]. The geometry of the model was derived from CT scans of a male participant and comprised of nearly 26 000 hexahedral elements. The head was comprised of the scalp, skull, pia, falx, tentorium, cerebrospinal fluid, grey and white matter, cerebellum and brain stem. The model was validated for intracranial pressure and brain motion response conducted on cadavers [7].

## RESULTS

Table 1. Mean Peak Dynamic Impact Response and Brain Tissue Deformation by Helmet

Helmet	Dynamic Impact Response		Brain Tissue Deformation	
	Linear	Angular	VMS	MPS
A	78.2	6 962	13 842	0.459
B	80.8	7 151	15 195	0.518
C	72.0	5 870	13 113	0.448
D	76.4	6 966	14 966	0.522
E	80.2	6 353	13 869	0.465
F	80.7	7 393	14 125	0.483

## DISCUSSION

Employing injury thresholds as a means to determine the effectiveness of helmets is challenging at best; however, they do provide a reference for evaluating helmet performance. Current ice hockey helmet certification injury thresholds are based on linear acceleration values associated with a predicted risk of traumatic brain injury or skull fracture. This dependent measure has proven efficacious, as traumatic injuries have been virtually eliminated from the sport; however it is not well associated with mild traumatic brain injury and therefore alternative measures should be considered. The tissue deformation values did not follow the dynamic values in all cases. While helmet C consistently ranked the best in all four dependent variables this was not always the case. Helmet D ranked second in peak linear acceleration and last in Von Mises stress. When peak linear acceleration was considered by itself to assess the efficacy of ice hockey helmets under centric and non-centric impact conditions, it revealed that all helmets impacted at 7.5 m/s were below the 50% risk for mild traumatic brain injury [8, 9]. When angular acceleration was also considered, only helmet C was below the proposed 50% injury risk threshold.. This discrepancy indicated that perhaps angular acceleration was a more sensitive measure for the assessment of mild traumatic brain injury. When brain tissue deformation variables, maximum principle strain and Von Mises Stress, were considered predicted injury levels far exceeded the 50th percentile for all helmets tested. This data supports the importance of continuing research supporting the use of tissue deformation values in evaluating the efficacy of helmets in preventing brain injuries.

## REFERENCES

1. Wennberg, R.A. and Tator, C.H. National Hockey League reported concussions, 1986-87 to 2001-02. *Can. J. Neurol. Sci.* 2003; 30: 206-209.
2. Hoshizaki, T.B. and Brien, S.E. The science and design of head protection in sport. *Neurosurg.* 2004; 55: 956-967.
3. Gennarelli, T.A., Thibault, L.E., Adams, J.H. et al. Diffuse axonal injury and traumatic coma in the primate. *Ann Neurol* 1982; 12(6): 564-574.
4. Rousseau, P., Post, A., Hoshizaki, T.B. A comparison of peak linear and angular headform accelerations using ice hockey helmets. *J. ASTM int.* 2009; 6(1):11.
5. Post, A., Hoshizaki, T.B. and Gilchrist, M. Evaluation of American football helmet performance using finite element modeling. *8<sup>th</sup> ISEA Conf.* 2010; Vienna, Austria
6. King, A.I., Yang, K.H., Zhang, L. et al. Is head injury caused by linear or angular acceleration. *IRCOBI conference* 2003; Lisbon, Portugal.
7. Horgan, T.J. and Gilchrist, M.D. The creation of three-dimensional finite element models for simulating head impact biomechanics. *IJCrash* 2003; 8(4): 353-366.
8. Zhang, L., Yang, K.H. and King, A.I. A proposed injury threshold for mild traumatic brain injury. *J. Biomech. Eng.* 2004; 126: 226-236.
9. Kleiven, S. Predictors for traumatic brain injuries evaluated through accident reconstruction. *Stapp Car Crash J.* 2007; 51: 81-114.

## IMPACT ASSESSMENT OF JOCKEY HELMET LINER MATERIALS

A.S. McIntosh<sup>1,2</sup>, D.A. Patton<sup>1</sup>, K. Thai<sup>1</sup>

1. Risk and Safety Sciences, UNSW, Australia; a.mcintosh@unsw.edu.au
2. The Australian Centre for Research into Sports Injury and its Prevention (ACRISP), Monash University, Australia

### INTRODUCTION

Reducing head injury risks amongst jockeys has been identified as a health and safety priority in the horse racing industry [1]. Currently available jockey helmets are typically assessed against performance standards, which cater to equestrian helmets for all horse riding activities. However, it has been identified that head impacts, and therefore injuries, in horse racing are towards the severe end of the spectrum for all possible equestrian impacts.

The EN 14572 High Performance Helmets for Equestrian Activities Standard was introduced in 2005 [2]. EN 14572 promoted a higher level of impact protection than other standards; however, no helmet was certified to this standard. The energy attenuation requirements of this standard were peak headform acceleration < 250g and not exceeding 150g for longer than 5ms for the following three drop configurations:

- 3m drop on to a flat anvil
- 2m drop on to a hemispherical anvil
- 2m drop on to a 'hazard' anvil

An additional test was a 1m drop onto a flat anvil requiring peak headform acceleration < 80g. Compared to existing Australian, British and American standards for equestrian helmets, the high performance standard promoted a substantially higher level of protection. Currently, all helmet standards are based solely on linear acceleration, but it has been recommended that future standards should incorporate angular kinematics [3]; although not assessed here.

Equestrian helmets generally consist of a protective outer shell, an inner liner and a comfort liner. In terms of energy attenuation, the most important of these components is the inner liner, which is typically constructed from expanded polystyrene (EPS) foam.

A previous study investigated the development of a new shock-absorbing liner for helmets by impacting single- and dual-density samples [4]. Dual-density samples were constructed by embedding low-density EPS foam into the currently-used high density EPS

foam, in a 'unique' configuration. Samples had dimensions of 100mm x 100mm and thicknesses of 25mm or 40mm.

Finite element (FE) methods have been used to investigate the potential of layered foam liners [5]. It was found that peak linear accelerations could be lowered by modeling the liner as multiple foam layers of different densities. A functionally graded foam liner was investigated in a further study [6]. Results were similar to the layer configuration, but crack initiation and propagation issues would be avoided.

The aim of this study was to assess the performance in radial impacts of a range of energy attenuating materials that could be fabricated into a helmet liner considering usability issues, such as helmet mass and comfort. Selected foams and honey comb structures of different densities and thicknesses were assessed.

### MATERIALS AND METHODS

Five commercially available materials were selected for testing. Three foam materials with various densities were cut into samples with dimensions of 100mm x 100mm and thicknesses of 10mm:

- polyurethane (PU)  
(48kg/m<sup>3</sup>, 90kg/m<sup>3</sup> and 170kg/m<sup>3</sup>)
- expanded polypropylene (EPP)  
(46kg/m<sup>3</sup> and 86kg/m<sup>3</sup>)
- expanded polystyrene (EPS)  
(35kg/m<sup>3</sup>)

Two honeycomb structure materials were also cut into samples with dimensions of 100mm x 100mm and set thicknesses:

- polypropylene  
(15mm)
- aluminium  
(12mm)

Single-material samples were constructed using two and three layers of the same foam material with thicknesses of 20mm and 30mm, respectively. They were also constructed using one and two layers of either type of honeycomb structure material with total thicknesses ranging from 12mm to 30mm. Dual-material samples, were constructed using two and

three layers of two different materials with thicknesses ranging from 20mm to 32mm. The top layer material had a higher relative density, greater than  $50\text{kg/m}^3$ , and the bottom layer(s) consisted of a material with a lower relative density, less than  $50\text{kg/m}^3$ .

Samples were tested using a rigid ISO headform running in guided free-fall on two wires. The impact energy attenuating properties of each sample were measured. Each sample was lightly taped to the base of the rig so that the crown of the headform impacted the centre of the sample. Just before the impact, a light gate triggered data acquisition and high speed video capture. Samples were initially tested from a drop height of 1.5m. If the peak headform acceleration was  $< 300\text{g}$ , the sample was tested from a drop height of 2.0m. This successive elimination of samples was again repeated for the final drop height of 2.5m.

## RESULTS

Figures one and two present the main results of the impact tests across the materials and three impact severities.

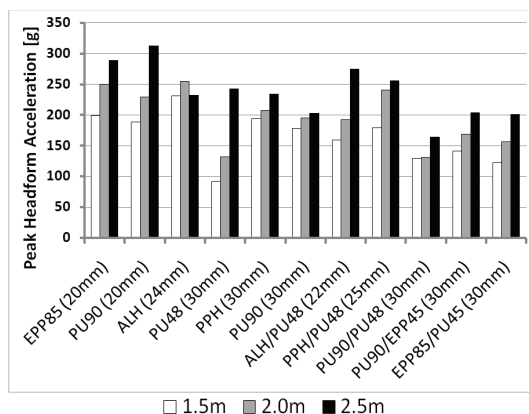


Figure 1: Peak headform acceleration across material samples and drop heights.

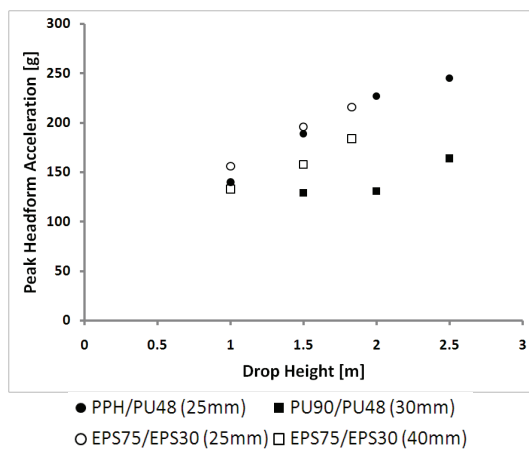


Figure 2: Comparison of material sample energy-attenuation performance with Morgan & Szabo (2001). Filled markers denote results from this study.

## DISCUSSION

In general dual-material samples performed better than single-material samples (Figure 1). For single-material sample impact tests, polyurethane ( $48\text{kg/m}^3$  and  $90\text{kg/m}^3$ ) returned the lowest headform acceleration values. The dual-material samples incorporating polyurethane ( $48\text{kg/m}^3$ ) all performed well. For impacts with a drop height of 2.5m, the lowest headform acceleration was recorded by the dual-material sample of polyurethane ( $48\text{kg/m}^3$  and  $90\text{kg/m}^3$ ).

For both single- and dual-material samples, energy attenuation performance increased with sample thickness. This result was expected due to the work-energy relationship.

When compared to the results presented in Morgan & Szabo (2001), the 30mm thick dual-material sample of polyurethane had the best energy attenuation performance (see Figure 3). Moreover, the best performing sample in the previous study had a thickness of 40mm. In both studies, the performance of 25mm thick samples resulted in similar peak headform acceleration levels.

The honeycomb materials tested showed promise. However, due to either mass or performance limitations were not pursued further. Changing the internal honeycomb blade stiffness and density may produce a material that has excellent impact energy attenuating characteristics. Consideration was also given to the difficulties of fabricating these materials into liners.

## REFERENCES

1. McCrory, P., et al., *An Analysis of Injuries Resulting from Professional Horse Racing in France During 1991-2001*. British Journal of Sports Medicine, 2006. 40(7): p. 614-618.
2. BSI, *EN 14572:2005 High Performance Helmets for Equestrian Activities*. 2005, BSI: London, UK.
3. Forero Rueda, M.A., L. Cui, and M.D. Gilchrist, *Finite Element Modelling of Equestrian Helmet Impacts Exposes the Need to Address Rotational Kinematics in Future Helmet Designs*. Computer Methods in Biomechanics and Biomedical Engineering, 2010. 13(3): p. 1-11.
4. Morgan, D.E. and L.S. Szabo, *Improved Shock Absorbing Liner for Helmets*. 2001, Australian Transport Safety Bureau: Canberra, Australia. p. 54.
5. Forero Rueda, M.A., L. Cui, and M.D. Gilchrist, *Optimisation of Energy Absorbing Liner for Equestrian Helmets. Part I: Layered Foam Liner*. Materials and Design, 2009. 30(9): p. 3405-3413.
6. Cui, L., M.A. ForeroRueda, and M.D. Gilchrist, *Optimisation of Energy Absorbing Liner for Equestrian Helmets. Part II: Functionally Graded Foam Liner*. Materials and Design, 2009. 30(9): p. 3414-3419.

## PASSIVE AND ACTIVE MUSCLE EFFECTS ON IMPACTS

Matthew TG Pain

School of Sport, Exercise and Health Sciences, Loughborough University;  
m.t.g.pain@lboro.ac.uk

### INTRODUCTION

Impacts in sports take many forms, from the mild and innocuous through to the debilitating or even fatal, but invariably all but a very limited number of sports involve impacts. Impacts can occur as the goals of the sport, as a by-product of the main aims of the sport, or accidentally. Combat sports and contact sports can aim to maximise impacts or utilise impacts in a skilful and controlled manner, locomotion during sports results in steady stream of impacts with the ground, and collisions with sports equipment, the environment or other athletes is something that is often best avoided altogether.

Globally much of the research into impacts has focussed on the most violent impacts that can cause catastrophic injury. Crash research has been at the forefront of impact injury research and has led to a greater understanding of the impact-injury relationship and improved safety and protective systems. However, this research does not transfer to the whole range of sporting impacts and tends to ignore at least one potentially important factor, living, dynamically active muscles. Muscle has the ability to change its mechanical properties by orders of magnitude in fractions of a second and in collisions between two athletes these differences can be an important factor. For instance the effects of tensing muscles in anticipation of an impact and the effect of that muscle tension on the impact is generally regarded as having a minor influence during crash studies. Early crash test studies found increased thoracic stiffness when impacting tensed human volunteers in a non-injurious range but a negligible difference in thoracic stiffness between tensed and relaxed muscle conditions was found above the threshold at which irreversible injury was found to occur<sup>1</sup>. Thus the affect of varying muscle tension on impact response is ignored, however, all combat athletes will always tense to take an impact if given the opportunity. With whiplash studies in crashes the damaging action occurs before reflexes can help stabilise the neck. The accelerations of the head in crashes are normally due to inertial changes or impact with large effective mass objects, such as a vehicle or the ground, and so muscle stabilisation in crash test dummies is ignored. But all combat sport athletes have rigorous neck strengthening regimes as without it they are far more

susceptible to knockout punches. The muscles in an athlete's body are also capable of producing very large forces. The quadriceps muscle group of a strong individual can produce a muscle and tendon force of between 10 – 15 kN. These forces are required to control the movements being made but they can also be used to help preload or counteract loading on the skeleton<sup>2</sup> or they can result in a substantial, even dangerous, levels of loading that is equivalent to the externally measured loads. This talk aims to cover a series of studies that look at active and passive muscle effects on impacts and show that for impact intensities commonly seen in sports including muscles is required for a full understanding.

### MATERIALS AND METHODS

The muscles and other soft tissues of the body react to an impulsive load by deforming within themselves and with respect to the more rigid skeletal structures. Experimental measures of soft tissue motion were made in a series of experiments and this motion included as lumped wobbling masses in various simulation models of impacts. The effect of the soft tissue motion on loading and energy transfer was calculated both numerically and within computer simulation models. Further modelling was performed that included the effects of muscle forces on skeletal loading when landing technique and landing surface were altered.

Subsequently studies involved direct surface measures of contact forces during rugby tackles, ball-thigh impacts and during martial arts kicks to the abdomen. These studies looked at the effects of involving the viscoelastic properties of the human in testing the load mitigation properties of padding and protective equipment on impact intensity. The Tekscan F-Scan measuring system was used with a custom dynamic calibration method<sup>3</sup> and high speed motion analysis. Comparisons between standard rigid body tests and human on human tests for protective garments were carried out with the recorded data. The effects of muscle tension on the forces and energy dissipation were also quantified for the ball-thigh impacts.

## RESULTS

During low level impacts of the arm soft tissue deformation could account for 70% of the energy lost from the forearm during these impacts, which in turn also accounted for the majority of the energy dissipation during the impact<sup>4</sup>. Measurements from the pendulum impact simulation indicated that heel pad properties changed from those found *in vitro* to those found *in vivo* as relative motion of the bone and soft tissue was allowed. The *in vivo* heel pad properties are also measuring the properties of the whole lower leg. The ability of the wobbling mass of the shank to dissipate energy during an impact was found to be significant. These results demonstrate the important role of soft to the dissipation of mechanical energy during impacts<sup>5</sup>.

In whole body simulations of landing from a drop, that utilized realistic wobbling masses, the peak vertical ground reaction for the subject was 16.4 bodyweights and 16.2 bodyweights for the model. If all wobbling masses were rigidly fixed to the rigid skeleton then the peak vertical ground reaction force increased to 40.5 bodyweights. The wobbling masses have a large influence on the loading on the system. In a similar fashion the resultant joint moments and forces were much larger for the rigid model than the wobbling mass model indicating the extent to which soft tissue motion can change the calculated loading<sup>6</sup>.

When landing models were optimized to look at reducing external and internal loading during landings in gymnastics it was intriguing to see the effect that muscle forces had on the internal loading. Optimizing the landing strategy, via change muscle activations, to minimize the GRFs reduced the peak GRFs by up to 48% compared to a matching simulation. However, most internal loading measures (bone bending moments, joint reaction forces, muscle forces) increased compared to the matching simulation. Optimizing the landing strategy to minimize the peak bone bending moments resulted in reduced internal loading measures, up to 27%. Using a reduction in ground reaction forces, due to a change in landing strategy as a basis for a reduction in injury potential may not be appropriate since internal loading can increase due to muscle forces<sup>7</sup>.

*In vivo* impact testing of rugby shoulder pads results showed that the pad significantly reduced peak impact force by up to 35% when impacted with an object and by 40% overall for all tackles. However, this reduction in force was localized directly above the acromioclavicular joint, while forces in the surrounding areas were not reduced. However, the peak loads and loading rates were different from those seen in standardized testing and markedly different in the soft tissue areas<sup>3</sup>. Testing of taekwondo chest protectors via the standards method and *in vivo* tests shown that the performances of TKD protectors were extremely dependent on the impactor and anvil used in

its assessment. The development of biofidelic sports impact testing dummies would seem to be required for greater understanding of how protective equipment truly functions once on an athlete<sup>8</sup>.

Tensing has been shown to change the kinetics of impacts, but its exact role in injury prevention is unclear. In the impact test between a medicine ball and the thigh tensed muscle was found to increase force by 11%, decrease energy absorption by 10% whilst producing significantly less discomfort (relaxed:  $4.2 \pm 1.1$ ; tensed:  $1.4 \pm 0.8$ ). Athletes with a greater proportion of muscle mass also experienced less discomfort. Increased force has been considered to create higher internal stress and a greater likelihood for injury, but tensing seemed to reduce discomfort, and possibly injury, by increasing the effective mass of the impacted limb. Tensing also created a more rigid impact which reduced soft tissue deformation and increased its energy dissipative properties<sup>9</sup>.

## DISCUSSION

Both passive and active muscle effects can play an important part in impact response at the impact levels seen in sports. Direct transfer of results and knowledge from the crash and ballistic impact literature may not describe all the important aspects of impact response in lower intensity sports impacts.

## REFERENCES

1. Kent RW, Bass CR, Woods WA, Salzar RS, Sang-Hyun Lee, and Melvin J. The role of muscle tensing on the force-deflection response of the thorax and a reassessment of frontal impact thoracic biofidelity corridors. *Proc. IMechE*, 2006; 220: 853-868
2. Bertram JEA and Biewener AA. (1988). Bone Curvature: Sacrificing strength for load predictability? *J Theor Biol* 1988; 131:75-92.
3. Pain MTG, Tsui F and Cove S. *In vivo* determination of the effect of shoulder pads on tackling forces in rugby. *J. Sport Sci* 2008; 26: 75-82.
4. Pain MTG and Challis JH. Soft tissue motion during impacts: their potential contribution to energy dissipation. *J Appl Biomech* 2002; 18: 231-242
5. Pain MTG and Challis JH. The role of the heel pad and shank soft tissue during impacts: A further resolution of a paradox. *J Biomech* 2001; 34: 327-333.
6. Pain MTG and Challis JH. The influence of soft tissue movement on ground reaction forces, joint torques and joint reaction forces in drop landings. *J Biomech* 2006; 39: 119-124.
7. Mills C, Pain MTG and Yeadon MR. 2009. Reducing ground reaction forces in gymnastics' landings may increase internal loading. *J Biomech* 2009; 42: 671-678
8. Tsui F and Pain MTG. The effects of testing techniques on the performance of chest protectors in Tae Kwon Do. Proceedings of the 32<sup>nd</sup> Annual Meeting of ASB, Penn State, USA, 2009
9. Tsui, F., and Pain, M.T.G. The effects of muscle tension on human biomechanical response and perceived impact intensity. Proceedings of the 4th NACOB, Ann Arbor, USA, 2008.

## VALIDATED 3D FINITE ELEMENT MODEL OF WRIST JOINT

V. Balden, Y.Iyer and G.N. Nurick

Blast Impact and Survivability Research Unit, BISRU, Department of Mechanical Engineering University of Cape Town, South Africa victor.balden@uct.ac.za

### INTRODUCTION

The forearm and hand give humans the defining ability to manipulate their environment and perform vital daily activities. When a person falls, reflex reactions cause them to make instinctive use of their hands to protect the body and head from injury. In the process they are often subject to injurious forces, therefore inhibiting their use for necessary activities.

Fracture of the radius bone has been found statistically to be the most common injury, after a fall onto an outstretched hand. This has been found to be the case in children [1], the elderly [2] and during sport [3]. The wrist joint is composed of two joints; the mid-carpal and the radio-carpal. The bones involved are the radius, the ulna, the carpals and metacarpals.

This study aimed to create a validated finite element model of the wrist joint. This model was developed to simulate and understand the force transmission to the radius bone and give insight into the contact stress distributions within the wrist joint.

### MATERIALS AND METHODS

The forces applied to the hand and wrist has been studied experimentally by having subjects fall onto force plates [4 for example]. Such studies have been conducted to determine possible preventative methods to decrease the load applied to the wrist during a fall. These studies can only be used to simulate falls that do not cause injury.

Injury causing loads have to be studied using cadaveric specimens. The fracture load of individual cadaveric radius bones has been studied through compression testing, while the pressure and force transfer through the wrist joint has been studied through various loading methods of cadaveric wrist joints [5 for example].

Investigating numerous loading conditions can not be studied without the use of numerous cadaver arms and therefore numerical techniques are developed. Finite Element models [6 amongst others] and Rigid Body Spring Models [7, 8, 9] are used to simulate these

various loading conditions and to study the effect of injurious loading conditions [10].

Bone solid geometry is created by extracting the edges contours from CT images with image segmentation software, MIMICS. The material properties for each bone were assigned based on the Hounsfield units, extracted from the CT dataset of a volunteer 40 year old male subject. Following surface mesh optimisation in MIMICS the surface mesh was converted into a volume mesh and imported into the general purpose finite element software, ABAQUS. The completed model is shown in Figure 2.

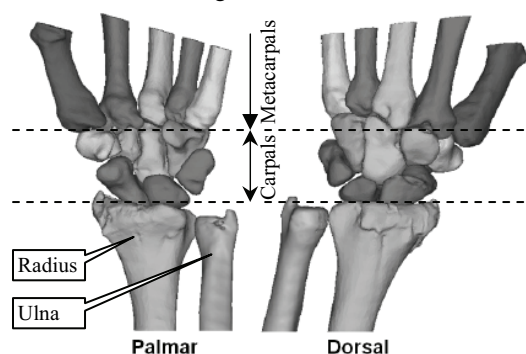


Figure 1: Wrist Joint Bone Geometry

CT scan data does not give a clear description of the articular cartilage present covering the bones. To account for the presence of cartilage in the model, an exponential contact pressure-cartilage thickness relationship was defined for the regions of bones where cartilage and cartilage-cartilage contact occurs.

The ligaments that connect the metacarpals to the carpals, the carpals to each other and the carpals to the radius were included in the FE model. Ligaments were simulated as axial connectors, with prescribed linear stiffness.

### RESULTS

For the validation procedure the FE model the results were compared to multiple experiments, which may be summarised as four validation criteria. The experimental results of cadaver tests are given in the

form of experimental corridors as different cadavers subjected to the same load give a spread of different results. The ability of the model to simulate the cadaver tests can be determined by how closely the simulated response falls within the corridor defined by the experiments. The published experimental work used for validation is summarised in Table 1.

Reference	Load		Experiment or Numerical Model
	Magnitude (N)	Application	
Blevens et al. [11]	178	Wrist tendons	Experiment
Teurlings et al. [13]	300	Wrist	Experiment
Horii et al. [8]	140	5 metacarpals	2D rigid body spring model
Majima et al. [9]	140	5 metacarpals	2D rigid body spring model
Veigas et al. [5,12]	50,100,200,400	5 metacarpals	Experiment
Pietruszczak et al. [10]	700	Fossa on radius	FE model

Table 1: Published experimental work used in validation procedure.

The first validation criteria considered was the contact area of scaphoid and lunate on the radius articular surface. The model results fit well within the experimental corridors for the two different parameters of total contact area/joint area ratio and scaphoid/lunate contact area ratio.

The second validation criteria considered the maximum contact pressure on the radius articular surface. The model fits within the experimental corridors for two parameters of the three used in this criterion. These two parameters were total maximum contact pressure with increasing load and ratio of scaphoid to lunate maximum pressure.

The third parameter was the individual maximum contact pressures of the radius-scaphoid and radius-lunate articulations. Here the model only fell within the boundaries for the radius-scaphoid case. The model over-predicted the maximum value boundaries for the radius-lunate.

The contact pressure distribution in the mid-carpal joint was qualitatively compared to the work of Majima et al. [9] which showed general agreement on the locations of contact pressure.

The third criterion was a qualitative comparison as to which ligament carried the most tensile force in the model. The hamate-triquetrum ligament was predicted to carry the greatest tensile load. This was not the ligament that carried the largest tensile load in the validation work. The difference is thought to be due to the validation work being a 2D model, where out of plane movement is prevented.

The final criterion was the force transmission percentages through the radio-carpal and mid-carpal joints. The predicted radio-carpal force transmission percentages are within the experimental boundaries. The capitate-lunate and scaphoid percentages are also within these boundaries. The scaphoid-trapezoid and trapezium force transmission is however below the boundary of the experimental work.

## DISCUSSION

The developed finite element model generally satisfied the imposed validation criteria 1, 2, and 4. Validation criteria three was decided to be ineffective as a comparative criterion as the data is extracted from a 2D model, thereby restricting out of plane bone movement of the scaphoid and lunate which occur naturally.[14]

## REFERENCES

- [1] M. Kramheft and S. Bedtker. Epidemiology of distal forearm fractures in danish children. *Acta Orthopaedica*, 59(5):577-559, 1988.
- [2] P.W. Thompson, J. Taylor, and A. Dawson. A annual incidence and seasonal variation of fractures of the distal radius in men and women 25 years in Dorset, UK. *International Journal of the Care of the Injured*, 35:462-466, 2004.
- [3] C. Hill, M. Riaz, A. Mozzam, and M.D. Brennen. A regional audit of hand and wrist injuries: A study of 4873 injuries. *Journal of Hand Surgery*, 23B(2):196-200, 1998.
- [4] J. Chiu and S.N. Robonovitch. Prediction of upper extremity impact forces during falls on the outstretched hand. *Journal of Biomechanics*, 31:1169-1176, 1998.
- [5] S.F. Viegas and R.M. Patterson. Load mechanics of the wrist. *Hand Clinics*, 13(1):109-128, 1997.
- [6] P. Ledoux, D. Lamblin, and R. Targowski. Modifications to the mechanical behaviour of the wrist after fracture of the scaphoid modeling by finite element analysis. *Acta Orthopaedica Belgica*, 67:236-241, 2001.
- [7] F. Schiund, W.P. Conney, R.L. Linscheid, K.N. An, and E.Y. Chao. Force and pressure transmission through the normal wrist. a theoretical two-dimensional study in the posteroanterior plane. *Journal of Biomechanics*, 28:587-591, 1995.
- [8] E. Horii, M. Garcia-Elias, K.N. An, A.T. Bishop, W.P. Cooney, R.L. Linscheid, and E.Y. Chao. Effect on force transmission across the carpus in procedures used to treat kienbock's disease. *The Journal of Hand Surgery*, 15(A):393-400, 1990.
- [9] M. Majima, E. Horii, H. Matsuki, H. Hirata, and E. Genda. Load transmission through the wrist in the extended position. *The Journal of Hand Surgery*, 33(A):182-188, 2008.
- [10] S. Pietruszczak, K. Gdela, C.E. Webber, and D. Inglis. On the assessment of brittle-elastic cortical bone fracture in the distal radius. *Engineering Fracture Mechanics*, 74:1917-1927, 2007.
- [11] A.D. Blevens, T.R. Light, W.S. Jablonsky, D.G. Smith, A.G. Patwardhah, M.E. Guay, and T.S. Woo. radio-carpal articular contact characteristics with scaphoid instability. *The Journal of hand surgery*, 14A (5):782-790, 1989.
- [12] S.F. Veigas, R. Patterson, P. Peterson, J. Roefs, A. Tencer, and S. Choi. The effect of various load paths and different loads transfer characteristics of the wrist. *The Journal of Hand Surgery*, 14A:458-465, 1989.
- [13] L. Teurlings, G.L. Miller, and T.W. Wright. Pressure mapping of the radioulnar carpal joint: effects of ulna lengthening and wrist position. *The Journal of hand surgery*, 25B:346-349, 2000.
- [14] R. Schmitt, S. Froehner, G. Coblenz, and G. Christopoulos. Carpal instability. *European Radiology*, 16:2161-2178, 2006.

## TRAMPOLINE FRAME IMPACT ATTENUATION: PADDED METAL-FRAME VS SOFT-EDGE SYSTEM

David Eager<sup>1</sup>, Chris Chapman<sup>1</sup>, Peter Davidson<sup>2</sup>

1. University of Technology Sydney, Australia; David.Eager@uts.edu.au
2. University of Otago, Dunedin, New Zealand; Peter.Davidson@otago.ac.nz

### INTRODUCTION

Trampolines are a major source of childhood injury both in Australia and around the globe. In Australia, trampolines account for approximately 31% of all childhood injuries. In the age groups 0-4 years and 10-14 years they are the most common source of injury accounting for 40% and 46% of cases respectively.

The aim of this research was to measure the impact force that users would experience if they sustained a head impact on a trampoline frame.

### MATERIALS AND METHODS

A SpringFree™ soft-edged trampoline and variety of padded metal-frame trampolines were tested in accordance with Australian Standard AS 4989:2006 Amdt2 Trampolines – Safety aspects Appendix C ‘Test method for frame padding and other soft-edge systems.



Figure 1: SpringFree Trampoline with instrumented 5 kg J-headform at 1.5 m above the soft-edge safety system prior to release

Following AS4989:2006 the pass/fail criteria are:  $g_{max}$  shall be less than 200 g; and the duration of the largest acceleration pulse shall be greater than 6 ms.

The maximum jerk ( $j_{max}$ ) was also recorded.

### RESULTS

The results of this research are contained in Figures 2 to 6 below.

Figure 3 depicts the test results from an impact onto a vinyl covered pad directly above a support leg. A failure was recorded for both magnitude at 328 g and duration of the first acceleration pulse at 1.3 ms. A maximum jerk of 326,000 g/s was also recorded.

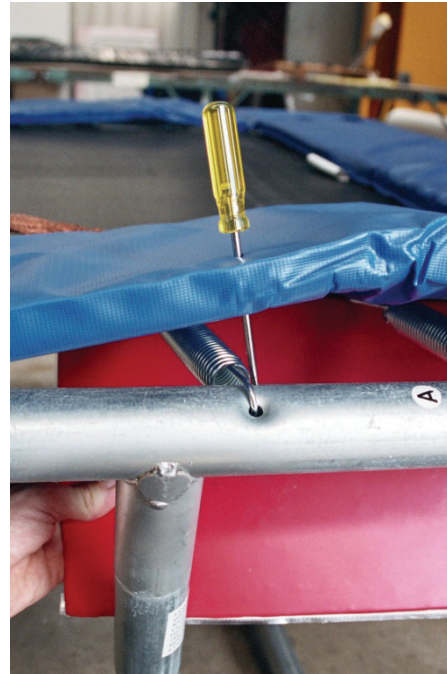


Figure 2: Padded metal-frame trampoline where the pad has been impacted above a spring connection. The pad and cover have been sheared by the impact, resulting in a FAIL

Figure 4 depicts the test results from an impact onto at a vinyl covered pad directly above a

spring connection. A failure was recorded for the duration of the first acceleration pulse at 2.7 ms and a technical fail was recorded for the  $g_{max}$  at 199.4 g. A maximum jerk of 187,600 g/s was also recorded.

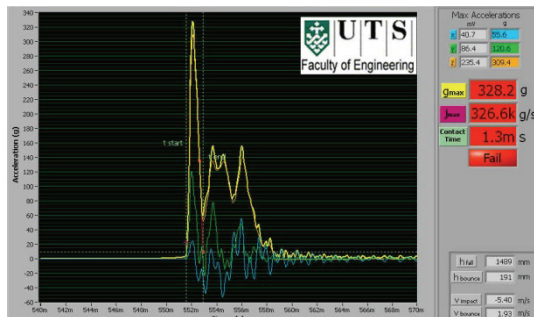


Figure 3: Padded metal-frame trampoline impact onto the pad above a leg ( $g_{max}$  328 g;  $j_{max}$  326,000 g/s; Time duration 1.3 ms = FAIL)

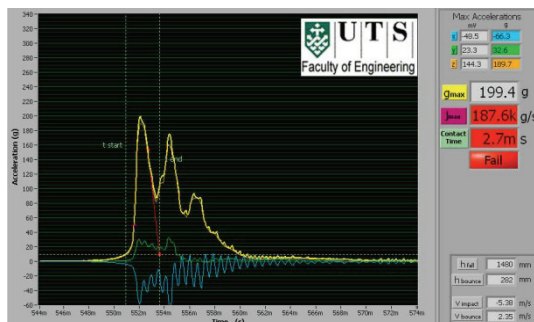


Figure 4: Padded metal-frame trampoline impact onto the pad above a spring connection ( $g_{max}$  200 g;  $j_{max}$  187,600 g/s; Time duration 2.7 ms = FAIL)

Figure 5 depicts the test results from an impact onto a vinyl covered pad directly above the tubular frame 200 mm from a leg support. A failure was recorded with the duration of the first acceleration pulse at 4.2 ms. A maximum jerk of 132,400 g/s was also recorded.

Figure 6 depicts the test results from a SpringFree™ trampoline being impacted onto the soft-edge safety system. A pass was recorded for the  $g_{max}$  at 16 g and duration of the first acceleration pulse at 50.4 ms. A maximum jerk of 10,700 g/s was also recorded.

## DISCUSSION

It was found that the test location influenced the results significantly. For example it was noted that if there was a protrusion beneath the padding system such as a bolt or spring connector the pads were permanently damaged and the magnitude of the impact forces was greater.

The performance of the SpringFree™ soft-edge trampoline was quite remarkable compared to that of all the traditional padded metal-frame trampolines.

The design of the SpringFree™ trampoline is inherently safer than the traditional trampoline in that it removes the hard metal spring and frame from the plane of the jumping surface and thus relocates all hard impact points away from the user.

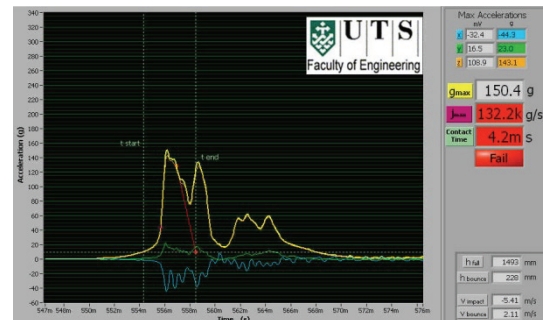


Figure 5: Padded metal-frame trampoline impact onto the pad 200 mm offset from leg ( $g_{max}$  150 g;  $j_{max}$  132,400 g/s; Time duration 4.2 ms = FAIL)

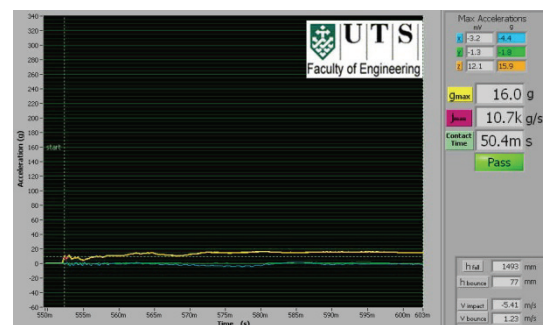


Figure 6: SpringFree™ trampoline impact onto the soft-edge safety system ( $g_{max}$  16 g;  $j_{max}$  10,700 g/s; Time duration 50.4 ms = PASS)

## REFERENCES

1. Cassell E and Ashby K. Hospital-treated falls and other injury involving trampolines. *VSIU* 28 April 2011.

## FALLS INTO VIA FERRATA CLIMBING SETS CAN CAUSE SEVERE INJURIES FOR LIGHTWEIGHT CLIMBERS

Emrich Pasching, Eckehart Diem, Stefan Litzenberger, Anton Sabo

University of Applied Sciences Technikum Wien, Institute for Sports Engineering & Biomechanics, Hoehstaedtplatz 5, A-1200 Vienna; litzenberger@technikum-wien.at

### INTRODUCTION

A via ferrata (ital. for: “iron road”) is a climbing route with fixed iron climbing aids in steep, rocky mountain terrain. Vie ferrate can be found mainly in Europe, North America and Asia. Currently more and more are built. Climbers are using special protective equipment: a via ferrata set which should prevent injuries by attaching a break that is attached to the via ferrata and the harness worn by the climber.

As the via ferrata set is part of the climber's protective equipment it has to fulfill certain standards. Whereas these standards vary in different parts of the world the standards for falling behavior are tested and limits are set. The European standard [1] specifies that when a steel mass of 80kg is dropped from 5 meters in the set the breaking forces are not to exceed 6 kN and the breaking distance has to be less or equal 120mm.

The fact that falling in a via ferrata set would be rather uncomfortable was never doubted nonetheless it never was examined which consequences a fall within the standard's limitations would have on the human body. Whereas the via ferrata set should react as expected for climbers with the same or more weight as is used for testing the effect on (much) lighter persons (e.g. children, lightweight females) remained unclear.

Therefore the Deutscher Alpenverein (German Alpine Association - DAV) initiated a test series with crash dummies of various sizes and weights.

### MATERIALS AND METHODS

Four different NCAP Frontal Crash Dummies (First Technology Systems, Plymouth, MI, US) representing humans of different weights and ages (3 yrs. (15kg); 10 yrs. (34kg); female adult (48kg); male adult (77kg)) were dropped from a height of 5 meters into different via ferrata sets to acquire realistic data (Fig. 1). A total of 108 measurements were conducted within 3 days. During a fall the acceleration of the dummies and breaking forces were A/D converted with a frequency of 1024Hz and 1000 Hz, respectively and recorded on a PC. Additionally synchronous video

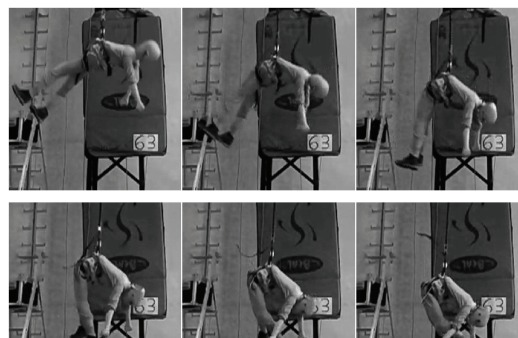


Fig. 1: Still frames of a drop test (fall height = 5m)

data were recorded with two Sanyo VPC HD 2000 cameras (240fps, 448x336px).

The used via ferrata sets were of two different types: (1) modern web based sets where a webbing is ripped apart and absorbs energy and (2) cheaper rope breaking systems which absorb energy by friction. The used systems were (company - model): for (1) Black Diamond - Easy Rider; Edelrid - Cable Light; Mammut - Via Ferrata Tec Step; Petzl - Scorpio; Salewa - G4 Attac Premium; for (2) Mammut - Via Ferrata Y; Petzl - Zyper; Salewa - Attac G3.

Data were evaluated for the measured absolute values and the degree of injury, respectively. For the latter the Abbreviated Injury Scale (AIS) [2] was used where the degree of injury is assessed in 7 AIS classes (0: uninjured – 6: maximum injury, no chance of survival). According to this scale each via ferrata set was rated sufficient ( $\leq$  AIS class 3, severe injury not perilous, no permanent damages) or insufficient ( $\geq$  AIS class 4, perilous, survival likely) for certain climbers' weights.

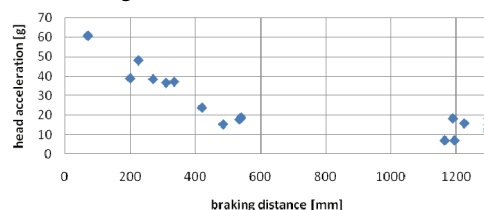


Fig. 2: Head acceleration of the 48kg dummy plotted versus the breaking distance

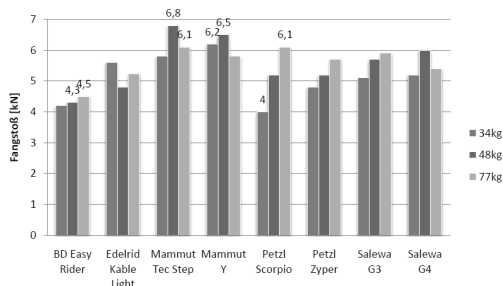


Fig. 3: Braking forces for different via ferrata sets and different climbers' (dummies') weights, maxima and minima for each weight are displayed in the plot.

## RESULTS

As expected the breaking forces of the via ferrata sets raised with raising dummy weight and shorter braking distance (Fig. 2). The braking forces for the different via ferrata sets and different climbers' (dummies') weights are displayed in Fig. 3. It is noticeable that the

maximum braking force allowed in the European standard (6kN) is exceeded in several cases although the masses are lower than the mass used for standard testing (80kg) (Fig. 3).

AIS class analysis for weights of 15kg (3 yrs.), 48 kg (female adult) are already fully evaluated. For the 15kg measurements all climbing sets exceeded an AIS of 3 (in 3 cases AIS = 5, in 3 cases AIS = 4). For the 48kg measurements three climbing sets were sufficient (AIS ≤ 3) all others showed AIS = 3,5.

## DISCUSSION

The results of the tests showed, that modern web based sets have less breaking force than rope breaking systems. 3 breaking systems out of 8 had higher breaking forces than the European standards allow.

Most of the via ferrata sets showed a positive weight-breaking force behaviour for lightweight users. Braking force decreased with increasing user's weight which is related to the expected injuries. Modern web based via ferrata sets showed lower breaking forces than rope breaking sets.

Although detailed results according to injury levels still have to be verified to specify a weight limit for falling into a via ferrata set it can be stated that persons weighing less than 50kg should not in any case risk a drop in a via ferrata set, as – according to AIS evaluation – severe injuries are to be expected for lightweight climbers.

According to the gathered data a minimum weight limit for via ferrata sets should be established. European standards should be adopted in consideration of the presented results of this study.

## REFERENCES

1. DIN EN 958, *Climbingequipment – Energy absorbing systems for via ferrata*; German version EN 958:2006, march 2007.
2. Madea B and Brinkmann B. Abbreviated Injury Scale. *Handbuch gerichtliche Medizin*, Springer-Verlag Berlin Heideberg New York, vol. 1, ch. 5.6, pp. 294-296

## UPLOAD YOUR HEAD INJURY!

A NOVEL METHOD FOR BIOMECHANICAL PREDICTION. IS IT FEASIBLE?

Andrew Glenn<sup>1</sup>, Andrew Short<sup>1,2</sup>

1. University of Melbourne, Biomedical Engineering Department
2. BioForensic Consulting, Melbourne

### INTRODUCTION

Current understanding of human injury is largely based on cadaver work conducted between 25<sup>1</sup> and more than 100 years ago<sup>2</sup>. While one million head injuries occur in the US each year<sup>3</sup>, obvious ethical and procedural barriers slow the progress of traditional laboratory means of further understanding.

We rely on a criterion that requires the instantaneous measurement of acceleration at a rate greater than every millisecond<sup>1</sup>. This will not be generally available and certainly not in the ballooning stores of on-line video which includes many head impacts.

If a simpler criterion were to be used as a predictor along with the large numbers of injuries captured on video in the online community, it may be possible to make progress.

Furthermore, the simple tracking required in this proposal is very achievable when we consider the wealth of computer vision functions already been demonstrated and readily available to the commercial market.

This abstract considers the power of a simpler head injury predictor put together with a much larger data set.

### BACKGROUND

The worldwide benchmark for predicting head injury is the Head Injury Criteria (HIC). The criteria were based on a limited number of tests performed on cadavers mainly in the 1960s to 1990s. The resulting criteria identify the key factors of head injury as a complicated integral of translational acceleration.

Alternative models have been proposed including GAMBIT, Finite Element Models<sup>4</sup>, HIS and the ATB to help improve the predictability of head injury with some claiming improved accuracy over the HIC<sup>5</sup>.

Our point is that increased data must parallel these improved analysis methods and that the stores of

laboratory orientated data is low compared to the volume of real world data. Using video is not a new idea, but to use a simple criterion with it may be novel. While a parallel study considers a simpler criterion of impact speed, this study considers the volume, quality and value of the available on-line video.

### MATERIALS AND METHODS

A feasibility checklist was devised as follows:

1. Is there enough data/video available to work with?
2. Can heads be tracked using such generally poor quality video?
3. And what is the resolution at which impact speed can be measured?
4. Given the limitations will there be any useful data?

#### Is there enough data?



Figure 1: a still from a youtube video which shows a head impact.

We performed a preliminary analysis of YouTube videos to see how many head injury videos we could identify over time. We looked at videos discovered in the first 10 minutes and every subsequent 10 minute period up until 1 hour (See Table 1). We also looked at the ratio of sports-based injury to other injuries.

Table 1. Table of YouTube videos discovered

Time Period (minutes)	Total Videos Found	Sports-based
0-10	42	80%
10-20	45	85%
20-30	38	82%
30-40	43	70%
40-50	32	65%
50-60	34	70%

The drop-off rate was low and the indications are that there are hundreds of suitable videos.

### Can heads be tracked using such generally poor quality video?

Image based systems already provide high-performing and reliable object detectors, motion trackers and impact detectors. These systems are commercially available at prices dramatically less than from-scratch creations. In this scenario however, we have no control over hardware or image quality and thus there are fundamental issues arising from low frame rates, poor camera angles and video quality (noise). Even if we can overcome these, we then need to identify a good method for predicting injury accurately against what may be limited input data. In so doing, we need to identify what data the end-user (our video up loader) can reliably provide to us in order to make correlations between inputs and outcomes. Accordingly, we breakdown our software architecture into 3 subsystems and consider each independently:

A: Video Analyser: performs object recognition, motion tracking and impact detection for video

B: The upload site: The video and data Upload function for users

C: The predictor model: uses the data to learn what might predict head injury likelihood

Figure 2 shows algorithms for noise reduction, edge detection and object tracking which can aid the user in detecting impact speed in terms of the apparent head size.

### What resolution can be achieved in measuring the impact speed?

Speed is determined by how large the object appears in the field of view and the number of frames for which it is visible prior to impact. Given that life threatening injuries to pedestrians begin at 18km/h and become 50% likely at 60km/h, the resolution in the measured speed needs to be to the nearest 5km/h.

In normal video footage, a head impact itself is often poorly captured due to the high acceleration and the short duration of impacts, the approach speed may

have many frames with reasonably clear view as the head approached the impact. It is likely that primarily in-plane motion will be selected for analysis over motion in line with the view.

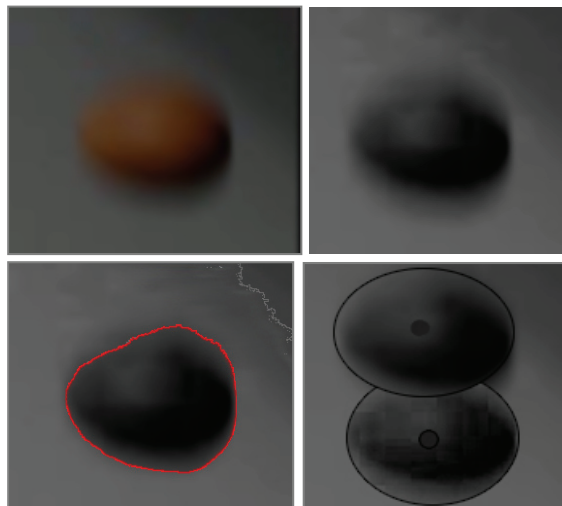


Figure 2: An example of a sequence of image processes that could aid the user in detecting motion in the view.

## DISCUSSION

While the injury outcomes will be self-reported, which has its own problems, this study states simply that the vast array of on-line video can be utilized to trial and possibly validate a simple impact speed based head injury predictor.

## REFERENCES

1. Prasad P & Mertz, H, (1985) The Position of the United States Delegation to the ISO working group 6 on the use of the HIC in the Automotive Environment, Government/ Industry Meeting & Exposition, Washington DC. ISSN 0148-7191
2. O. Messerer, Ueber die gerichtlich-medicinische Bedeutung verschiedener Knochenbruchformen. *Friedreichs Blätter f. Gerichtl. Med.* 36 (1885), pp. 81–104
3. Bakay L and Glassauer FE, (1980) *Head Injury*, Boston Little Brown
4. Head impact biomechanics simulations: A forensic tool for reconstructing head injury?, *Legal Medicine* 11 (2009) S220–S222.
5. Franklyn, Fildes, Zhang et al, 2005. Analysis of finite element models for head injury investigation: reconstruction of four real-world impacts. *Stapp Car Crash J.* 2005 Nov;49:1-32.

## A COMPARISON OF PEAK LINEAR AND ANGULAR RESPONSE BETWEEN THE HYBRID III AND THE HODGSON-WSU HEADFORMS

Marshall Kendall, Evan Stuart Walsh and Thomas Blaine Hoshizaki

Neurotrauma Impact Science Laboratory, University of Ottawa; mkend072@uottawa.ca

### INTRODUCTION

In brain injury research, linear and angular resultant acceleration data have been considered important mechanisms contributing to various level of brain injury [3, 5]. Previous research used animal models or cadaveric heads to gather this information. These methods can be time consuming and somewhat difficult to gather the necessary resources. The development of biofidelic head forms with similar dimensions and weight to that of a real human head has allowed for researchers to repeatedly collect data related to the effects of different impacts on the human head. Currently, there are different types of head forms available for impact testing each with varying degrees of biofidelity and repeatability. Two commonly used head forms are; the Hybrid III and the Hodgson – WSU (NOCSAE). The Hybrid III head form was developed by Dr. Robert Hubbard and Donald McLeod as part of a larger GM project aiming to build a crash test dummy for simulating humans in car accidents. The main goal in the development of this head form was to have the head durable enough to sustain multiple high impacts without breaking, however still producing data within the ranges found in cadaveric head drop studies [1]. The NOCSAE head form was developed from the cadaveric impacts of Hodgson et al. (1971) and is still currently used in certifying football helmets. It is believed that some of the characteristics, i.e density of urethane used for the skin, of this head form may improve the biofidelic response upon impacts. The purpose of this research was to compare the peak dynamic head form responses between the Hybrid III and Hodgson-WSU head forms for similar impacts velocities.

### MATERIALS AND METHODS

Two head forms were used in this study; one Hybrid III and one Hodgson-WSU head form. The Hybrid III head form, engineered by FTSS, weighed  $4.54 \pm 0.01$  kg with dimensions of 154.90 mm and 195.60 mm in breadth and depth. The Hodgson-WSU head form developed by Hodgson et al. from Wayne State University had mass of 4.85 kg and a circumference of  $5.78 \times 10^{-1}$  meters. These two head forms were outfitted with nine single-axis (Endevco

7264C-2KTZ-2-300) accelerometers positioned orthogonally following a 3-2-2 array. The head forms were dropped, unhelmeted and unrestrained, onto a steel anvil on the front (forehead) location. This location was chosen for several reasons. The first being that for comparison with cadaveric data from Hodgson et al. (1971) where the forehead region was chosen as the impact site [1]. The forehead location has been deemed one of six high risk areas for mTBI [4]. Finally, this region is also a principle impact site in helmet testing certifications. Using the monorail drop system, the head forms were dropped from four heights. Processing of the nine signals allowed for the determination of the complete three-dimensional motion of the head. The filtered (SAE 1000 class) [6] acceleration data was collected at 20 kHz. Peak linear and angular data was calculated for each impact condition. Polynomial line of regression curves were calculated from the peak linear and angular acceleration data and compared between the hybrid III head form and the Hodgson-WSU head form, along with Hodgson et al. (1971) cadaveric head drop data. Pearson correlations were calculated for the regression curves created by each data set.

### RESULTS

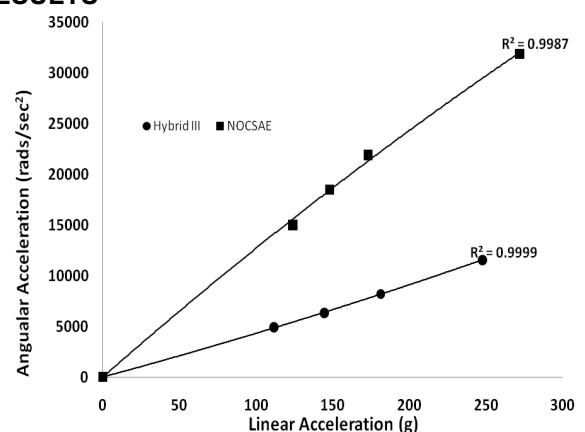


Figure 1. Linear resultant acceleration data in relation to angular resultant acceleration (with  $R^2$  values) for frontal impact of the hybrid III head forms (circle) and the Hodgson-WSU (square).

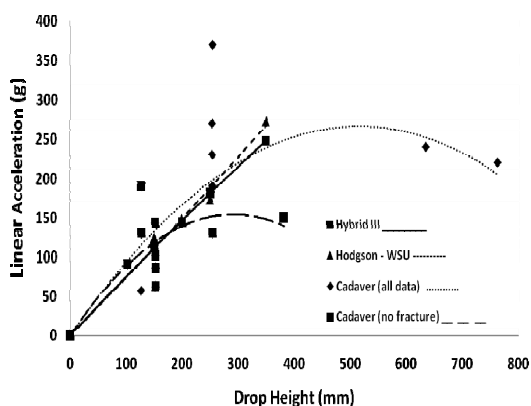


Figure 2. Shows peak linear acceleration and lines of regression for the hybrid III, Hodgson – WSU and cadaveric head drop data (Hodgson et al. (1971) [1].

Table 1.  $R^2$  values for peak linear and angular resultant acceleration of Hybrid III and Hodgson-WSU head forms.

	Hybrid III	Hodgson-WSU	Hodgson (1971 – no fracture)	Hodgson (1971 – all data)
Peak Linear (g)	0.9996	0.9786	0.4616	0.4913
Peak Angular (rads/s <sup>2</sup> )	0.9983	0.9960	N/A	N/A

Table 2. Peak linear acceleration correlation values between Hybrid III, Hodgson – WSU and Cadaveric data.

	Hodgson-WSU	Hodgson (1971 – no fracture)	Hodgson (1971 – all data)
Hybrid III	0.999	0.903	0.995
Hodgson-WSU headform	-----	0.888	0.991

## DISCUSSION

The results of this study show that there exists a very high correlation between peak linear, angular accelerations and impact velocity for both the hybrid III and Hodgson-WSU head forms ( $R^2$  values for all tests of 0.970). This supports a study done earlier which compared the hybrid III head form to other head forms [2] for frontal impacts only. With both head forms, the forehead impacts demonstrated a nearly linear relationship to increasing velocities for both linear and angular accelerations (Figure 1). Though this data is only preliminary, peak linear data from both head forms seem to be very close. There are however, at this point in the data collection, large differences in terms of peak angular response between the two head forms. The Hodgson-WSU produced peak angular values almost three times higher than the Hybrid III.

Comparing the hybrid III and the Hodgson – WSU peak linear acceleration data with previous cadaveric head drop data, it shown in Table 2 that there is good correlation between all three conditions (Table 2). The  $R^2$  values for the cadaveric head drops is quite low in comparison with the Hybrid III and WSU head forms. This is likely due to the inconsistencies associated with the actual human head (geometric differences, size etc...).

It is hypothesized that the different biofidelic characteristics of the two head forms as being the main cause of these peak angular acceleration differences. Density of the urethane used to mimic the facial skin, different resonance frequencies and mass may be some of the parameters causing the differences seen in this study.

The purpose of this study was to compare peak linear and angular responses of the Hybrid III and Hodgson-WSU head forms in terms of linearity related to impact velocity and head form response and differences in peak accelerations between two head forms (Hybrid III and Hodgson-WSU). The results of this research show that there is indeed good correlation between peak accelerations and increased impact velocity for each head form. In comparing peak linear acceleration data from these two head forms to cadaveric data, there also seems to be good correlation. Due to the fact that peak angular acceleration data was not collected in the cadaveric study, no comparisons are possible.

The preliminary data collected thus far seem to show that both head forms produce similar results with regards to Peak linear accelerations. Where they differ seems to be with the peak angular accelerations. Since we do not currently have any angular acceleration data from cadaveric research to compare to, it becomes difficult to determine which head form produces the most realistic dynamic response through impact reconstructions. This is important information as continuing research looks at abilities of different head forms to produce more biofidelic response to reconstructed impacts. Future research should investigate differences in shape of the dynamic response curve of different head forms and its effects on brain tissue deformation using FE modelling.

## REFERENCES

1. Hodgson V.R. et al., NHTSA report no. DOT-HS-800-583, June 1971.
2. Mertz H., Society of Automotive Engineers Inc., 851245: 1-9, 1985.
3. Ommaya AK., et al., *J Biomechanics*, 4:13-31, 1971.
4. Walsh et al., ISBS conference proceedings, Limerick, Ireland, August 2009.
5. Society of Automotive Engineers International, Instrumentation for Impact Testing – Part 1- Surface Vehicle Recommend Practice, J211-1, 2007.

## COLLISION INJURIES IN RUGBY UNION

John Ryan

Leinster Rugby, Dublin, Ireland J.Ryan@st-vincents.ie

### INTRODUCTION

Rugby Union is a full contact team sport which initiated in the early half of the 19th century in England. Over the last 170 years it has undergone many modifications. The game is played by two opposing teams of fifteen players. The game is played on a grass pitch measuring 100 metres long and 70 metres wide and lasts for two periods of 40 minutes each. Recently synthetic surfaces have been developed but are not yet commonplace. The aim of the game is to carry an oval leather ball across the opponents' line or to score points by kicking it over the crossbar of a set of goal posts.

The laws of the game have changed in response to a variety of influences including spectator opinion, commercial needs and not least player welfare. Until 1995 rugby union was an amateur sport where players often participated from their first years in school until the age of 35 or so. In 1995 all restrictions on payment of players were removed and the sport turned 'professional'. This led to the sport being played by fitter, stronger and faster athletes who in turn have contributed to a higher profile of injuries sustained playing the game.

Injuries can occur during any part of the game. The game is played around a number of set pieces known as scrums and lineouts. A second more loose type of play includes competing for possession of the ball in 'rucks' and 'mauls'. Players in possession of the ball may be tackled by opponents below the neck in an attempt to retrieve the ball.

### RUGBY INJURIES

When considering injuries sustained in collisions during the games Newton's second law of physics is highly applicable.  $Force = Mass \times Acceleration$ . Thus the greater the force applied to an individual's body the greater the potential damage that can result. Clearly therefore the bigger a player and the faster he is travelling at the time of a collision then the more likely he is to cause and sustain a physical injury.

The mechanism of injury is highly relevant in understanding how injuries are sustained. A number of movements which can occur in a game can lead to specific injury patterns. Hyperflexion, hyperextension and axial forces can lead to spinal and ankle injuries. Valgus and Varus forces are frequently associated with knee and elbow injuries as is rotation. Abduction with external rotation contributes to anterior shoulder dislocations. Direct blunt trauma is associated with head injuries, collapsed lungs and solid organ injury such as liver and splenic tears as well as bowel perforations. Genital injuries are uncommon but are exposed to blunt trauma as well as penetrating wounds from football boot studs. In general penetrating injuries are uncommon but injuries to the eye from fingers are unfortunately seen and not always accidental. Traction injuries occur with tendon attachments being avulsed with or without bone fragments.

### INJURY RESEARCH AND PREVENTION

Over the last 30 years the sport has attracted an increasing volume of research interest addressing the epidemiology, mechanism and prevention of injuries. The 'tackle' has been identified as the phase of play producing most injuries. Research has also identified risk factors and individual playing positions in a match as presenting risk for injury which has led to the need for individual position specific injury-prevention programmes in rugby. The injury rate per game has been variably reported ranging from 10.8 in youths to 57.2 in under 20 tournaments and 83.9 per 1000 player-match-hours in the 2007 International Rugby Board World Cup tournament. Injury rates among youths are lower than in adults. The risk and the severity of injury appears to increase with age.

The volume of injury research publications has increased since the advent of the professional game in 1995. Numerous rule modifications which have changed the game have nevertheless been associated with high risk injuries to particular sites including the shoulder, thigh, ankle and head. Increasingly the tackle has become the phase of play in which most

injuries occur followed by rucks and mauls. Furthermore injuries are more likely to occur in the second half of a game, and forwards are more likely to be injured than backs. The consequences of injuries sustained during games are significant not only for the player but also the club who can expect to have 18% of their players unavailable for selection as a consequence of match injuries.

Injury prevention has become a key function of governing authorities. In New Zealand the introduction of the RugbySmart programme coincided with a reduction in the rate of disabling spinal injuries arising from scrums. Other interventions such as the introduction of padded headgear to prevent head injury has not met with similar gains. Headagear will however reduce scalp lacerations and mouth guards lower the risk of orofacial injuries. Well fitting shoulder pads may decrease the extent of soft tissue injury but have not been shown to decrease the incidence of severe shoulder injuries.

Of all injuries sustained in rugby union, catastrophic neck injuries have perhaps been the most reported over the last 30 years. In particular this was highlighted by the high profile case of Tom Evans a Scottish player who sustained a serious neck injury in an international match against Wales in 2010 (Figure 1).

## CONCLUDING REMARKS

Although the overall incidence remains low the injury attracts emotive and reactions and strong public concern. Injury rates have changed in response to

scrum laws. Appropriately injury prevention strategies should be focused on weight training activities and scrummaging. The use of injury databases is crucial going forward if the effects of changes and interventions are to be appropriately evaluated. However for a variety of reasons, to date, national governing unions and the International Rugby Board have yet to make meaningful strides in this regard.

Rugby Union remains a highly popular collision sport. The introduction of professionalism has paralleled an increase in the severity of injuries due to changes in body mass and speed. Rugby Unions are responding to changing injury patterns with law modifications. In the future injury data bases and close monitoring of trends in injury profiles will hopefully contribute to safeguarding player welfare.



Figure 1: Tom Evans in match against Wales.

## CLASSIFICATION OF COLLISIONS IN ELITE LEVEL RUGBY UNION USING A WEARABLE SENSING DEVICE

Daniel Kelly<sup>1</sup>, Garrett Coughlan<sup>2</sup>, Brian Green<sup>2</sup>, Brian Caulfield<sup>1</sup>

1. Clarity Center, University College Dublin; daniel.kelly@ucd.ie
2. Irish Rugby Football Union, Ballsbridge, Dublin

### INTRODUCTION

Elite rugby union teams currently employ the latest technology in order to monitor and evaluate the physical demands of training and games on their players. Tackling has been shown to be the most common cause of injury in rugby union (Fuller et al. (2007a), Garraway et al. (1999)). However, current player monitoring technology does not effectively evaluate player tackling measurements. Currently, in order to evaluate measurements specific to player tackles, a time consuming manual analysis of player sensor data and video footage is required. The purpose of this work is to investigate tackle modelling techniques which can be utilized to automatically detect player tackles and collisions using sensing technology already being used by elite international and club level rugby union teams. In this paper we discuss issues relevant to automatic tackle analysis, describe our technique to detect tackles using sensing data and validate our technique by comparing automatically detected collisions to manually labelled collisions using data from elite club and international level players.

### MATERIALS AND METHODS

Sensing devices, currently being used by elite rugby union teams, contain a GPS receiver and a 3-axis accelerometer. GPS receivers track player position over time, and have primarily been used to measure player speed and distance travelled during training sessions or competition. However, GPS technology does not measure details of the consequences of player actions on the body such as tackles. Tackles are the main cause of injury in rugby; therefore a system which can automatically measure tackle specific information could be vital in making decisions on training content, aimed at reducing the incidence of injury, for individual players and the team.

Accelerometers can quantify body impact by measuring the acceleration experienced by the player. However, while analysis of positional movement (i.e. intensity and duration of running bouts) can be carried out automatically, analysis of physical loads during specific actions (i.e. tackles and collisions) requires a significant amount of time consuming manual analysis. Owing to the lengthy time that manual tackle analysis takes for each player, it is impossible to provide staff with real time tackle information that could be used to make decisions on training content for individual players and the team. In contrast, an automatic system could provide coaches and medical staff with real-time tackle information which could give practical guidance in training volumes and loads. An automatic system could also monitor the number and load sustained in tackles throughout a season (in matches and training sessions) and flag players who are at risk to injury.

In recent years, machine learning and pattern recognition techniques have become increasingly important in the area of movement evaluation (Pfeifer & Hohmann(2011)). Pfeifer & Hohmann (2011) propose that simple linear models are inadequate in understanding and explaining human behaviour or movement and more complex, non-linear, methods of analyzing movement characteristics are needed. In this work we propose a combination of a number of different non-linear pattern recognition techniques in order to understand and classify the complex movements of a rugby tackle. Due to the complexity of the different types of impacts which can occur in a training session or a match, the tackle detection system must have the flexibility to configure itself to these different signals. We utilize two machine learning models to create a framework which can learn the complex relationship between the source data (acceleration signals) and the target data (decision of what is and is not a collision). Support Vector Machine (SVM) and Hidden Conditional Random Field (HCRF) models were selected to learn the relationship between the source and target data. The

goal of the tackle classification system is to discriminate between impacts (peaks in acceleration) which are tackles and impacts which are not tackles. This is a difficult problem due to the fact that, on average, 99% of the impacts which occur during a match represent events which are not tackles. The first step in the algorithm is the learning model used to train the system to detect tackles. Due to the large ratio of non-tackles impacts to tackles impacts, there is a large variation in the types of acceleration signals which can occur during a non-tackle impact. Given a labelled training set of tackle and non tackle impacts, it is difficult to train a single model to discriminate between the tackle and non tackle impacts. We propose a solution to this by automatically splitting the training set up into subsets and training different types of classifiers to model different aspects of the relationship between tackle and non tackle impacts. Each classifier is then fine tuned such that an optimal subset of the classifiers can be combined to create a linear combination of complimentary classifiers. The classification results from each of the classifiers in the linear combination are then utilized to make an overall decision as to whether or not the input data is a tackle.

## RESULTS

In order to evaluate the performance of our proposed system in detecting collisions, we compare the output of our system with that of manually labelled tackles. We use data collected from three players, which we will refer to as player A, B and C, to test the system. Data for player A and B was collected during an elite club level rugby union match and data for player C was collected during an elite international rugby union match. Each player's data set was pre-processed to extract a set of tackle features. A total of 1179, 619 and 383 impacts peaks were detected for player A, B and C respectively. Each impact peak was then classified by our tackle detection technique. The automatically detected collisions were then compared to the set of manually labelled collisions and the number of true positives (TP), false positives (FP), true negatives (TN) and false negatives (FN) were counted.

Player	#TP	#FP	#TN	#FN	Precision	Recall
A	23	1	1153	1	0.958	0.958
B	24	1	591	3	0.96	0.888
C	23	1	351	1	0.958	0.958
<b>All</b>	<b>70</b>	<b>3</b>	<b>2102</b>	<b>5</b>	<b>0.958</b>	<b>0.933</b>

## DISCUSSION

Movement sensing technology is now extensively used by professional rugby union teams in order to improve physical conditioning and to reduce injury risk. This technology is used to analyze the type, frequency and duration of movement activities performed by a player, and their relationship to the team's respective tactics. While current

implementations of this technology can be used to quantify overall physical work and therefore be utilized to build appropriate training programs to improve physical conditioning, the current technology cannot be effectively used to evaluate injury risk. A number of works have investigated the cause of injury in rugby union and have reported that the main cause of injury in training and match situations is player collisions. In order for GPS/ Accelerometer technology to be effectively utilized as an injury risk assessment and performance tool, a method to automatically identify player collisions using the GPS/ Accelerometer data is needed.

This work addresses the need for an objective and real-time tackle analysis system by developing a technique to automatically classify player collisions using sensing devices already being used by elite rugby union teams. We have shown that our technique performs well at detecting collisions using data collected from two players during an elite club level match and from one player during an elite international level match. When compared to manually identified collisions, our learning grid approach achieved a recall of 0.933 and a precision of 0.958. These measures demonstrate that our system is able to consistently identify collisions with very few false positives and false negatives. The high performance of our collision classification technique means that coaches, medical and strength and conditioning staff can obtain reliable and objective collision measurements in real-time for individual players. These collision measurements can then be utilized to develop injury management protocols and return to play criteria for individual players and teams. Future studies, in a larger sample size, could investigate more detailed classification of collisions with the aim of identifying successful or unsuccessful tackles, which would have applications in player performance evaluation, as well as the identification of the location on the player's bodies which received the impact.

## REFERENCES

1. Fuller, C. W., Brooks, J. H. M., Cancea, R. J., Hall, J., & Kemp, S. P. T. (2007a). Contact events in rugby union and their propensity to cause injury. *British Journal of Sports Medicine*, 41, 862-7.
2. Garraway, W., Lee, A., & Macleod, D. (1999). Factors influencing tackle injuries in rugby union football. *British Journal of Sports Medicine*.
3. Pfeifer, M., & Hohmann, A. (2011). Applications of neural networks in training science. *Human movement science*.

## AN INTEGRATED MEASUREMENT SYSTEM FOR ANALYSING IMPACT BIOMECHANICS IN THE RUGBY SCRUM

E. Preatoni<sup>1</sup>, A. Wallbaum<sup>1</sup>, N. Gathercole<sup>2</sup>, S. Coombes<sup>2</sup>, K. Stokes<sup>1</sup>, G. Trewartha<sup>1</sup>

1. Sport, Health & Exercise Science, Department for Health, University of Bath, Bath, UK; e.preatoni/a.wallbaum/k.stokes/g.trewartha@bath.ac.uk,
2. Department of Mechanical Engineering, University of Bath, Bath, UK; n.gathercole/s.coombes@bath.ac.uk

### INTRODUCTION

Competitive scrummaging is a fundamental component of rugby union. Given its intense physical nature and the presence of impacts, the rugby scrum may engender very high biomechanical demands on the players' musculo-skeletal structures and may thus expose rugby forwards to the risk of both acute and chronic (overuse) injuries. Epidemiological studies of rugby injury (1, 2) have shown a moderate incidence of scrum-related injuries (6-8% of all rugby injuries), but have also evidenced the potential seriousness of these occurrences. In fact, even though recent data have suggested a relative decline of scrum related injuries, about 40% of the catastrophic (typically spinal cord) injuries that occur in rugby are related to scrummaging.(3) Furthermore, players may appear asymptomatic while they are active, but they may experience repeated micro-trauma (4) that can contribute to the emergence of long-term pathologies of the spine, including abnormalities (5, 6), reduced mobility (7), and impaired proprioception (8).

While rugby scrums may be associated with a number of potential injury risk factors, there is currently very little quantitative data that tries to identify and describe them. There is a lack of information about the forces and motions involved in actual scrummaging, and, consequently, little objective knowledge about how performance could be optimized and injuries prevented. Quantitative researches about the rugby scrum have been occasional (9-11) but these findings are now limited in applicability due to lack of ecological validity (e.g. scrummaging against rigid frames), measurement issues (e.g. sampling rates, players only analysed individually), and the fact that engagement techniques and playing styles have changed over the years.

Therefore, the aim of this work was to design, realise and test a new unobtrusive measurement system for assessing the kinematics and kinetics of rugby forwards while scrummaging on the pitch in realistic environmental conditions. At this stage the analysis

was focused on the biomechanics of machine scrummaging, leaving to the second phase of the project the analysis of live conditions with two forward packs involved. The reason behind this choice was the need for controllable and repeatable experimental conditions as well as the unavailability of devices that can directly measure forces in live scrums.

### MATERIALS AND METHODS

The measurement system (Figure 1) integrated three different subsystems for: (I) measuring forces exerted by players; (II) capturing players' movements; and, (III) triggering/synchronizing all the sensors involved in I and II.

**I. Force measurement system:** a commercially available sled-type scrum machine (Dictator, Rhino Rugby, UK) was instrumented with a set of force sensors and accelerometers. Strain gauges transducers (8 elements in full bridge configuration for compression; 4 pairs in full bridge configuration for bending) and a piezoelectric accelerometer (3055B2 LIVM, Dytran Instruments, USA) were positioned on each of the four pusher arms of the machine so that the three components (lateral, longitudinal and vertical) of the applied force and the acceleration imposed by front row players on each arm of the machine could be measured. An Instron testing system was used to calibrate transducers in a range between 0 and 10 kN for compression and between -1 and +1 kN for shear forces. During data collection the scrum machine remained stationary due to its weight and the attachment of additional ratchet straps connected to metal pegs driven into the ground. Any relative movement was negligible and the assumption of rigid body was reasonably respected.

**II. Motion analysis system:** the players' movements were synchronously captured by 4 digital video cameras from 3 different views (top, left and right). Side cameras (Sony HDR-HC9) were placed on tripods at a distance of about 18m from the centre of

the scrum. Top cameras operated at 200 Hz (Sony HVR-Z5) and 50 Hz (Sony TRV-900E) respectively, and were positioned at a height of about 8 m and oriented vertically downwards from the ground by means of two winch-stands and a horizontal truss. A rigid frame 3D calibration object (3.0 x 1.8 x 0.9 m) was used at the beginning of each testing session for multiple 2D calibrations using 4-point projective scaling. Vicon Motus software (v.9, Vicon Motion Systems, USA) was used for the digitisation of selected body landmarks and for the estimation of kinematic variables (displacements, angles and their derivatives).

**III. Synchronization and audio** the synchronization of the measuring devices was carried out through a reconfigurable embedded control and acquisition system (cRIO-9024, National Instruments, USA) operating real time, and specially designed software implemented in Labview (v.2010, National Instruments, USA). This system was also used to: excite strain gauge circuits; collect force and acceleration signals at a frequency of 1000 Hz; and, simulate the referee's calls during a real scrumming, by playing pre-recorded audio files with standardised timing between the subsequent vocal commands. The control system also triggered LED arrays visible in each camera view to allow subsequent time synchronisation of video data and force data to within 1 ms.



Figure 1. Experimental set-up

## RESULTS AND DISCUSSION

The implemented measuring system proved to be effective for the analysis of impacts biomechanics in the rugby scrum. The system can be transported to a standard pitch or a suitable patch of ground ( $\geq 36 \times 12$  m) and assembled in less than 2 hours. It allows measurement of the 2D kinematics of the players from two different planes of motion (lateral and horizontal) and the 3D kinetics of the interaction between the scrum machine and the front row players. This gives the opportunity of gathering and analysing data about the forces/movements developed by forward packs as they engage in a scrum and how these forces/movements vary across different playing levels and with different engagement techniques (see Figure 2 for an example). This will give the possibility to gain more insight into the type and intensity of demands placed on forwards during scrummaging and, hence, to understand the factors related to the occurrence of acute and chronic injuries. It will also

form the quantitative basis for any potential coaching, refereeing modifications or other (on field) recommendations to manage injury risk whilst maintaining or improving performance levels. Ultimately, the system is open to future developments that include the integration of further measures (e.g. pressure distribution, wearable sensors) and the study of live, competitive (two teams) scrummaging.

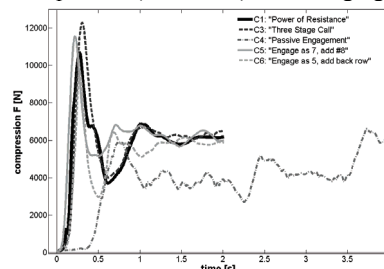


Figure 2. Example of the overall compression force (sum of the 4 arms) under 5 different engagement conditions.

## REFERENCES

- Brooks JH, Fuller CW, Kemp SP, Reddin DB. Epidemiology of injuries in English professional rugby union: part 1 match injuries. *Br J Sports Med.* 2005 Oct;39(10):757-66.
- Targett SG. Injuries in professional Rugby Union. *Clin J Sport Med.* 1998 Oct;8(4):280-5.
- Quarrie KL, Cantu RC, Chalmers DJ. Rugby Union injuries to the cervical spine and spinal cord. *Sports Med.* 2002;32(10):633-53.
- Berge J, Marque B, Vital JM, Senegas J, Caille JM. Age-related changes in the cervical spines of front-line rugby players. *Am J Sports Med.* 1999 Jul-Aug;27(4):422-9.
- Castinel BH, Adam P, Milburn PD, Castinel A, Quarrie KL, Peyrin JC, et al. Epidemiology of cervical spine abnormalities in asymptomatic adult professional rugby union players using static and dynamic MRI protocols: 2002 to 2006. *Brit J Sport Med.* 2010;44(3):194-9.
- Scher AT. Premature onset of degenerative disease of the cervical spine in rugby players. *S Afr Med J.* 1990 Jun 2;77(11):557-8.
- Lark SD, McCarthy PW. Cervical range of motion and proprioception in rugby players versus non-rugby players. *J Sport Sci.* 2007;25(8):887-94.
- Pinsault N, Anxionnaz M, Vuillerme N. Cervical joint position sense in rugby players versus non-rugby players. *Phys Ther Sport.* 2010 May;11(2):66-70.
- Du Toit DE, Venter DJL, Buys FJ, Olivier PE. Kinetics of rugby union scrummaging in under-19 schoolboy rugby forwards. *S. Afr. J. Res. Sport Phys. Educ. Recreation.* 2004;26(2):33-50.
- Milburn PD. The kinetics of rugby union scrummaging. *J Sport Sci.* 1990;8(1):47-60.
- Quarrie KL, Wilson BD. Force production in the rugby union scrum. *J Sport Sci.* 2000;18(4):237-46.

## ACKNOWLEDGMENTS

This research is funded by the International Rugby Board (iRB).

## IMPACT RECONSTRUCTION FROM DAMAGE TO PEDAL- AND MOTOR-CYCLE HELMETS

A.S. McIntosh, D.A. Patton

Risk and Safety Sciences, UNSW, Australia; a.mcintosh@unsw.edu.au

### INTRODUCTION

Pedal and motor cycle helmets have been shown to offer a high level of protection to the wearer's head [1-4]; however, debate continues over the how to optimize helmet performance [5, 6]. Unlike motor vehicle crashes, in typical motorcycle and pedal cycle crashes there are limited witness marks or interpretable vehicle damage patterns from which the crash severity, e.g. impact velocity, change in velocity or acceleration, can be estimated. Central to debates over helmet performance are the issues of impact severity (velocity, energy and profile of impact surface) and impact type (radial, tangential or oblique). Helmet standards must resolve the complex challenge of providing a suitable reduction in injury risk across a population, e.g. amateur or professional sport, through dynamic tests of helmet performance. Understanding how helmets perform in the real world is one element in the process of driving helmet improvement and standards. One possibility is to utilise helmet damage to estimate crash severity [7].

A previous study replicated 21 motorcycle accident cases, covering a broad range of head injuries, using experimental impact tests [8]. One case was used to validate the helmet damage replication method and was reconstructed using a full Hybrid III ATD mounted on a motorcycle, which was impacted against a car. For the remaining cases, the helmet damage was replicated with a series of impact drop tests. Standard targets used in motorcycle helmet tests were used to replicate struck objects and textured slabs were used to simulate road surfaces. It was found that (1) shell damage indicated the impacted object and (2) damage to the liner and shell structure indicated the angle and velocity of the impact. The results of this study suggested that rotational kinematic tolerance values of 40rad/s and 5000rad/s<sup>2</sup> could be incorporated into standards requirements.

This study examined whether helmet deformation caused by impacts can be utilized as a reliable measure of the impact severity. The following questions were addressed:

- are maximum headform acceleration and impact force repeatable for a helmet brand/model and type?

- is residual deformation correlated with maximum headform acceleration, maximum force and impact severity?

### MATERIALS AND METHODS

A selection of commonly available pedal- and motor-cycle helmets was obtained. The motorcycle helmet models included a full-face road style, an open-face road style and an off-road motocross style. The pedal cycle helmets included a relatively inexpensive generic style and a more expensive in-mould construction style. Six helmets of each type were obtained, five were tested, and one was used as an undamaged reference. Impact tests were conducted against a flat anvil: 18 pedal cycle helmet impacts and 26 motorcycle helmet impacts.

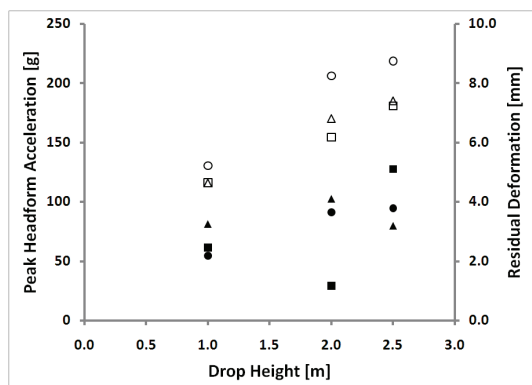
The helmets were tested using a helmet impact test rig; linear acceleration and impact force were used as measures of the energy attenuating capabilities of each helmet. The helmet impact test rig consisted of a drop carriage running along two guide wires. A rigid headform was attached to the drop arm, which contained an accelerometer array at the centre of mass. A force platform comprising of three uniaxial force transducers, constructed to measure impact force, was sandwiched between the anvil and the base of the impact test rig.

Each helmet was fitted onto the headform and retained by its retention system or adhesive tape for all motorcycle and pedal cycle helmets, respectively. The anvil was painted red so that the impact area was clearly marked. Impacts were conducted from drop heights of 1.0m, 2.0m and 2.5m onto comparable helmet locations.

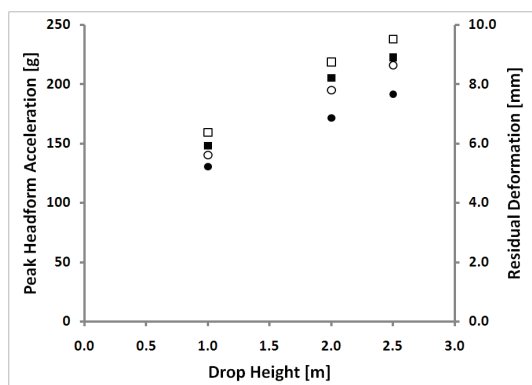
A protocol for assessing the damage sustained by the helmets during the impact tests was established and followed for all helmets. The helmets were weighed, labeled and photographed from multiple angles. Details of the helmet's construction were recorded including the make, model, date and country of manufacture, nominal mass, standards achieved, colour, shell material, inner liner material, and details of the retention system. The inner liner of the helmet was carefully removed and the impact location was

identified. The thickness of the inner liner at four points surrounding the impact area and at one point in the centre of the impact area was measured. The residual deformation was calculated by comparing the average thickness of the surrounding four points with the thickness at the central point.

## RESULTS



□ Road ○ Open △ MX ■ Road ● Open ▲ MX  
Figure 1: Mean peak headform acceleration and residual deformation, against drop height, for each motorcycle helmet type. Hollow and solid markers denote acceleration and deformation, respectively.



□ Generic ○ Expensive ■ Generic ● Expensive  
Figure 2: Mean peak headform acceleration and residual deformation, against drop height, for each pedal cycle helmet type. Hollow and solid markers denote acceleration and deformation, respectively.

The coefficient of variation (CV) for pedal cycle helmet acceleration ranged between 6.9% and 8.8%; for deformation between 26.0% and 29.2%. CV's for motorcycle helmets were greater: acceleration between 11.1% and 14.7% and deformation 55.9% and 67.2%

Force and acceleration were highly and significantly correlated across all impacts as expected (Pearson correlation coefficient of 0.977,  $P < 0.001$ ). Some variation occurred due to the differing helmet masses.

Table 1: Pearson correlation coefficients (r) and P-values for acceleration and deformation distributions against drop height in Figures 1 & 2.

	Acceleration		Deformation	
	r	P	r	P
Pedal Cycle	0.920	<0.001	0.520	0.027
Motorcycle	0.843	<0.001	0.272	0.179

## DISCUSSION

CV data for headform acceleration demonstrated a high level of repeatability. Table 1 shows that acceleration was highly correlated with the impact severity (drop height). Correlations between drop height and deformation were not as strong, although significant for pedal cycle helmets. This suggests that bicycle helmet damage can be used to estimate the severity of the crash. The effect of the motorcycle helmet shell in attenuating impact energy and the consequences for liner deformation are evident in the results. Further work is required on a range of anvils. Whether the headform accelerations are indicative of those experienced by the human head during actual accidents is a separate issue. Ideally, exemplar pedal cycle helmets of the same make and model need to be assessed in laboratory impact tests to determine their performance and this information used when assessing crashed helmets [7].

## REFERENCES

- McDermott, F.T., et al., *The Effectiveness of Bicycle Helmets: A Study of 1710 Casualties*. Journal of Trauma, 1993. 34(6): p. 834-845.
- Attewell, R.G., K. Glase, and M. McFadden, *Bicycle Helmet Efficacy: A Meta-Analysis*. Accident Analysis & Prevention, 2001. 33(3): p. 345-352.
- Coben, J.H., C.A. Steiner, and T.R. Miller, *Characteristics of Motorcycle-Related Hospitalizations: Comparing States with Different Helmet Laws*. Accident Analysis & Prevention, 2007. 39(1): p. 190-196.
- Savolainen, P. and F. Mannering, *Probabilistic Models of Motorcyclists' Injury Severities in Single- and Multi-Vehicle Crashes*. Accident Analysis & Prevention, 2007. 39(5): p. 955-963.
- Mills, N.J. and A. Gilchrist, *Oblique Impact Testing of Cycle Helmets*. International Journal of Impact Engineering, 2008. 35(9): p. 1075-1086.
- Richter, M., et al., *Head Injury Mechanisms in Helmet-Protected Motorcyclists: Prospective Multicenter Study*. Journal of Trauma, 2001. 51(5): p. 949-958.
- McIntosh, A.S., B. Dowdell, and N. Svensson, *Pedal Cycle Helmet Effectiveness: A Field Study of Pedal Cycle Accidents*. Accident Analysis & Prevention, 1998. 30(2): p. 161-168.
- Chinn, B., et al., *COST 327: Motorcycle Safety Helmets*. 2001, European Commission, Directorate General for Energy and Transport: Belgium.

## HEAD IMPACT CONDITIONS IN CASE OF BICYCLIST FALLING

Nicolas Bourdet<sup>1</sup>, Caroline Deck<sup>1</sup>, Pedro Carreira<sup>2</sup>, Rémy Willinger<sup>1</sup>

1. University of Strasbourg, bourdet@unistra.fr
2. Oxlane Research Villeneuve d'Ascq

### INTRODUCTION

The cyclist accident rate remains high among the whole road users. According to Linn *et al.*'s study in 1998 [1], the three parts most often hit during cyclist accident are the arms, legs and head for 50% of cases. Moreover, Otte *et al.* [2] showed that 70% of fatal cases are due to head injuries. Currently only few information are available concerning the head impact condition for this kind of accidents, especially concerning windscreen impact. In 2000 and 2003, Maki *et al.* [3]-[4] studied the pedestrian and cyclist kinematics according to the vehicle geometry. It appeared that the impact zones, the impact velocity and angle were different between cyclist accidents and pedestrian accidents. Hence, the authors concluded that the existing pedestrian tests were not applicable to cyclists. In 2001, Werner *et al.* [5] studied the human-cycle decoupling. He showed that in case of off-center impact or a cycle velocity over 5 m/s, the cyclist was often thrown to the ground without touching the car. Several authors have reconstructed many accidents between car and bicyclists in order to identify the cyclists kinematics during impact, as Serre *et al.* in 2007 [6]. But falling alone was rarely studied because of the huge quantity of scenarios and the difficulty to identify an accident type. Therefore, the objective of the present work is to identify the initial condition of head impact in case of cyclist fall alone by simulating a great numbers of accident situations.

### MATERIALS AND METHODS

The present study proposes a methodology based on a parametric study. A total of 512 simulations have been automatically carried out using Madymo® software coupled with a special designed program allowing computing and analyzing all the scenarios. Two fall situations have been studied according to real accident cases configuration. The analyzed outputs are successively head initial position and speed before impact and order of impact to other body parts.

The model used to represent the bicyclist is the TNO pedestrian human one. This model has deformable

legs and shoulders and can be scaled with the madyscale function in Madymo® software and is represented in figure 1.

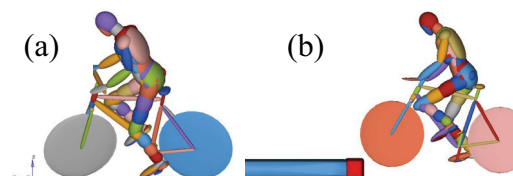


Figure 1. Representation of the bicyclist model with a cycle model used for the simulations of falling alone (a) after sliding, (b) against a curb.

The automatic parametric study enabled to obtain three major results: velocity, orientation and the head impact area, to establish the conditions of head impact just before contact.

Two configurations of falling were considered: against a curb and after sliding. For each configuration a set of parameters was studied such as cycle velocity, torso posture, human height, pedals position handlebars rotation and bike type.

### RESULTS

For a cyclist moving with 5.5 m/s (20 km/h) and falling alone as simulated in this study, the resulting head velocity is 5.7 m/s and 6.7 m/s for curb impact and sliding configuration respectively. Considering normal component, the velocities are 4.4 m/s and 5.7 m/s for curb impact and sliding respectively against 3.5 m/s for tangential component. The obtained values are in the velocity range recommended by testing standards for certification of helmets.

Whereas when the cycle speed is 11.1 m/s (40 km/h), the resultant head velocity is 8.8 m/s (4 m/s normal and 7.8 m/s tangential) for curb impact and 11.4m/s (6.5 m/s normal and 9.5 m/s tangential) for sliding. It can be observed that for this cycle speed the tangential component is higher than normal one for both configurations. Figure 3 illustrates the distribution of zone impact on the head for latitude and longitude partitions showed in figure 2.

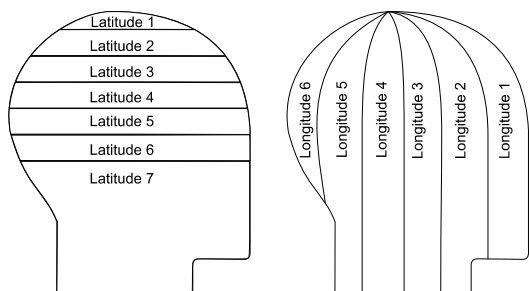


Figure 2. Representation of head partition (a) in latitude and (b) in longitude.

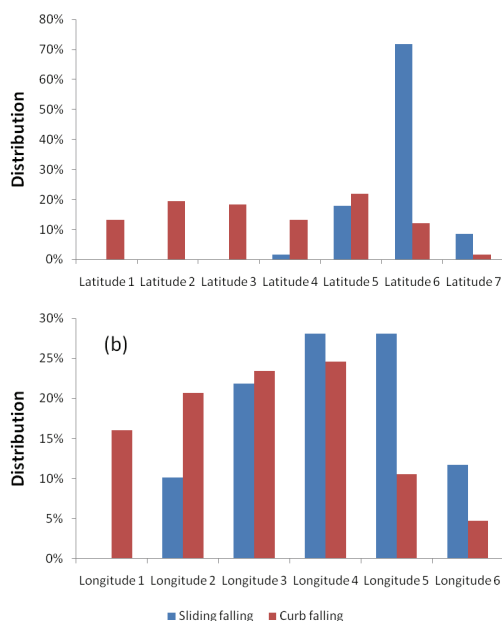


Figure 2. Distribution of head impact zone (a) in latitude and (b) in longitude for both configuration of falling.

## DISCUSSION

The study of impact locations at head level showed that the majority (70%) of these impacts are on helmet line level (latitude 6) for sliding falling. These results are consistent with other studies presented in the literature as Ching *et al.* [7] who noted 84%. But more spread for a fall against curb. Otherwise, for both configuration of falling, the most impacted in longitude area is occipital with more than 50%. Moreover, during head impact on the ground, a significant tangential component (60% to 80% and 145% to 195% of normal velocity for an initial cycle speed of 5.5 m/s and 11.1 m/s respectively) of the velocity is observed. This component generates a rotational acceleration of the head and thus increases the injury risk. Therefore, the standard test for bicycle helmet should include this tangential component in future.

The work has provided a solid information base for future work to carry on bicyclists' accidents. A parametric analysis was used to study the effects of environmental parameters poorly known in case of fall alone accidents as bike velocity or body posture with a great quantity of simulations. This constitutes a set of bicycle falling scenarios which allows to evaluate the head impact area and velocity during impact, especially the tangential and normal components. Finally, this work will contribute to improve our knowledge on the loading parameters of head during bicycle accident, especially in case of falling alone, and thereby understand better, how to optimize the helmet.

## REFERENCES

1. Linn, S., Smith, D. & Sheps. S. (1998). Epidemiology of bicycle injury, head injury, and helmet use among children in British Columbia: a five-year descriptive study. *Injury Prevention*, 4, 122-125
2. Otte, D., Injury mechanism and crash kinematics of cyclists in accidents—an analysis of real accidents, SAE STAPP 892425, 1989.
3. Maki Tetsuo, Asai Toshiyuki, Kajzer Janusz, The behavior of bicyclists in accidents with cars, JSAE Review Volume 21, Issue 3, July 2000, Pages 357-363.
4. Maki T.; Kajzer J.; Mizuno K.; Sekine Y., Comparative analysis of vehicle-bicyclist and vehicle-pedestrian accidents in Japan, *Accident Analysis and Prevention*, Volume 35, Number 6, pp. 927-940, 2003.
5. Werner SM, Newberry WN, Fijan RS, Winter M. Modeling of bicycle rider collision kinematics. SAE Technical Paper Series, 2001-01-0765, SAE 2001 World Congress, Detroit, MI, March 7, 2001.
6. Serre T., Masson C., Perrin C., Chalandon S., Llari C., Cavallero C., Py M., Cesari D., Pedestrian and Bicyclists accidents: in-depth investigation, numerical simulation and experimental reconstitution with PMHS *International Journal of Crashworthiness* (2007), vol 12, n°2, pp227-234
7. R.P. Ching, D.C. Thompson, R.S. Thompson, D.J. Thomas, W.C. Chilcott, F.P. Rivara, Damage to a bicycle helmets involved with crashes, *Accid. Anal. And Prev.*, Vol. 29, No. 5, pp 555-562, 1997

## HUMAN BRAIN TOLERANCE THRESHOLDS FOR TRAUMATIC BRAIN INJURY FROM RECONSTRUCTIONS

Andrew Post<sup>1</sup>, Blaine Hoshizaki<sup>1</sup> and Michael Gilchrist<sup>1,2</sup>

1. University of Ottawa Neurotrauma Impact Science Lab; apost@uottawa.ca
2. University College Dublin, Dublin, Ireland

### INTRODUCTION

In an effort to better understand traumatic brain injury research has focused using finite element modelling was employed in conjunction with accident reconstruction. Often, the purpose of these reconstructions is to correlate dependent variables of the injury. However, these reconstructions are difficult to perfect and the influence of factors such as impact vector (angle), mass and others on brain deformation are not well described.

Several researchers have attempted to reconstruct brain injury events in American Football, motorcycling accidents and falls with varying results [1; 2]. The American Football reconstructions had limitations due to the challenges of the reconstructions and errors in the estimation of velocity of impact and impact vector. The other simulations were also limited in their reconstructive accuracy, but provides a possible baseline for future research.

Advancements in methodology have been developed by Kleiven [3] and Doorly and Gilchrist [4]. These researchers used medical imaging to define brain lesion site for FE analysis. While an improvement, limitations still existed in accurately defining the vector of the impact and low sample sizes from which to develop a statistically significant result.

The purpose of this research is to reconstruct traumatic brain injury events using a combination of hybrid III headform, FE modelling and medical imaging to examine brain deformation based metrics which may be linked to the injury. A secondary purpose is to examine how the various impact conditions produced in this reconstruction influence the brain deformation dependent variables.

### MATERIALS AND METHODS

The participant in this case was 85 years old and had received a subdural hematoma from a fall without the presence of skull fracture. Clinical assessment of the brain injury was conducted by a neurosurgeon on site and corresponding CT scan along with injury reports were used to define the initial conditions for the reconstructive protocols.

The subject fell head first into concrete, with the contact site being to the right side of the frontal bone. The subject did not experience a loss of consciousness (assessed at a GCS of 15) and filled out a reconstructive report form describing the incident. The information on the form was further validated by a description of the incident by the subject's wife. A CT scan following the incident showed a subdural hematoma in his left frontal lobe.

As this incident was a falling injury, the reconstruction was conducted using a monorail device with a Hybrid III instrumented with a 3-2-2-2 accelerometer array. The impact conditions were a velocity of 4.5 m/s +/- 0.5 m/s and angle of impact variations of 0, 12 and 23 degrees. The material was composed of concrete similar to the original impact surface. The impact location on the Hybrid III was chosen to mimic the impact site as shown on the initial CT scan.

The finite element model used for the reconstruction was the University College Dublin Brain Trauma Model (UCDBTM) [5]. The head was comprised of the scalp, skull, pia, falx, tentorium, cerebrospinal fluid, grey and white matter, cerebellum and brain stem. In total, the model had approximately 26,000 elements [5]. The validation of the model was found to be in good agreement with intracranial pressure and brain motion data taken from cadaver experiments [5]. In this reconstruction the UCDBTM was scaled to the head size of the subject, and extra element sets were created to represent the area affected by the subdural hematoma and the bridging veins local to the injury site.

The loading curves from the physical reconstructions were input at the centre of gravity of the model and brain deformations calculated. Results in von Mises stress, maximum principal strain, strain rate, product of strain and strain rate were taken from the subdural hematoma region identified by CT scan as well as global peaks from the cerebellum element set of the model.

### RESULTS

The results for the reconstruction are shown in tables 1 and 2. Table 1 shows the kinematic input and brain deformation response for the subdural region

and table 2 shows the values for the bridging veins closest to the injury site.

The results indicate a range of dynamic response across velocity of 300 to 567 g and 29.9 to 41.8 krad/s<sup>2</sup>. The deformation metrics shown in these tables also vary by velocity. When the results are examined by angle of impact, there is also variance showing an interaction between impact angle and resulting dynamic response and brain deformation metric.

## DISCUSSION

The results of this reconstruction suggest that for this case the subdural hematoma was produced at a range between 25 to 34% maximum principal strain, which is somewhat higher than those values found in the literature [4]. The values found for this reconstruction for the overall brain response (cerebrum) was also found to be largely in excess of the current values for human reconstruction that exists in literature.

The dynamic response and resulting brain deformation as a result of the different impact conditions were found to vary. The change in velocity as expected would produce a more severe impact; however the change in impact angle produced corresponding decreases in linear acceleration, and increases in rotational acceleration. These variations in impact angle would have a significant influence on the resulting magnitudes of the dependent variables used to predict a brain injury when doing reconstructive research.

This reconstruction differs from some of the previous TBI reconstruction research as it employs the use of physical models as well as finite element. In the case

of physical models, the head is more rigid than most computational models under impact, which can influence the results greatly. The impacting mass can be difficult to ascertain from injury reports, though in this case the weight of the head itself was likely the impacting mass. Other factors that would influence the dynamic response data would also be the type of impacting surface used and the mechanism of injury which is being reconstructed (head impacting object vs object impacting the head).

There are further limitations to reconstructive research as is evidenced through the use of finite element models. They are best approximations and not perfect representations of human physiology. Also, in this case the unique physiology of the elderly brain was not reflected by the UCDBTM, although the model was adjusted to size.

## REFERENCES

1. Zhang, L., Yang, K.H. and King, A.I. A proposed injury threshold for mild traumatic brain injury. *J biomech eng*, 2004; 126:226-236.
2. Willinger, R. and Baumgartner, D. Numerical and physical modelling of the human head under impact – towards new injury criteria. *Int. J. Vehicle Design*, 2003; 32:94-115.
3. Kleiven, S. Predictors for traumatic brain injuries evaluated through accident reconstruction. *Stapp Car Crash J*. 2007; 51: 81-114.
4. Doorly, M.C. and Gilchrist, M.D. The use of accident reconstruction for the analysis of traumatic brain injury due to head impacts arising from falls. *Comput Method Biomec* 2006; 9(6): 371-377.
5. Horgan, T.J. and Gilchrist, M.D. The creation of three-dimensional finite element models for simulating head impact biomechanics. *IJCrash* 2003; 8(4): 353-366.

Table 1. The brain deformation metric responses for the subdural hematoma region

	4.0 m/s			4.5 m/s			5.0 m/s		
	0°	12.6°	23.7°	0°	12.6°	23.7°	0°	12.6°	23.7°
Linear acceleration (g)	414	353	300	485	422	351	567	467	436
Rotational acceleration (krad/s <sup>2</sup> )	30.0	31.3	29.9	35.5	38.1	34.6	39.6	41.6	41.8
Maximum principal Strain	0.258	0.313	0.308	0.28	0.329	0.316	0.344	0.322	0.342
von Mises Stress (kPa)	9.2	9.9	10.0	11.3	10.3	10.8	10.4	11.7	11.5
Strain rate (s <sup>-1</sup> )	64	89	88	43	94	90	41	92	114
Strain X Strain rate	17	28	27	12	31	28	14	30	39

Table 2. The brain deformation metric responses for the bridging veins closest to the subdural hematoma region

	4.0 m/s			4.5 m/s			5.0 m/s		
	0°	12.6°	23.7°	0°	12.6°	23.7°	0°	12.6°	23.7°
Linear acceleration (g)	414	353	300	485	422	351	567	467	436
Rotational acceleration (krad/s <sup>2</sup> )	30.0	31.3	29.9	35.4	38.1	34.5	39.6	41.6	41.8
Maximum principal Strain	0.14	0.11	0.074	0.088	0.112	0.075	0.11	0.11	0.109
Strain rate (S <sup>-1</sup> )	22	17	13	16	19	15	18	17	18
Strain X Strain rate	3	1.87	0.96	1.41	2.13	1.13	1.98	1.87	1.96

Symposium Programme: 2011 IUTAM Symposium on Impact Biomechanics in Sport, University College Dublin, Room 326, Engineering Building, July 7th-9th 2011		July 9, 2011	
July 7, 2011		July 8, 2011	
8:00-9:00	Registration and welcome		
9:00-9:45	<b>Keynote lecture</b> K.T. Ramesh, JHU Adding insult to injury: The dynamics of human tissues	<b>Keynote lecture</b> A. McIntosh, UNSW Biomechanical considerations in the design of equipment to prevent sports injury	<b>Keynote lecture</b> J. Ryan, Leinster Rugby Collision injuries in Rugby Union
9:45-10:15	A. Ni Annaidh, UCD Modelling the anisotropic behaviour of skin	Andrew Post, Univ. of Ottawa Analysis of loading curve characteristics on the production of brain deformation metrics	Garrett Coughlan, UCD Classification of Collisions in Elite Level Rugby Union using a Wearable Sensing Device
10:15-10:45	Katrien Baeck, KULeuven Experimental characterization of the mechanical properties of the superior sagittal sinus – bridging vein complex	Manuel Forero, UCD Computational protective helmet component analysis	Grant Trewartha, University of Bath An integrated measurement system for analysing impact biomechanics in the rugby scrum
10:45-11:15	Coffee Break	Coffee Break	Coffee Break
11:15-11:45	Julie Motherway, UCD Modelling the impact response of cranial bone	Evan Walsh, Univ. of Ottawa Dynamic impact response characteristics of ice hockey helmets using a centric and non-centric impact protocol	A. McIntosh, UNSW Impact reconstruction from damage to pedal- and motor-cycle helmets
11:45-12:15	Esmeralda Forausbergher, KULeuven A new method to determine the young's modulus from fresh bone flaps	Blaine Hoshizaki, Univ. of Ottawa The application of brain tissue deformation values in assessing the safety performance of ice hockey helmets	Pedro Carreira, Orylane Research Head impact conditions in case of bicyclist falling
12:15-12:45	Badar Rashid, UCD Mechanical properties of brain tissue in tension at high strain rates	D.A. Patton, UNSW Impact assessment of jockey helmet liner materials	Andrew Post, Univ. of Ottawa Human brain tolerance thresholds for traumatic brain injury from reconstructions
12:45-14:15	Lunch	Lunch	
14:15-15:00	<b>Keynote lecture</b> S. Kleiven, KTH Biomechanics of traumatic brain injuries and head injury criteria	<b>Keynote lecture</b> M.T.G. Parn, Loughborough University Passive and active muscle effects on impacts	
15:00-15:30	Andrew Short, University of Melbourne The egg injury criterion. Can we learn more about head injury with an egg surrogate?	V. Balden, University of Cape Town Validated 3d finite element model of wrist joint	
15:30-16:00	D.A. Patton, UNSW Injury data from unhelmeted football: head impacts evaluated against critical strain tolerance curves	David Eager, Univ. of Technology Sydney Trampoline frame impact attenuation: padded metal-frame vs soft-edge system	
16:00-16:30	Coffee Break	Coffee Break	
16:30-17:00	Michael Gilchrist, UCD / Strasbourg University Traumatic brain injuries investigation using finite element modeling of rat brain	Stefan Litzenberger, UAS Technikum Wien Falls into via ferrata climbing sets can cause severe injuries for lightweight climbers	
17:00-17:30	Ryan Ouckama, McGill University Impact performance of ice hockey helmets: head acceleration versus focal force dispersion	Andrew Glenn, University of Melbourne Upload your head injury! A novel method for biomechanical prediction. Is it feasible?	
17:30-18:00		Marshall Kendall, Univ. of Ottawa A comparison of peak linear and angular response between the Hybrid III and the Hodgson-WSU headforms	
Irish Pub Night - Pick up at 18:00		Departure from UCD for Symposium Banquet - 18:00, Pick-up at Radisson Hotel - 18:15	